This is to certify that the

dissertation entitled

The development of a Rex-induced spiral exchange technique for mapping the ribosomal DNA of D. melanogaster and further investigations of the genetic properties of Rex

presented by

Peter Gerard Crawley

has been accepted towards fulfillment
of the requirements for
Doctor of Philosophy Zoology
_____ degree in _____

Leonard Robbins
Major professor

4-29-96
Date _____

THE DEVELOPMENT OF A *REX*-INDUCED SPIRAL EXCHANGE TECHNIQUE FOR MAPPING THE RIBOSOMAL DNA OF *D. MELANOGASTER* AND FURTHER INVESTIGATIONS OF THE GENETIC PROPERTIES OF *REX*.

By

Peter G. Crawley

A DISSERTATION

Submitted to
Michigan State University
in partial fulfillment of the requirements
for the degree of

DOCTOR OF PHILOSOPHY

Department of Zoology and the Genetics Program

1996

ABSTRACT

THE DEVELOPMENT OF A *REX*-INDUCED SPIRAL EXCHANGE TECHNIQUE FOR MAPPING THE RIBOSOMAL DNA OF *D. MELANOGASTER* AND FURTHER INVESTIGATIONS OF THE GENETIC PROPERTIES OF *REX*.

By

Peter G. Crawley

As a means of studying heterochromatin in *D. melanogaster*, we have chosen to examine the genetic properties of a particular heterochromatic element, *Rex* (*R*ibosomal *ex*change), and to use *Rex* as a tool to further investigate the structure and properties of the ribosomal RNA (rDNA) genes. The three central accomplishments of this study are:

1. The development of a *Rex*-induced spiral mapping technique that greatly improves the efficiency of mapping molecular variants in rDNA arrays.

2. The estimation of total and active gene copy number in twenty one recombinant nucleolus organizer (NO) and the demonstration of the absence of a correlation between either of these parameters with the ability of an array to function as a site for *Rex*-induce spiral exchange.

3. The demonstration that *Rex* can induce changes in repeat copy number in rDNA arrays.

To my parents.

TABLE OF CONTENTS

LIST OF TABLES

LIST OF FIGURES

Chapter 1

INTRODUCTION

Background Information

The impetus for the research presented in this study is guided by a desire to learn more about a poorly understood chromosomal domain called heterochromatin. Perhaps the most salient feature of heterochromatin is its ubiquity. It is present, to varying degrees, in every eukaryotic organism that has been examined to date (Brown, 1966). In addition, in many organisms, heterochromatin occupies a substantial fraction of the genome (Brutlag et al, 1977). In the fruit fly, *Drosophila melanogaster*, for instance, heterochromatin comprises approximately forty percent of the total nuclear genetic material (Peacock and Appels, 1980). Yet, for a number of reasons, many of which are presented below, heterochromatin has been regarded as structurally simple and functionally inert; in other words, 'junk' DNA. The results of studies in the past twenty years, however, indicate that heterochromatin exhibits an enormous variety of functions and that although the molecular composition is simple, the overall structure is much more complex.

In order to reveal more about heterochromatin in general, we have chosen to examine, in detail, the genetic properties of one heterochromatic 'element' (the term 'element' will be used throughout the text to differentiate heterochromatic sequences with defined functions from euchromatic genes) called *Rex*, for *R*ibosomal *ex*change, and to use *Rex* as a genetic tool to examine the structure and properties of a large heterochromatic repeated array, the ribosomal DNA (rDNA) array. Specifically, we have used *Rex* to construct a type of map of rDNA arrays that defines the relative positions of a class of molecular variants that can be identified among the repeating units of an array. The original intent of this research was not only to develop a more rapid means of generating maps of rDNA arrays using mapping principles that had already been developed in our laboratory, but to use the new, 'quick mapping' protocol to address other

questions about the rDNA. One question that was particularly intriguing to me was how copy number of the repeating units in an rDNA array is maintained. This question could, in theory, be addressed using a 'quick mapping' strategy. Because an increase in mapping efficiency would allow us to examine a large number of arrays, we could start by mapping a particular array, then introduce conditions that caused changes in copy number in that array, and finally map those arrays that showed an increase in copy number. By comparing the before and after maps, we hoped to address the underlying mechanism controlling these changes. However, because of the difficulties in actually developing the quick mapping system, I was unable to put the system to use in the way it was originally intended. Consequently, the bulk of my thesis involves the development of the mapping procedure itself. The remainder involves further genetic studies of the properties of *Rex*, including evidence that *Rex* itself can cause increases in copy number of the repeating units of single rDNA arrays.

The thesis is divided into four chapters. The first chapter serves as a general introduction to heterochromatin, the structure and function of the rDNA array in *D. melanogaster*, and some of the basic properties of *Rex*. In addition, the three major areas of investigation are introduced. These are: 1. development of the spiral mapping technique and the use of the technique to map one rDNA array, 2. genetic attempts to more precisely define a 'target' region for *Rex*-induced rDNA exchange and 3. examination of the role of *Rex*, if any, in the maintenance of copy number in rDNA arrays. Each of these three topics is then covered in detail in chapters two, three and four, respectively.

Heterochromatin

The study of heterochromatin began nearly 70 years ago, in 1928, when a German cytologist, E. Heitz, used a dye that stained nucleic acids to examine different stages of the cell cycle. Heitz observed two cytologically distinct chromosomal domains (Heitz, 1929). One region,

which Heitz named heterochromatin, remained darkly staining throughout the entire cell cycle. A second region, the euchromatin, stained darkly only during mitosis, when the chromosomes were in a highly compact state. During interphase, the euchromatin did not stain as darkly. This suggested to Heitz that the darkly staining heterochromatin was always in a compact mitotic state. Because it was, and still is, believed that chromosomal function is paused during mitosis, Heitz reasoned that the permanently compact, darkly staining heterochromatin was inert nuclear material. A more modern term for inert DNA is 'junk' DNA and the idea that heterochromatin is primarily 'junk' has remained a prevalent notion among geneticists today even in the face of a large body of evidence suggesting otherwise.

Heitz's initial hypothesis has enjoyed such staying power because a number of important observations have been interpreted as further indicators of the inert nature of heterochromatin. First, a number of model organisms, most notably fruit flies and corn, are much less sensitive to homozygous deletions of heterochromatin than they are to deletions of regions of euchromatin of comparable physical size (Hilliker, 1976) . This observation implies that there are few necessary genes in heterochromatin. Second, when euchromatic genes are brought in close proximity to heterochromatin by chromosomal rearrangements, they are transcriptionally inactivated (Muller, 1930; for reviews see Spofford, 1976; Henikoff, 1990). For instance, in *D. melanogaster*, when a gene responsible for normal eye pigmentation, the white gene, w^+, is translocated near heterochromatin, the eye develops with a mottled or variegated pattern of pigmentation. This phenomenon, known as position effect variegation (PEV), is caused by the inactivation of the translocated gene in a cell-lineage dependent manner during development. During the development of the eye, for instance, those cells in which inactivation of the translocated white gene has occurred give rise to daughter cells that also have an inactive white gene. Conversely, cells in which the gene remains active, producing red pigment, give rise to daughter cells that also produce

red pigment. The result is an eye that is composed of patches of white and normally pigmented, red sectors. Because heterochromatin does not provide a hospitable environment for the normal transcription of these euchromatic genes, it has been argued that it does not provide a hospitable environment for the transcription of *any* genes (Miklos, 1985; Smith, 1976). Third, a large fraction (60-80%) of heterochromatin is comprised of highly repetitive short sequences called satellite sequences (Peacock et al., 1976). The position of particular satellite sequences does not appear to be well conserved between closely related species (Peacock et al., 1976), implying that the actual sequence of the satellite DNAs is dispensable. Finally, heterochromatin exhibits a much reduced frequency of homologous meiotic recombination compared to euchromatin. For instance, homologous recombination within the heterochromatin of the *X*-chromosome of *D. melanogaster* occurs at a frequency about 10^3 times lower than recombination in *X* euchromatin (Williams and Robbins, 1992). This observation has been used as supporting evidence for the 'junk DNA' hypothesis (John and Miklos, 1989). The argument is that recombination provides a means for creating genetic diversity upon which the forces of evolution can then act. A region that has no evolutionary consequence would not need to recombine. Junk recombining with junk is still, after all, just junk.

Yet, even in the face of what appears on the surface to be strong evidence against an important functional role, the fact remains that heterochromatin is everywhere. How, then, can we reconcile these contradictory observations? In recent years, a closer examination of heterochromatin and its properties, suggests that heterochromatin is actually far from inert. In *D. melanogaster*, for instance, fifty-four functional heterochromatic elements have been discovered (Wakimoto, 1989; Gatti, 1994). A brief description of some of these elements will illustrate the functional diversity of heterochromatic elements and serve as a means of addressing some of the errors in the 'junk' DNA hypothesis.

Although it is clear that the distribution of heterochromatic elements is relatively sparse in comparison to genes in the euchromatin, it is also clear that the structure and nature of heterochromatic genetic elements is very different from euchromatic genes. Many of them show complex interactions with euchromatic counterparts. For instance, *Responder* (*Rsp*) is a heterochromatic element that is located immediately adjacent to the centromere of chromosome two in *D. melanogaster* (Ganetzky, 1977). *Segregation distorter* (*SD*) is a euchromatic gene, located near the heterochromatic/euchromatic breakpoint on the second chromosome, that interacts with *Rsp*. There are two types of *Rsp* alleles that have been identified based on their interactions with *SD*, *Rsp* sensitive and *Rsp* insensitive alleles. In flies carrying a *SD* bearing chromosome and an SD^+ bearing homologue, *SD*-bearing chromosomes are recovered in 99% of the progeny if the SD^+ homologue also bears a *Rsp* sensitive allele. The *SD* gene product interacts with the *Rsp* sensitive site on the SD^+ homologue in such a way as to poison those sperm that carry the sensitive site (for review see Lyttle, 1991). *Rsp* is by no means unique in showing interactions with euchromatin. Duplications of a heterochromatic segment called ABO can rescue the embryo from the lethal effects associated with a euchromatic maternal effect recessive mutation called ***abnormal oocyte***, or *abo* (Tomkiel et al., 1992). Interactions of the heterochromatic *crystal* element with the euchromatic *Stellate* locus have dramatic effects on spermatogenesis (Palumbo et al., 1994). To some extent, euchromatic genes, readily exposed by deficiencies, are simply easier to find than heterochromatic genes.

Studies of the regulation of a number of heterochromatic genes have dramatically shown that transcriptional inactivation of euchromatic genes juxtaposed with heterochromatic sequences is not caused by an inherent transcriptional inertness. When some heterochromatic genes are moved from their heterochromatic environment to euchromatic regions, their regulation is also disrupted in a variegated manner. For example, the heterochromatic *light* gene is one of the genes responsible

for pigment deposition in the eye. When *light* is placed in a euchromatic environment, either by chromosomal rearrangements or by P-element transposition, the eye takes on a mottled appearance analogous to PEV of the *white* gene (Wakimoto, 1990). In fact, *light* **requires** surrounding heterochromatin for correct temporal and spatial regulation. This suggests that there are at least two distinct nuclear environments and that genes or elements evolve expression mechanisms for their own particular environments (Henikoff, 1990).

The *Y*-chromosome fertility factors are a group of five elements necessary for fertility in the *D. melanogaster* male and provide an example of how simple sequence DNA can be functionally complex. The fertility factors are comprised of megabase-length simple sequence repeats that are transcriptionally active in the developing spermatocyte (Bonoccorsi et al., 1990). A complex of proteins binds the actively transcribed fertility factors to form enormous Y-chromosome loops. The function of the loops is still unknown. It has been hypothesized, however, that, when transcribed, the fertility factors may serve as a structural framework necessary for normal sperm development (Bonaccorsi et al, 1990). Another example of simple sequences with critical functions has come from studies attempting to define the sequences that make up a *D. melanogaster* centromere. Recent evidence suggests that satellite sequences surrounding a complex 'island' of single copy material known as Bora Bora in the basal heterochromatin of the *X*-chromosome is responsible for sister chromatid adhesion and play a role in ensuring proper segregation of sister chromatids during mitosis (Karpen and Murphy, 1995).

Although there is very little recombination occurring within heterochromatic sequences, this does not necessarily imply that homologous heterochromatic sequences never interact. In fact, for two heterochromatic gene arrays, the histone genes and the ribosomal DNA genes, there is evidence that homologous regions must interact. Current evidence suggests that these two multigenic arrays have evolved a mechanism for homogenizing the repeat units within an array.

The evidence for some sort of homogenizing force comes indirectly from observations that there is as much or more sequence variation between the repeat units of closely related species as there is between distantly related species, implying that once a variant arises within an array of a population, it can either spread quickly throughout the population or be removed from the array. The homogenization of arrays, called concerted evolution, suggests that, at least for these two heterochromatic elements, a means of homologous 'communication' does exist.

Our understanding of the structure and function of heterochromatin is extraordinarily primitive. However, it has become increasing clear in recent years that Heitz's initial cytological description of heterochromatin as inert genetic material does not accurately reflect either the complex functional components of heterochromatin or the intricacies of its molecular structure. Instead, current evidence strongly suggests that the eukaryotic genome can be subdivided into two separate subgenomes with very different structures and properties. The two most widely studied genetic differences between the two regions, suppression of recombination in the heterochromatin and position effect variegation, may be reflections of different evolutionary demands and different regulatory strategies of the two subgenomes. The molecular organization of the two types of chromatin is also very different. The euchromatin is comprised of relatively densely packaged unique coding sequences while heterochromatin is made up mainly of moderately and highly repetitive sequences with relatively few unique coding sequences. In *D. melanogaster*, the middle repetitive sequences residing in the heterochromatin are (retro)transposable elements that appear to be quiescent (Franz and Kunz, 1981; Glatzer, 1979; Jamrich and Miller, 1984; Kidd and Glover, 1981; Long and Dawid, 1979). The proteins associated with the two classes of chromatin also differ. In 1989, Wustmann et al. identified a novel protein, based on it's ability to suppress position effect variegation, now referred to as HP1, for heterochromatic-specific chromosomal protein 1. HP1 is the first cloned gene whose product was shown to bind specifically to

heterochromatin (for review see Eisenberg, 1991). Since then, a large number of proteins have been isolated because of their ability to suppress or enhance position effect variegation. Many of these proteins have also been shown to bind specifically to heterochromatin. Currently, these proteins are thought to function to generate and maintain the heterochromatic state.

Finally, the two regions are cytologically separable. In addition to the differential staining that is seen during interphase, heterochromatin exhibits a number of cytological differences relative to euchromatin. In many insect species, certain cell types undergo multiple rounds of DNA replication without cellular division, producing giant polytene chromosomes. For instance, in the larval salivary glands of *D. melanogaster*, the heterochromatin is the only chromosomal region not to be over-replicated. Furthermore, the heterochromatin in polytenized cells is associated in a centralized region called the chromocenter. Heterochromatin is also late-replicating and shows tight adhesion of sister chromatids in neuroblast mitotic spreads. Together, the cytological , genetic and molecular differences describe two very different nuclear domains.

Despite our improving knowledge of heterochromatin and its properties, there are many fundamental questions about heterochromatin that remain unresolved. What defines a heterochromatic gene? Is some sort of repetitive structure required for heterochromatic function? How are heterochromatic elements expressed? In an attempt to more clearly define the structure and function of heterochromatin as a whole, we have chosen to examine the genetic properties of a particular heterochromatic element, *Rex*, and to use *Rex* as a genetic tool to examine the structure of a complex multigenic heterochromatic array, the ribosomal DNA array, in a manner that has not been possible for other large repeated arrays. In order to fully understand how we use *Rex* to examine the structure of the rDNA, it is necessary to understand both the structure of a single rDNA repeat unit and the basic genetics of *Rex*.

The ribosomal DNA of *D. melanogaster*

The rDNA of *D. melanogaster* is organized as two large (3-4 Mb) multigenic arrays. One array is in the basal heterochromatin of the *X* chromosome. The other is on the short arm of the entirely heterochromatic *Y* chromosome. Each wild-type array contains between 200-250 copies of the same transcriptional unit. Each repeat encodes two of the major RNA species, the 18 and 28S, and two of the minor species, the 5.8 and 2S that go into forming a mature ribosome. Between each of the repeating units there is a nontranscribed intergenic spacer (IGS) comprised mainly of a 240 bp repeating unit that is about 80% homologous to the functional promotor region. This promotor-like repeat is responsible for ensuring *X:Y* pairing in males (Mckee, 1993). The IGS can vary in length from 2-20 kb depending on the number of 240bp promotor-like repeats. The structure of the rDNA array and of a single repeat is shown in Figure 1. Cytologically these arrays can be seen in the nucleus as the site of ribosome assembly and are referred to as the nucleolus organizers (Schwarzacher and Wachtler, 1993). Genetically, complete or partial deletions of rDNA arrays are defined as bobbed (*bb*) alleles. Flies that have approximately a quarter (100) of the wild type copy number are phenotypically "bobbed" (*bb*). They are developmentally retarded, have thin shortened bristles and exhibit abdominal etching. Each of the three terms used to describe the ribosomal arrays, the rDNA, the nucleolus organizer (NO), and the *bb* gene, are molecular, cytological and genetic definitions of the same locus.

Many (up to 70%) of the 28S subunit rRNA coding region are interrupted by one of two classes of retrotransposable elements called R1 and R2, although the number of repeats varies greatly from strain to strain. (Lyckegaard and Clark, 1991) . The R1 and R2 elements are not related, although both are families of non-LTR retrotransposons. The insertion sites of the two inserts are located 74 bp apart (Eickbush, 1995). The full length R1 insertion contains two open reading frames, ORF1 and ORF2. The second ORF contains a region that shares homology with

the general consensus sequence for reverse transcriptase. The R2 insertion sequence also encodes a putative reverse transcriptase. There is no direct evidence, however that either of these elements is capable of transposition.

In Figure 1, the structure of the rDNA in *D. melanogaster* is shown. At the top of the figure, a schematic diagram of the mitotic *X*-chromosome is shown. Euchromatin is depicted as a white box and heterochromatin as a black box. The centromere is represented by the circle at the right most end of the chromosome. The rDNA array occupies the central one third of the basal heterochromatin. The first magnified view illustrates two important aspects of the array. First, the transcribed portion of each repeat, shown as triangles, is uniform in length, but the nontranscribed, intergenic spacer (IGS) region is variable in length. As detailed later in this study, it is IGS length variation that is used as a molecular landmark in constructing maps of arrays. Second, the repeats are not tandemly arranged (Swanson and Robbins, 1989). The consequences of this nontandem structure will become evident during the discussion of *Rex* in the following section. In this single heterochromatic region, three different functional elements have been identified: 1) the rDNA is the site of ribosome assembly and provides a number of the structural components of the ribosome, 2) it is the *X* and *Y* chromosome pairing site in Drosophila males and 3) *Rex* itself maps to within this region.

Rex

Rex is a heterochromatic element that can cause recombination between rDNA arrays (Robbins, 1983). The recombination that *Rex* mediates is unusual for a number of reasons. First, there is normally very little measurable recombination between homologous heterochromatic sequences, including ribosomal arrays. *Rex*-induced exchange in the rDNA, however, occurs at frequencies approximately 100-fold higher than spontaneous homologous exchange. Second, the exchange mediated by *Rex* is mitotic. The exchange occurs very early (sometimes prior to the first

round of DNA synthesis) in the fertilized egg; furthermore, *Rex* acts maternally. That is, the piece of DNA upon which *Rex* resides need not be present in the zygote in order to see it's effects. Instead, *Rex*-bearing females presumably dump the *Rex* product into the developing oocyte and the product then functions to generate the exchange events. Finally, the types of chromosomes used to detect *Rex*-induced exchange are a class of structurally unusual chromosomes that we call target chromosomes. The common feature of all target chromosomes is that each possesses two rDNA arrays separated by the entire length of an *X*-chromosome.

Figure 2a shows a cross typical of those used to detect *Rex*-induced exchange, the types of exchanges that *Rex* can generate, and the results of each of two types of exchange events. In this scheme, only sex chromosomes are followed. The female fly has two *X*- chromosomes, only one of which is *Rex*-bearing. Both maternal *X*-chromosomes, however, are 'marked' with a recessive mutant allele, *yellow* (*y*), that affects the color of the fly body. The male fly carries a normal *Y*-chromosome and an *X*-chromosome that is a target for *Rex*-induced exchange. In this example, the target chromosome carries a wild-type y^+ allele. Flies bearing this allele will have dark brown bodies. The target also carries a dominant mutant allele called *Bar* (*B*) that affects the shape of the fly's eye. The rationale behind choosing these particular markers for the target chromosome will become obvious when the scheme for detecting one class of *Rex*-induced events is discussed in Figure 2b.

The *Rex* mother will occasionally produce an egg in which a mitotic exchange occurs immediately following fertilization. *Rex* causes two types of exchanges, depending upon how the arrays pair. Pairing of the arrays in a spiral configuration, as shown on the left hand side of Figure 2a, when followed by exchange will result in two products; an acentric ring chromosome that is lost during subsequent divisions because it lacks a centromere and a mini-fragment chromosome. The overall consequence of the spiral exchange is to delete all material between exchange points.

Figure 1 - The structure of the ribosomal DNA in *D. melanogaster*

A schematic diagram of a mitotic *X*-chromosome is shown at the top of the figure. The positions of a number of relevant genetic markers used during the course of this study are shown. Heterochromatin other than the ribosomal array is shown as a black box. The centromere is shown as a circle at the base of the chromosome. The rDNA occupies the central third of the basal heterochromatin. Euchromatin is shown as a white rectangle. The first expanded view of the array shows that the repeating units are comprised of both an intergenic spacer (rectangular sections) and coding regions (triangles). The intergenic spacer (IGS) separates each coding region and is composed mostly of varying numbers of a 340bp repeating sequence. The repeating units are not tandemly arranged. The final blow-up shows the structure of an individual repeat unit (see text for details). The 28S subunit is sometimes interrupted by one or both of two different types of insertion sequences, Type I and Type II inserts.

Figure 1 - The structure of the ribosomal DNA in *D. melanogaster*

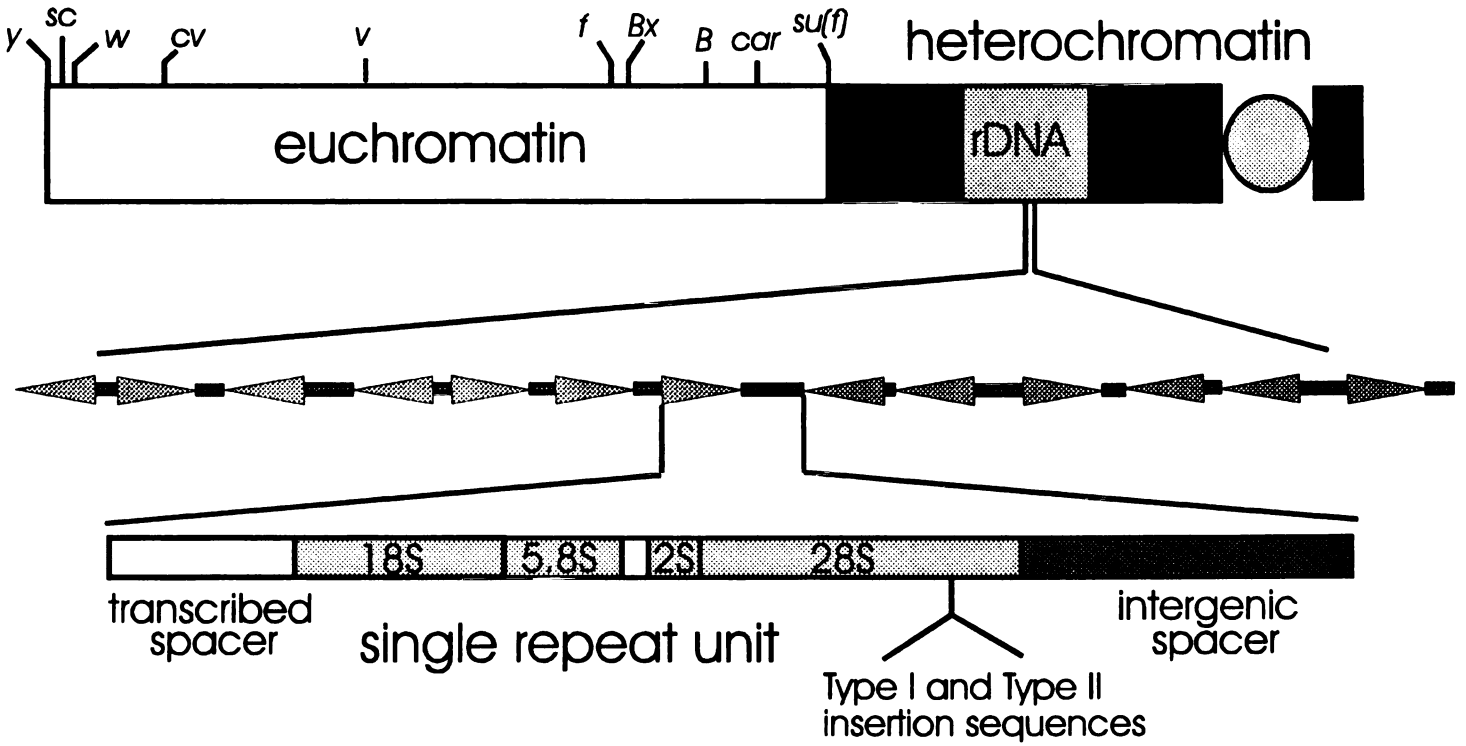

IDENTIFIED FUNCTIONS IN THE rDNA

1. encodes four of the five ribosomal RNA species
2. serves as the *X:Y* pairing site in males
3. contains *Rex* and *Su(Rex)*

Because the *Bar* allele is between the two exchange points it ends up on the acentric ring chromosome and is lost. The y^+ allele, located at the very tip of the *X*-chromosome, is outside the two arrays. It ends up on the fragment chromosome and is expressed in flies that bear it, thereby affecting their phenotype. Pairing of the two arrays in a hairpin orientation, followed by exchange, will invert all material between the exchange points. If the target chromosome is inverted to begin with, as shown on the right hand side of Figure 2a, then a hairpin exchange will result in a reinversion back to a chromosome with normal orientation. As previously mentioned, hairpin events are much more difficult to detect since no material is lost. A means of identifying chromosomes that have undergone *Rex*-induced hairpin exchange will be discussed in some detail in the third chapter where hairpin exchange mapping is used in an attempt to further characterize the target site of *Rex*.

Because *Rex*-induced spiral exchange can result in offspring with a unique phenotype, spiral exchange can be used as a means of detecting *Rex*. Figure 2b diagrams a Punnett square from the mating described above. Normal disjunction in the female will produce an *X*-chromosome bearing a *y* allele. Gametes arising from nondisjunction will be either diplo-*X*, carrying two maternal *yellow*-bearing *X*-chromosomes, or nullo. Sperm will carry a *Y*-chromosome or the target *X*-chromosome. Flies that receive the target from the male will occasionally undergo a *Rex*-induced spiral exchange. As a consequence of the exchange, flies that would normally develop into females bearing a single maternal *X*-chromosome and the target chromosome, are converted to phenotypically unique males that bear the maternal *X*-chromosome and the fragment chromosome. (In flies, sex is determined by the ratio of *X*-chromosomes to autosomes, not by the presence of a *Y*-chromosome, as it is in mammals. Flies that have a single *X*-chromosome and two of each Bar-eyed.autosome have the normal 1:2 male sex chromosome to autosome ratio). Because the *Y*-chromosome is required for fertility in males, the X/fragment males are viable but infertile.

Figure 2 - *Rex*-induced Exchange in the rDNA of *D. melanogaster*

2a. The two types of *Rex*-induced exchange, spiral exchange and hairpin exchanges, and the products of each of these exchanges are shown. A female fly homozygous for *yellow*, *y*, (a body-color mutant) and heterozygous for *Rex* is mated with a male that carries a marked target *X*-chromosome. A y^+ marker lies outside the two blocks of rDNA that define the target. An additional dominant marker, *B*, lies between the two separated blocks of rDNA. A *Rex*-induced hairpin exchange will result in inverting all material between the exchange points. A *Rex*-induced spiral exchange event will delete the *B* marker between the two rDNA blocks and will produce a fly with a unique phenotype.

2b. A fly resulting from a spiral exchange will be easily detectable, as shown in this Punnett square. This fly will carry one of the two maternal *X*-chromosomes but will have a small fragment chromosome that bears only the y^+ marker from his father. This fly, has a normally shaped eye, but y^+ body color, and is easily distinguishable from all other progeny. If the exchange occurs after the first mitotic round of DNA replication in the zygote, a gynandromorph will result (see text).

Figure 2- *Rex*-induced exchange in the rDNA of *D. melanogaster*

A. *Rex*-induced Mitotic Events

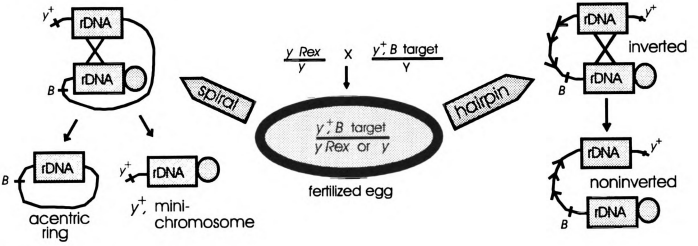

B. Detecting Spiral Exchanges

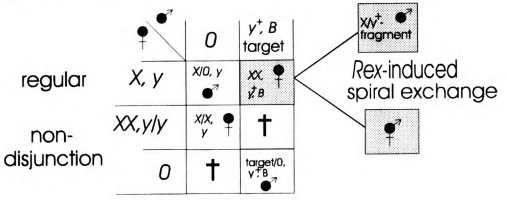

Phenotypically, they are unique. They are y^+ males with normally shaped eyes. This result is shown in the top box that stems from the box with target-bearing females. The only other y^+ males that can come from this mating are the result of nondisjunction; these males, however, are y^+ and

The box below shows a fly that is generated from a spiral exchange that occurs after the first round of DNA replication in the zygote. After the first round of replication, there are two target chromosomes upon which *Rex* can potentially induce exchange. If exchange occurs in one of these and not the other, half the cells of the fly will bear the fragment and half will not. The consequence of this event is a gynandromorph, a fly that is comprised of half male and half female tissue. Whether the exchange occurs before the first round of replication, producing an entirely male fly, or after the first round of replication, producing a gynander, the result is easily detected and provides a simple assay for *Rex* activity.

Our current working hypothesis is that *Rex* is an active version of one of the normally quiescent retrotransposable-like elements that reside in the rDNA. The evidence for this hypothesis is indirect. First, *Rex* itself is located within an rDNA array (Rasooly and Robbins, 1989). Second, *Rex* increases levels of exchange between arrays. Finally, both genetic and molecular data indicate that the *Rex*-induced exchanges are sometimes accompanied by deletions at the site of exchange (Rasooly and Robbins, 1989; and this work). Apparently, *Rex* is acting to generate breaks in the rDNA and these breaks are occasionally resolved by recombination. Thus, *Rex* may generate breaks in rDNA by producing a transposase that is packaged in the maturing oocyte. The transposase can presumably make cuts in rDNA arrays even before S phase of the first mitotic division of the developing embryo. Eickbush and Xiong (1988) have shown that the R2 homolog of the silkmoth *B. mori*, encodes an endonuclease activity that can generate cuts at a specific site within the 28S subunit region of the rDNA array. The *Rex* phenotype may be due to recombinational repair of cuts generated by just such an element. That is, when two rDNA arrays

are present on the same paternally-derived chromosome, a break in one or both of these arrays could initiate repair by recombination. If one of the arrays has two breaks, a piece may be deleted during the exchange, thus yielding a deletion that maps to the exchange site. More recent cytological evidence suggests that many more breaks in the rDNA are occurring than can be repaired in the rapidly dividing early embryo. When fertilized eggs from *Rex*-bearing mothers are allowed to develop for fifteen minutes, fixed, stained with DAPI, and viewed with fluorescence microscopy, up to 60% of the embryos show severe chromosomal damage (Robbins and Pimpinelli, 1995). This implies that in *Rex* matings we recover only the small minority of damaged eggs that escape death by recombination repair (Robbins, 1995).

High levels of mitotic recombination between rDNA clusters is not unique to the *Rex* system. In the budding yeast, *Sacchromyces cerevisiae*, mutants lacking either DNA topoisomerase I or II show highly elevated levels of mitotic rDNA recombination (Christman et al, 1989). Topoisomerase I and II are also required for the stability of chromosomal rDNA clusters in yeast (Kim and Wang, 1990). In a S. cerevisiae strain deleted for TOP1 and temperature sensitive for TOP2, most of the rDNA exists as extrachromosomal elements. Kim and Wang suggest that the rDNA topology changes in the double mutants and leads to a shift in the equilibrium of an excision/integration rDNA recombination pathway. Topoisomerase I is a component of the nucleolus organizer of Drosophila (Fleisman et al., 1984). Recently, Williams et al. (personal communication) have suggested that the presence of increased numbers of topoisomerase I DNA binding sites relative to euchromatin may be a distinguishing characteristic of all heterochromatic sequences. A second mutation in yeast, rrm3, stimulates recombination in rDNA and in a second repeated gene, the copper chelatin genes, without affecting a variety of other repeated sequences (Keil and McWilliams, 1993).

In *S. cerevisiae*, a *cis*-acting sequence, called HOT1, comprised of an rRNA transcription initiation site and an RNA polymerase 1 enhancer, can stimulate recombination (Keil and Roeder, 1984). When the HOT1 sequence is inserted at a variety of chromosomal sites, recombination levels in the vicinity of the transposed HOT1 element are elevated.

Curiously, there are many different types of insertion elements that reside within nuclear, mitochondrial and chloroplast rDNA from a wide variety of organisms that share the ability to make breaks in rDNA. A class of mitochondrial rDNA group-1 introns of fungi encode putative site-specific endonucleases (Carbone et al., 1995). A murine retrotransposon, B2, has recently been shown to 'hop' into 18S rDNA in mice (Oberhaumer, 1992). Interestingly, a group-1 intron from *Physarum polycephalum*, that encodes a rDNA-specific endonuclease that generates double-strand breaks in a conserved region of the rDNA, has recently been cloned into *S.cerevisiae* (Muscarella and Vogt, 1993). The expression of the endonuclease using the GAL10 inducible promoter caused a lethal phenotype as a result of double strand breaks in rDNA. It would be interesting to see if the expression of this gene in *D. melanogaster* would lead to *Rex*-like events.

Areas of investigation

This study focuses on three areas: 1. development of a 'quick' system for mapping rDNA arrays using *Rex*-generated spiral exchanges; 2. determination of whether the frequency of *Rex*-induced spiral exchange correlates with the total number of rDNA repeats or the total number of actively transcribed rDNA repeats; and 3. showing that *Rex* can induce heritable changes in the copy number of single, paternally-derived rDNA arrays.

Chapter 2 describes the methodology used to develop a system that allows us to rapidly map the positions of molecular variants in rDNA arrays. Briefly, this system relies on using *Rex* to induce spiral exchange chromosomes in a novel target chromosome. That target is itself a product

of *Rex*-induced hairpin exchanges, and allows us to replace the proximal array with any array that we wish to map. In addition, this new target yields fragment chromosomes that can be recovered as viable and fertile male offspring. The details of the construction of the novel target, the matings designed to allow recovery of fragment exchange chromosomes and the methods used in generating a map from these fragment chromosomes are presented.

Chapter 3 details experiments designed to further define the nature of the *Rex* target. Previous studies have shown that rDNA is sufficient to generate exchanges (Swanson, Ph.D. thesis;) and that nearly all of *Rex*-induced exchange is in the rDNA. Whether or not there are specific sites or specific regions within an array that are sensitive to *Rex* is not known. By constructing a family of target chromosomes that differed in the amount and composition of rDNA in one of the two target chromosome arrays, we looked for correlations between the frequency of spiral exchange in these new chromosomes and the amount of total and active repeat units within the differing arrays. Using maximum likelihood methods we compared hypotheses based on no correlation between our measured parameters and an hypothesis based on a linear correlation. Our results indicate that there is no correlation between either the total number of repeats or the number of active repeats in an array and the spiral exchange frequency. This suggests that there are in fact regions within arrays that respond better to *Rex* than do other regions and it is not simply a quantitative effect.

Chapter 4 examines another phenotype of *Rex*. We know that *Rex* can cause inter-array exchange events, but could *Rex* also be generating breaks that are resolved by intra-array recombination? The intra-array events would normally escape detection because, unlike the inter-array events that generate spiral exchanges, there is no obvious phenotypic consequence of exchange occurring within an array. One possible result of an intra-array event is an alteration in gene copy number due to resolution of breaks either by recombination or by some other, as yet

unidentified, mechanism. Ribosomal gene copy number alterations in the rDNA of Drosophila, a phenomenon known as magnification, are known to occur under a variety of conditions. To test whether *Rex* was capable of magnifying an rDNA array, we looked for changes in copy number of an allele of *bb*, bb^2, that had been "exposed" to the maternal activity of *Rex*. We found that indeed, *Rex* could induce stable increases in copy number of the bb^2 allele at frequencies comparable to the rate of spiral exchanges. Although the mechanism of these changes is still unknown, the spiral exchange mapping technique makes an examination of the mechanism of *Rex*-induced magnification, as well as other types of magnification, feasible. By comparing maps of premagnified alleles with those of magnified arrays it may be possible to distinguish between a number of current hypotheses on how copy number changes take place.

Because there are a number of chromosomes used throughout the course of the work that the reader may be unfamiliar with, the following tables point out their relevant properties.

Table 1 - Standard and Previously Constructed Chromosomes

Chromosome	Description	Reference
C(1)DX	an attached-*X* chromosome that is lacking all rDNA	Lindsley and Zimm, 1987
FM7	standard *X*-chromosome balancer, males viable and fertile	Lindsley and Zimm, 1987
Df(1)X1	deficient for approximately 80% of the basal heterochromatin and a small region of neighboring euchromatin. Completely rDNA$^-$.	Lindsley and Zimm, 1987
In(1)sc^{V2}	*X*-chromosome inversion with distal breakpoint at scute and proximal breakpoint approximately at midpoint of rDNA	Lindsley and Zimm, 1987
In(1)sc^{4}sc^8	inverted chromosome lacking rDNA	Lindsley and Zimm, 1987
In(1)w^{m51b}L$_w$m4R	parental chromosome used to map *Rex* target site	Swanson, 1984
Dp(1)w^{m51b}L$_w$m4R	*Rex*-generated hairpin exchanges from *In(1)w^{m51b}L$_w$m4R*	Rasooly, 1989
Tp(1)w^{m51b}L$_{,\#}$	left end arrays from *In(1)w^{m51b}L$_w$m4R$_{,\#}$*	Rasooly, 1989
NOw$^{m4R}_{,\#}$	right end arrays from *In(1)w^{m51b}L$_w$m4R$_{,\#}$*	Rasooly,1989

Table 2 - Novel Chromosomes Constructed During This Study

Chromosome	Description
Tp(1:1)sc^{V2}, #1- 5	*Rex*-induced hairpin exchanges of *In(1)sc^{V2}*
Dp(1:1)sc^{V2},3L,bb^{2}R	*Dp(1:1)sc^{V2}, 3a* with basal heterochromatin replaced with *bb^{2}*
Dp(1:f)sc^{V2}bb^{2}R	*Rex*-induced fragment chromosomes generated by spiral exchange
Dp(1:1)w^{m51}L$_{w}$m4R, 7L, #R	Recombined hairpin exchanges, 7L with all other right ends
Dp(1:1)w^{m51}L$_{w}$m4R, #L, 5R	Recombined hairpin exchanges, 5R with all other left ends

Chapter 2

THE DEVELOPMENT OF A SPIRAL MAPPING TECHNIQUE FOR THE rDNA OF *D. MELANOGASTER*

Introduction

Our understanding of the both the structure and function of heterochromatin is limited, in part because it has been historically labeled as an uninteresting region, but also because it is difficult to study using techniques that were developed for euchromatin. The repetitive nature of heterochromatin and the enormous size of many of the repeated gene arrays makes classical molecular techniques, like chromosome walking and restriction mapping, tedious at best, and in many cases, simply impossible. Also, because there is very little recombination between homologous heterochromatic regions, it is extraordinarily refractory to analysis using classical genetic techniques. As a result, what we do know about the structure of heterochromatin comes primarily from *in situ* cytological analysis. For instance, using multiple sequence-specific biotinylated probes, Pimpinelli et al. have shown that the distribution of a number of transposable elements located in heterochromatin is conserved evolutionarily (Pimpinelli, in press). A combination of cytology and pulse field gel electrophoresis is being used to construct gross physical maps of two large repeated arrays, the 600 kb *Rsp* element composed primarily of a 240 bp XbaI repeating unit (Lyttle et al., 1995) and the 2.0 Mb region of a *Y*-chromosome lampbrush loop in *D. hydei* (Kurek, Trapitz and Bunemann, 1995).

A second approach at understanding large heterochromatic arrays has been taken for the histone genes. The histone gene array spans a 500 kb region in the heterochromatin of 2L. The histone genes are arranged as a tandemly repeating array with interspersed regions of nonhistone coding sequences. Williams et al. have cloned and sequenced multiple copies of the histone repeat unit to look at the structure of small regions of the cluster. These studies have shown that neighboring repeat units have greater sequence homology than more distant repeats. The implication is that variants spread outwards from their points of origin (Williams et al., 1992).

Both the regional molecular approach and the more general *in situ* approach have been instructive in further understanding the complexity of arrays containing repeating units.

However, both approaches are limited. Examining clones containing multiple copies of repeat units yields detailed information about the local structure of arrays, while *in situ* analysis yields information about the large scale placement of arrays without telling us about the relative positions of particular variants. By combining both genetic and molecular techniques, mapping rDNA arrays has provided a unique system that allows us to position different molecular variants with respect to one another along the length of an array. This type of information is potentially important, not simply because it offers an entirely novel approach to examining the large scale organization of heterochromatic multigenic arrays, but also because it provides us with a framework with which we can more clearly define the functional components of the rDNA, and a means of addressing more complex mechanistic questions. For instance, rDNA mapping has been used to show that *Rex* and one type of suppressor of *Rex* are repetitive elements that occupy discrete regions within the ribosomal array (Rasooly and Robbins, 1990). In addition, mapping has been instructive in understanding the mechanism of exchange within arrays; Robbins and Williams have shown that exchanges between rDNA arrays are single crossover events . However these exchanges can often be unequal, and in the case of *Rex*-induced exchange, can also be accompanied by deletions at the point of exchange (Rasooly and Robbins, 1990).

Although the strategy for mapping molecular variation in rDNA arrays differs somewhat from euchromatic mapping, the requirements are the same. To construct a map it is necessary to identify polymorphisms and it is necessary to recover exchange progeny. Any type of polymorphism could potentially be mapped in the rDNA. To date, however, only the positions of IGS length variants have been mapped. Two different methods have previously been used to generate IGS maps of arrays. One method relies on recovering spontaneous exchanges between homologous arrays. The second method, hairpin exchange mapping, uses *Rex* as a genetic tool to boost the frequency of exchange between two separated arrays on the same *X*-chromosome. *Rex* elevates the level of exchange within rDNA arrays to more usable frequencies, but the hairpin

event inverts the chromatin between the two arrays, yielding a product that is difficult to detect. Spontaneous rDNA exchanges are infrequent, and mapping a single array in this manner requires roughly one person-year of effort (Williams and Robbins, 1992). A third method, developed during the course of this study, relies on recovery of *Rex*-induced spiral exchanges. Although only one of the two recombinant arrays is recovered in *Rex*-induced spiral exchanges, the obstacles presented by this are far outweighed by the simplicity of identifying spiral exchange progeny. Because understanding spiral exchange mapping will be simplified by understanding spontaneous mapping first, an outline of spontaneous mapping is presented in Materials and Methods.

Materials and Methods

Genomic DNA extraction

Genomic DNA from *D. melanogaster* was isolated using a modification of the protocol of Pinol et al (Nucleic Acids Research, v.16, no 6, 1988). 1.5 ml eppendorf tubes filled to 1 ml with flies frozen at -70°C for at least 10 min. and up to 6 months were added to 4 mls of ice cold buffer A (100 mM NaCl, 10 mM EDTA, 0.5% Triton X-100 and 20 mM Tris.HCl pH 7.5) in a 15 ml teflon homogenizer. Twelve strokes at 1500 RPM are made with the pestle and the homogenate is passed through 150 mesh nylon sieve. The nuclei were then pelleted by centrifugation at 10000 RPM for 5 min. The supernatant is discarded and the nuclear pellet is gently washed 3X with ice-cold buffer B (buffer A without Triton X-100) and finally resuspended in 1.5 mls of buffer B. 1 ml of 4% SDS and 1 ml of 4M Sodium perchlorate are added. This mixture is gently mixed until a flocculent layer rises to the top. The lysate is then extracted twice with chloroform-isoamylalchol (24:1). DNA is precipitated with 7 mls of 100% Ethanol. Precipitate is washed twice with 70% Ethanol and vacuum dried. Dried samples are dissolved in 1 ml of 10 mM Tris, pH 8.0, 1 mM EDTA. Samples were dissolved overnight at room temperature and the final concentration was determined using a Hoefer TKO-100 Fluorometer.

Description of probes

During the course of this study, a number of probes from a variety of sources were used. Except for the IGS clone, all plasmid DNAs are maintained in DH5α cells. Because of the instability of the IGS clone in DH5α cells, the spacer plasmid is maintained in SURE cells.

1. Intergenic spacer (IGS) probe, pDm103HH2, amp^r, high copy

The spacer probe is a 5.1kb *Hin*dIII/*Hae*III fragment of an entire rDNA cistron subcloned into pAT153. ref. Nature, vol. 295, 1982.

2. Insertion-sequence probe, pA56, amp^r, high copy

The insertion-sequence probe is a 307 bp *Bam*HI/*Hin*dIII fragment of the right hand junction of the type I insertion sequence insertion site cloned into pUC18. ref. Jacubzak, 1990

3. Urate oxidase, single copy gene probe, amp^r, high copy

The single copy probe is a 1600 bp *Sal*I fragment cloned into pCK7. ref. Wallrath, 1991

4. *D. melanogaster* c-ras probe, alternative single copy gene probe.

ref. Steinman, personal communication.

Probe labeling

All probes were labeled using a variation of the oligonucleotide labeling technique developed by Feinberg and Vogelstein (1982). Random 9-mers were heat denatured with 25-50 ng of probe DNA, according to the recommended specifications of Amersham's Megaprime DNA labeling protocol. Labeling reactions were allowed to run for 1-3 hrs at 37°C. Unincorporated labeled nucleotides were removed from the reaction mix using Stratagene push columns. Radioactive nucleotide incorporation was measured in a scintillation counter and approximately 1-5 X 10^6 CPM/ml hybridization solution was used in all hybridizations.

Stocks and Matings

Flies were reared and matings were carried out on cornmeal, molasses and Brewer's yeast medium at 25°C. A standard five count schedule was used to score progeny in all matings.

Detecting IGS variants

Intergenic spacer variation in rDNA arrays was visualized by Southern blotting. Arrays of interest were isolated in rDNA$^-$ backgrounds. 400 ng of genomic DNA from each genotype was digested with HaeIII which cuts on either side of the IGS (see Fig 2). Cut DNA was electrophoresed in 1.2% agarose gels prepared with 1X TBE. The DNA in the gels was alkali-denatured by soaking in 0.5M NaOH for 50 min. and then neutralized. DNA was transferred to Hybond-N (Amersham) nylon membranes by capillary action or pressure blotting. Membranes were UV-fixed and prehybridized in a Robbins hybridization incubator in 7-10 mls of 50% formamide, 0.5mg/ml alkali-sheared salmon (or herring) sperm competitor DNA, 1X prehybridization mix (2.5X pre-hybridization stock = 250 mM Pipes, 2M NaCl, 0.5% sarkosyl, 0.25% Ficol, 0.25% PVP-40, 0.25% BSA, fraction V, pH 6.8). Prehybridization was carried out overnight at 42°C. Membranes were then hybridized with 1-2 X 10^6 CPM/ml of hybridization solution of ^{32}P-labeled plasmid purified spacer probe. Hybridizations were carried out at 42° for 8-12 hrs in 1X prehybridization mix; 40% formamide; 0.2% alkali-sheared salmon or herring sperm DNA; 10% dextran sulfate. After hybridization, membranes were washed twice at 25°C with mild scrubbing in 2X SSC, 0.1%SDS and 0.1% pyrophosphate, and then 3X for 15 min. at 50°C and 1X at 60°C in 0.1X SSC, 0.1% SDS, 0.1% pyrophosphate. After washing, membranes were immediately wrapped in saran wrap and placed in autoradiograph cassettes.

Spontaneous exchange mapping

Because the procedure for generating molecular variant maps of rDNA arrays using *Rex*-induced spiral exchange is based upon an established procedure using spontaneous exchange between rDNA arrays on homologous chromosomes, and because understanding the methodology

for spiral exchange mapping will be made easier with an understanding of spontaneous mapping, a simple example showing how maps can be constructed using spontaneous exchanges is presented below.

The first step in mapping the positions of a particular type of variant is to identify those variants that are unique to that array. In order to ensure that the variants examined come from a particular array, the array must be isolated in an otherwise rDNA$^-$ background. This can be accomplished for *X*-chromosomal arrays in two ways. Either *X/0* males bearing the array of interest can be collected, or females that bear the *X* array of interest and an *In(1)sc^{4}sc^8* rDNA$^-$ *X*-chromosome can be used. For *Y*-chromosomal arrays, *In(1)sc^{4}sc^8/Y* males are used. To visualize IGS variants, genomic DNA is cut with *Hae*III, an enzyme that cuts at either end of the spacer region (see Figure 1 for details). The cut DNA is then separated electrophoretically and the different size fragments are blotted onto nylon and probed with an IGS specific probe. By comparing the length variants of the two arrays from which we will recover recombinants, we can identify those variants that are unique to each of the two arrays.

The next step is to recover crossovers between the two arrays. Spontaneous exchange between homologous arrays is very rare, a single exchange/10^4-10^5 meioses (Williams et al., 1989). By using closely linked markers, however, crossovers between arrays are recovered. In Figure 3, the strategy, developed by Williams et al., for mapping the positions of unique variants using spontaneous exchanges is outlined. In this example, mapping variants using spontaneous exchanges between two *X*-chromosomal arrays is examined. The two arrays are shown as solid red and purple boxes. For the sake of clarity, the size of the arrays is greatly exaggerated relative to the rest of the chromosome. In maintaining the diagrammatic conventions of the thesis, heterochromatin other than rDNA is shown as a black box and euchromatin is shown as a white box. For simplicity, only three variants from each of the two arrays will be mapped. Unique variants from each of the two arrays are shown here as either colored circles or colored squares in an otherwise homogeneous background. Our goal is to position the variants with respect to one another along the length of the array.

Figure 3 - Spontaneous Mapping

The rDNA arrays to be mapped are represented as purple and red boxes. The surrounding black boxes are flanking heterochromatin. The white box represents euchromatin. Centromeres are depicted as white circles. The centromere attached to the red array is 'marked' with y^{+}. The centromere attached to the purple NO is unmarked and referred to in the text as the *y*-centromere. The size of the rDNA array is greatly exaggerated for clarity. Unique variants are shown as colored squares or circles attached to the arrays. Square shaped variants are associated with the purple NO and circular variants with the red NO. The positions of three independent exchanges and the recombinant chromosomes that result from each of the three exchanges is also shown. The presence/absence of each of the unique variants is scored and used to map the limits of the variants in the array (see text for details).

Figure 3 - Spontaneous Mapping

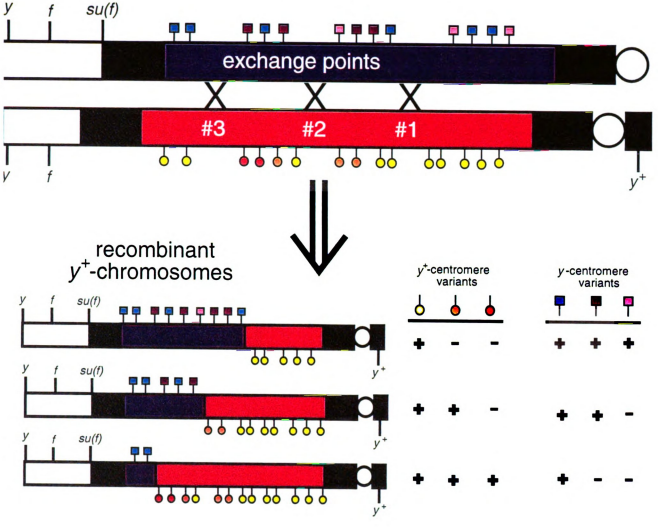

Figure 4 - Proximal and Distal Variant Limits

A. The proximal limits of the variants in the red array, attached to the y^+-bearing centromere, are shown in A. The proximal limit of the yellow variant cannot be determined because the yellow variant is found in the recombinant array derived from the proximal-most exchange point. The yellow variant must extend beyond this point and we arbitrarily extend it's limit to the end of the array. The orange variant, on the other hand is not found in the recombinant chromosome resulting from the proximal-most exchange, exchange #1, but is present in the recombinant array derived from the next most proximal exchange point , exchange #2. Therefore, this variant extends proximally beyond exchange point #2 but does not extend proximally beyond exchange point #1. Similarly, the red variant's proximal limit is exchange point #2. As explained in the text, the distal limits for the variants in this is array would be determined from data collected from recovery of recombinants bearing the *y*-centromere.

B. For variants in the purple array, distal limits, rather than proximal limits are determined from data recovered from the y^+-centromere recombinants. Because the blue square variant is present in the recombinant array that is a result of the distal-most exchange, we know that the distal limit of this variant extends beyond the distal-most exchange point. As with the yellow variant in the y^+-centromere array, we extend this variant to the limit of the array. The purple square variant is present in the recombinant array that is generated as a result of exchange #2. However, it is absent from the recombinant array derived from exchange #3. Therefore, the distal limit of this variant in the purple array is defined by exchange #3. Similarly, the pink variant does not extend beyond exchange point #2. The proximal limits of these variants would be determined by data collected from recovery of recombinant arrays bearing the *y*-centromere.

Figure 4 - Proximal and Distal Variant Limits

A. proximal limits of y^{+}-centromere variants

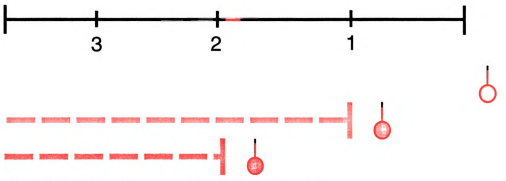

B. distal limits of *y*-centromere variants

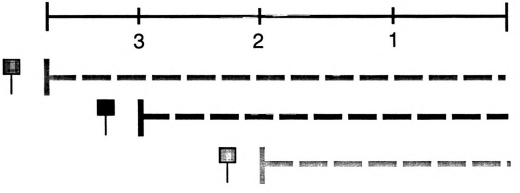

Our final maps, shown in Figure 4, will be incomplete because we will only show the results from one of the two reciprocal exchange classes, the exchange chromosomes bearing the y^+-centromere. In the construction of an actual map, we would also recover recombinant chromosomes bearing the opposite centromere, which, for the sake of clarity, is referred to as the *y*-centromere to distinguish it from the y^+- marked centromere. We select for recombinants based on their unique phenotype. In this particular cross, recombinants that bear the y^+-centromere are phenotypically wild-type.

The positions of three hypothetical exchanges and the recombinant chromosomes that result from these exchanges are shown. In this mapping exercise, we have predetermined the positions of the exchanges, and wish to show what data would be gleaned from each of these exchanges and how the data can be used to build a map. In actuality, the first step towards building a map is to order the exchange points relative to one another. Because exchange in the rDNA can be unequal, we must order the exchange points on each of the two arrays separately. First, let's consider how we order the exchange points in the y^+-array. In this simple example, the presence/absence data for the three color coded variants from each of the parental ends are shown next to recombinant chromosomes. Differences among the recombinant arrays with respect to which unique variants they have retained will allow us to determine the order of the exchanges that generated them.

The recombinant chromosome coming from exchange 1 is missing two of the three unique variants from the y^+-array, the orange and red variants. The only unique variant derived from the y^+-array is the yellow variant. The recombinant array generated by exchange 2, on the other hand, is missing only one of the y^+-array variants, the red variant. Since, the recombinant array that is produced by exchange 2 contains more of the y^+-array variants than the recombinant array produced from exchange 1 and that exchange 1 had to have occurred proximal to exchange 2 along the length of the y^+-array. Similarly, exchange 3 generates a recombinant array that has all of the unique variants from the proximal array. Therefore, exchange three occurred distal to the other two exchange points. This gives us the order that we see on the array. From proximal (closest to

the centromere) to distal (farthest from the centromere), we have exchange 1, then 2 and finally exchange 3.

Next, we can use the data from the recombinant arrays to define the limits of the variants with respect to the exchange points. For the unique variants in the y^+-array, the proximal limits of the variants can be determined from data collected from recombinant arrays bearing the y^+-centromere. Because the yellow variant is found in the recombinant array derived from the proximal-most exchange point, we know that there must be copies of this variant that are proximal to exchange point 1. The orange variant, on the other hand is not found in the recombinant chromosome resulting from the proximal-most exchange, exchange 1. Therefore, we know that there are no copies of this particular variant proximal to exchange 1. It is present, however, in the recombinant array derived from the next exchange point , exchange 2. Therefore, this variant extends proximally beyond exchange point 2 but is not present beyond exchange point 1. Exchange point 1, therefore, is defined as the proximal limit of the orange variant in y^+ this array. The distal limits for the variants in this is array cannot be determined from data collected from recombinant arrays bearing the y^+-centromere. In order to determine the distal limits of the unique variants in y^+-array, we would need to collect data from recombinant arrays bearing the other centromere.

We can, however, also determine the distal limits of the unique variants of the purple array. In this case, we know that exchange 1 was most proximal because it results in a recombinant chromosome that has all of the three square variants. The other two exchanges are missing either one or two of the unique variants from this array and therefore must have been generated from exchanges that occurred more distally. Exhange 2 is missing one of the variants, the pink variant, while exchange 3 is missing both the pink and purple variants. Therefore, exchange 2 occurred proximal to exchange 3 on the *y*-centromere chromosome. Recombinants bearing the y-centromere could be used to define the distal limits of variants from the y^+-array and the proximal limits of the variants from the *y*-array.

Results

Genetic components of a spiral mapping system

Although *Rex* increases the frequency of exchanges between rDNA arrays by at least 100-fold, recovering *Rex*-induced hairpin exchange products is still painstakingly difficult. Hairpin exchanges invert the euchromatin between the sites of exchange without any concomitant loss of phenotypic markers. In order to detect a hairpin exchange event, each paternally derived chromosome from a *Rex* cross must be tested for the classical inversion phenotype, suppression of exchange. This means that another generation of flies must be screened. Spiral events, on the other hand, delete all euchromatin between the exchange points. Consequently, detection of spiral exchanges is simple provided that the appropriate set of markers is used (see Fig. 2, Chapter 1). Detecting spirals is so much easier than detecting hairpins that the work involved in generating maps of individual arrays could potentially be reduced from 1 person-year/array in the case of hairpin mapping to 3 person-months/array using spiral exchanges. We therefore decided to develop a mapping system using spiral exchange chromosomes.

Although detection of spiral events is simple, the fragment chromosome generated is a source of anueploidy. Thus, recovery of spiral exchange products as viable and fertile flies requires some degree of chromosomal engineering. Developing a system using spiral exchanges for mapping multiple arrays also requires that we be able to easily substitute an array of interest into one end of the target chromosome. In other words, an inverted sequence target chromosome could not be used in a system developed specifically for spiral exchange mapping because of the difficulty of crossing an array of interest from a normal sequence chromosome onto an inverted target chromosome. Unfortunately, neither of the two targets that we had on hand met these criteria; production of viable, fertile fragment-bearing progeny, and easy substitution of arrays to be mapped. Therefore, the first step in attempting to develop a mapping system based on spiral exchanges required construction of a new target.

A chromosome called *In(1)sc*^{V2} seemed like an intelligent choice of starting material for the construction of the new target. First, *In(1)sc*^{V2} is itself a *Rex* target. It is a γ-ray induced

inversion of the *X*-chromosome with a proximal breakpoint cytologically mapped to near the midpoint of rDNA array, effectively splitting the array in half and moving half of it to a more distal location (see Lindsley and Zimm, 1985). Although this chromosome is itself an inverted chromosome, a *Rex*-induced hairpin exchange would generate a normal sequence chromosome with two separated NO's, designated $Tp(1;1)sc^{V2}$. Second, *Rex*-induced spiral exchange of $Tp(1;1)sc^{V2}$ would result in a duplication only of the euchromatin distal to scute. This duplication can be almost entirely compensated for by a known lethal deletion, *Df(1)259* (see Lindsley and Zimm). *Df(1)259* spans regions A1-A6 of the polytene chromosome map. The distal breakpoint of $In(1)sc^{V2}$ is at position B1-2 of the polytene map, within the achaete-scute complex. Therefore, the fragment chromosomes generated by *Rex*-induced spiral exchange, in a *Df(1)259* background, would result in flies duplicated for the region between the proximal most end of the deletion at A6 and the breakpoint at B1-2. This small amount of aneuploidy should affect neither viability nor male fertility. A schematic diagram of $In(1)sc^{V2}$, and the steps for generating the new $Tp(1;1)sc^{V2}$ target are shown in Figure 5.

In order to find *Rex*-induced hairpin events in $In(1)sc^{V2}$, we designed a mating scheme, shown in Figure 6, to detect reinverted chromosomes resulting from exchange in $In(1)sc^{V2}$. Reinversion events resulting from *Rex*-induced hairpin exchanges in paternally-derived $In(1)sc^{V2}$ chromosomes will give rise to daughters that contain two normal sequence chromosomes. Fertilized eggs in which there is no exchange will result in daughters that contain one normal sequence chromosome and one inverted chromosome.

Daughters that are inversion heterozygotes will show suppressed levels of exchange during meiosis. In inversion heterozygotes, chromatids involved in a single exchange event never make it into a mature oocyte. The reason for this stems from the biology of Drosophila oogenesis. Only one of the two terminal products of meiotic tetrad develops into a mature oocyte. If a single exchange occurs between two chromatids during meiosis, a dicentric bridge forms, excluding those cells from the terminal positions (Sturtevant and Beadle,).

Figure 5 - Generation of a novel target chromosome: *Tp(1;1)sc^{V2}*

In(1)sc^{V2} is an inverted chromosome with a distal breakpoint at *scute* and a proximal breakpoint near the middle of the ribosomal array. The inversion essentially splits the rDNA into two equal blocks. The separation of two blocks of rDNA on the same chromosome defines a *Rex* target. *Rex*-induced hairpin exchange occurring in *In(1)sc^{V2}* generates a normal sequence (non-inverted) chromosome that has a block of rDNA, without any surrounding heterochromatin, translocated to a distal position, near scute. We have named this new target chromosome, *Tp(1:1)sc^{V2}*.

Figure 5 - Generation of a Novel Target Chromosome: *Tp(1:1)scV2*

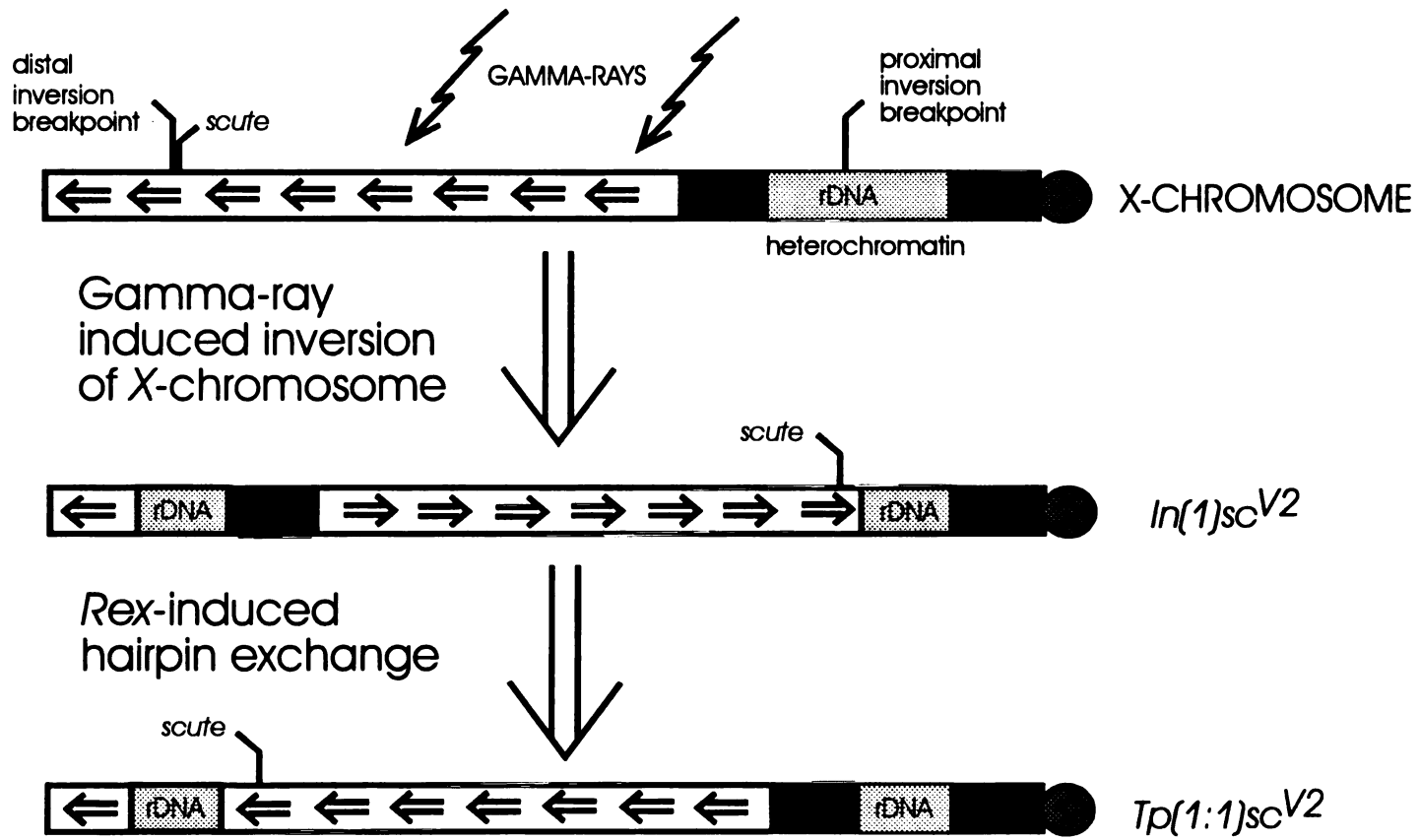

Figure 6 - Mating scheme to detect *Rex*-induced hairpin exchange in *In(1)sc*^{V2}

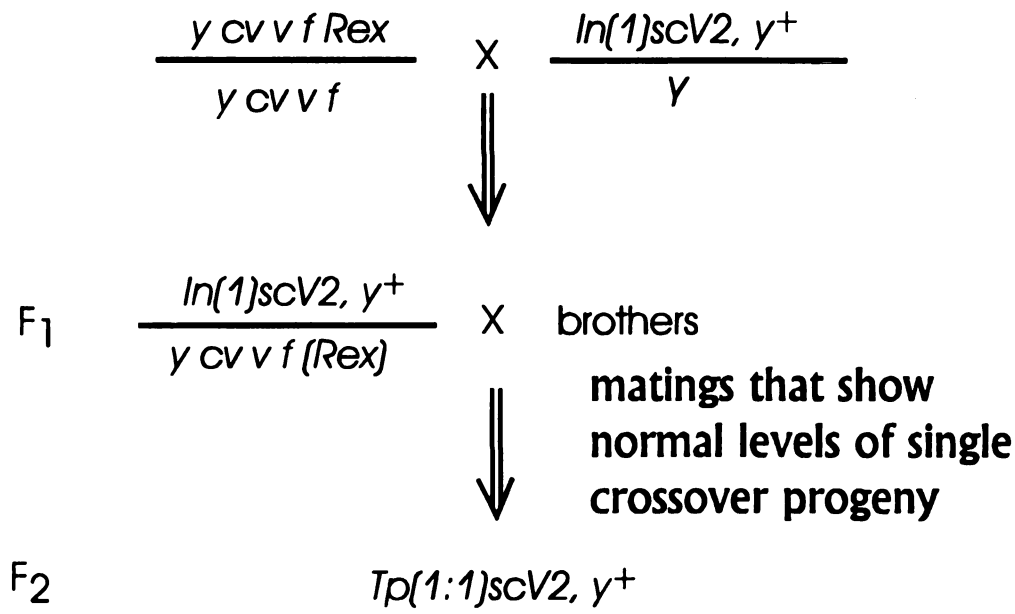

Rex-bearing females are crossed to *In(1)sc*^{V2} males. All F1 females are tested for levels of recombination. Reinverted *X*-chromosomes from those that exhibit normal levels of recombination are stocked. See text for details.

We can see this suppression of exchange among the F_1 daughters only by scoring their progeny. Progeny from flies that have undergone a hairpin exchange will exhibit normal levels of recombination, while female flies that develop from fertilized eggs that have not undergone an exchange event will exhibit suppressed numbers of single crossover progeny.

To test for normal levels of exchange, male progeny from individual matings of F_1 females were scored. We used the following logic in order to determine how many progeny we needed to score before we could be reasonably certain that a hairpin exchange had not occurred.

The frequency of single exchange meiotic tetrads, E_1's, in the *X*-chromosome of *D. melanogaster* is approximately 80%. Since two of the chromatids in a single exchange tetrad are not involved in the exchange, about 40% of all *X*-chromosomes are single crossover chromosomes. In inversion heterozygotes, those chromosomes are lost. The remainder, 60%, are non-crossovers and double crossovers (we do not consider triple crossovers since the frequency is so low). Because 3/4 of the double exchange tetrads (two strand and three-strand E_2's) generate dicentric bridges in an inversion heterozygote, the frequency of seeing a non-crossover or double crossover chromosomes in an inversion heterozygote is actually less than this value. However, by overestimating the frequency of non-crossovers in the following calculation we are less likely to mistake a reinverted hairpin chromosome for a chromosome that has not undergone a hairpin event. We would like the probability of counting N non-crossover and double crossover offspring without seeing a single crossover to be less than 1%. This gives 99% assurance that we do not miss a reinverted chromosome.

$$\begin{aligned} \text{Thus, } (0.6)^N &\leq 0.01 \\ N\log 0.6 &\leq \log .01 \\ N &\geq 9.01 \end{aligned}$$

In other words, to ensure that we are not overlooking a reinverted chromosome we need to look at just 10 male progeny. If none of the ten are single crossovers, then we can be assured,

with 99% certainty, that the target chromosome has not undergone a hairpin exchange event and we can discard the mating.

Five reinversions were recovered using the scheme presented in Figure 6. Each of the 5 novel chromosomes, designated *Tp(1;1)sc*^{V2}, #1-5 were then tested for their ability to respond to *Rex* and for viability of offspring carrying the fragment chromosome produced by a subsequent round of *Rex*-induced spiral exchange. All five are responsive to *Rex*, and the fragment chromosomes are viable in *X*/fragment males.

Although flies carrying the *Rex*-induced spiral exchange fragment chromosomes generated from the new targets were viable, in order to stock the fragments for further examination, we needed to recover them as *fertile* male flies; we need to bring in a set of Y-linked fertility factors. This can be done by using an attached-*XY* . Males that carry fragments and an attached-*XY* that bears *Df(1)259* are duplicated for just a very small region spanning from the distal breakpoint of *In(1)sc*^{V2} at 1B1-2 to the proximal end of the deficiency at 1A6. We would expect these males to be both viable and fertile. Thus, the problem of maintaining fragment chromosomes is reduced to setting up a mating that generates attached-*XY*/fragment males when a spiral exchange occurs. A mating scheme that generates these males is shown in Figure 7.

Genotypically *XXY* female flies that carry *Rex* on one *X* and the *Df(1)259* attached-*XY* are mated to males that have the D*p(1;1)sc*^{V2} target. At best this scheme only allows for the recovery of half of the spiral exchanges since half the males bearing the spiral will also carry the free *X*-chromosome and not the attached-*XY*. Additionally, any attached-*XY* to be used in such a scheme must be free of suppressors of *Rex*. Otherwise, *Rex* activity will be greatly reduced, decreasing the likelihood of recovering spiral exchange chromosomes.

Figure 7 - Generation of Fertile Males Containing the y^+-fragment Chromosome

To produce viable and fertile flies that carry the y^+-fragment chromosome generated from *Rex*-induced spiral exchange, a *Rex*-bearing female that also carries an attached-*XY* chromosome is used in the initial mating. Eggs that carry the attached-*XY* and the target (approximately 1/4 of all eggs) will occasionally undergo *Rex*-induced spiral exchange. These eggs, that normally would develop into female flies, loose most of the *X*-chromosome of the target as a result of the exchange. These eggs develop instead into male flies that have a complete complement of fertility factors brought in on the attached-*XY*. They are both viable and fertile, providing a means of stocking the fragment chromosome for further analysis.

Figure 7 - Generation of fertile males containing y^+-fragment chromosomes

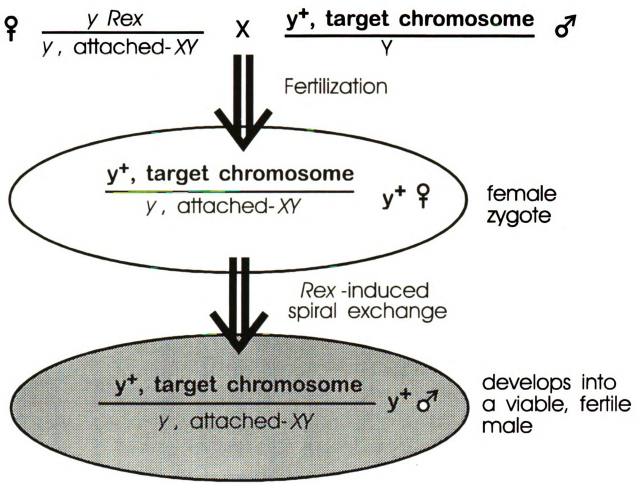

We tested two attached-*XY*s for suppressors. The results are shown in Table 3.

Table 3- Test of two attached *XY*'s for *Su(Rex)*

Attached-XY^{y}/ *y*, *Rex* X *Dp(1:1)sc*^{V2}, y^{+}/*Y*	wild-type females	spirals and gynandromorphs	exchange frequency
XY^{L}·Y^{S}, *Df(1)259, l(1)J1 y w*	2534	25*	1.0%
$Y^{S}X$·Y^{L}, *In(1)EN, y B*	4729	1	0.02%

*20 spirals (17 sterile, 3 fertile)

The attached-*XY* bearing *Df(1)259* showed normal levels of *Rex* activity, whereas the second attached-*XY* is obviously suppressing. It also confers other useful properties: 1) because it is deleted for much of the region of euchromatin that is present on the mini-chromosome, the degree of anueploidy is reduced, and attached-*XY* /mini-chromosome should be healthier, and 2) because the attached-*XY* is itself lethal, loss of the fragment chromosome from the stock is prevented.

Although we would expect half of the males bearing the fragment to be fertile, we in fact only see 3/20, a significant deviation from our expectations (x^2 = 9.8, 1d.f.). This may indicate that the small duplication does in fact affect fertility of the fragment bearing males or may reflect a difference in viability between the attached-*XY*/fragment males compared to *X*/fragment males. In

any event, we are able to recover viable fertile males, albeit at a slightly lesser frequency than anticipated, from a cross using an attached-*XY* and our new target.

Spiral mapping of bb^2

The rDNA array is genetically defined as the bobbed (*bb*) locus. Flies that do not produce adequate levels of rRNA are phenotypically "bobbed" (*bb*). Bobbed flies are slow to develop, have thin, short bristles and develop an abdominal cuticle that appears scratched or etched. In order to test the spiral mapping technique, we chose to map a particular bobbed allele, bb^2. The bb^2 allele has been used extensively in studies designed to determine both the conditions that induce changes in copy number and the mechanism of the change. Because one of the eventual purposes of establishing a spiral exchange mapping system is to examine how the position of molecular variants changes with changes in copy number, this allele seemed like an appropriate choice. To map bb^2 , we needed to replace the proximal NO of our $Tp(1:1)sc^{V2}$ target with bb^2 NO. The proximal end of each of the five $Tp(1:1)sc^{V2}$ chromosomes was replaced with bb^2. A schematic diagram of these crosses is shown in Figure 8. These new bb^2-bearing chromosomes are designated $Dp(1:1)sc^{V2}$.

The next step is to identify unique IGS variants in both ends of the bb^2 target, $Dp(1:1)sc^{V2}$ and $Dp(1:1)sc^{V2}bb^2$. This requires that the two arrays be isolated in rDNA$^-$ backgrounds. Figure 9a shows how the proximal bb^2 array and the distal *In(1)scV2*-derived array of $Dp(1:1)sc^{V2}$ were meiotically separated and Figure 9b shows the mating scheme for isolating the arrays in rDNA$^-$ backgrounds. One of the distal NO's, the distal NO from $Dp(1:1)sc^{V2}$ bb^2 1L, was bobbed lethal and therefore unusable. Distal arrays from the other four targets survived in otherwise rDNA$^-$ backgrounds. Genomic DNA was isolated from both proximal and distal ends, cut with *Hae*III, electrophoresed, blotted and screened for unique IGS variants (see Materials and Methods). Figure 10 is a Southern blot of the IGS variants in both the distal and proximal arrays of $Dp(1:1)sc^{V2}$ bb^2 3L, showing the unique bands in each end. The signal from probed membranes was stored on phosphor plates and scanned using the Molecular Dynamics

Figure 8 - Generating bb^2 targets

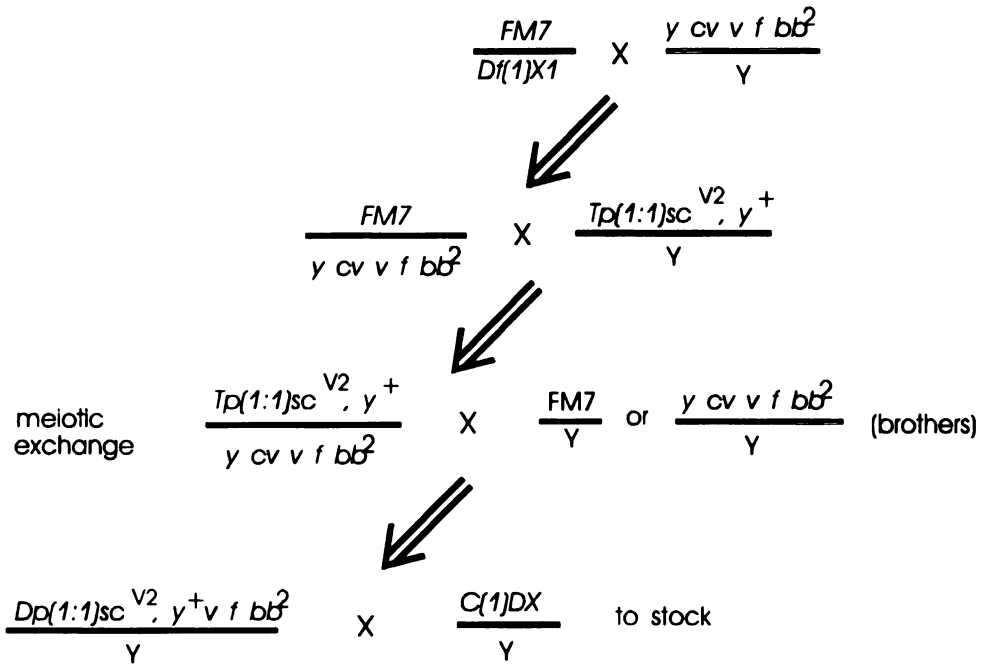

The mating scheme above shows how the bb^2 NO is crossed onto the *Tp(1:1)sc*^{V2}, *y*$^+$. The novel target chromosome, *Dp(1:1)sc*^{V2}, *y*$^+$ *v f bb*^{2},contains the distal array from *Tp(1:1)sc*^{V2}, and the proximal array from bb^2. Details are discussed in text.

Figure 9 - Separating the Proximal and Distal NO's of *Dp(1:1)sc^{V2}* and Isolating Proximal and Distal NO's in rDNA$^-$ backgrounds

A. We use *Df(1)X1* to separate the two NO's of *Dp(1:1)sc^{V2}*. This chromosome is deleted for approximately 80% of the proximal heterochromatin, including all of the rDNA , and is lethal when homozygous or hemizygous. Meiotic exchange between *Dp(1:1)sc^{V2}* and *Df(1)X1* generates two chromosomes, each with one of the NO's from *Dp(1:1)sc^{V2}*.

B. Both of the separated NO's can be placed in otherwise rDNA$^-$ backgrounds for further characterization. This is accomplished differently for the two stocks. 'Right' end stocks bearing the proximal NO can be stocked as males. These males can be mated to attached-*X/0* females and 'right' end chromosomes (in this case bearing the *bb^2* allele) can be recovered as *X/0* males. 'Left' end stocks cannot be maintained as males since they bear the *Df(1)X1* base. Left end females are mated to males that carry *In(1)sc^{4}sc^8* , a chromosome deficient for rDNA. Females that are genotypically *In(1)sc^{4}sc^8 /left end* are recovered for further analysis.

Figure 9a - Separating the proximal and distal NOs of *Dp(1:1)sc*^{V2}

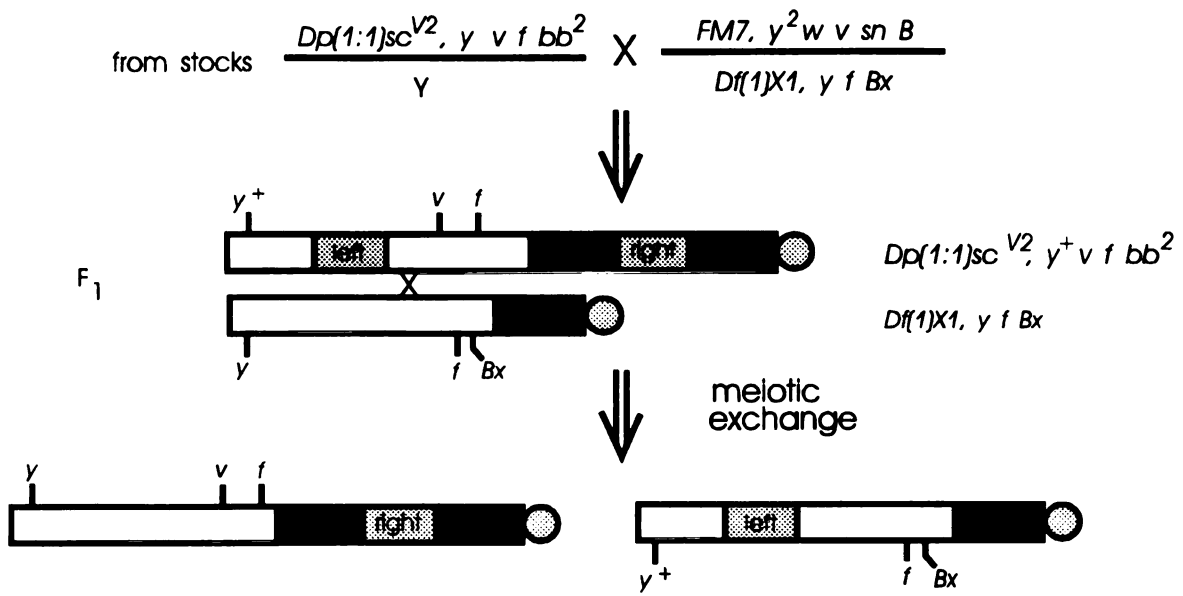

Figure 9b - Isolating the proximal and distal NOs of *Dp(1:1)sc* ^{V2} in rDNA$^-$ backgrounds

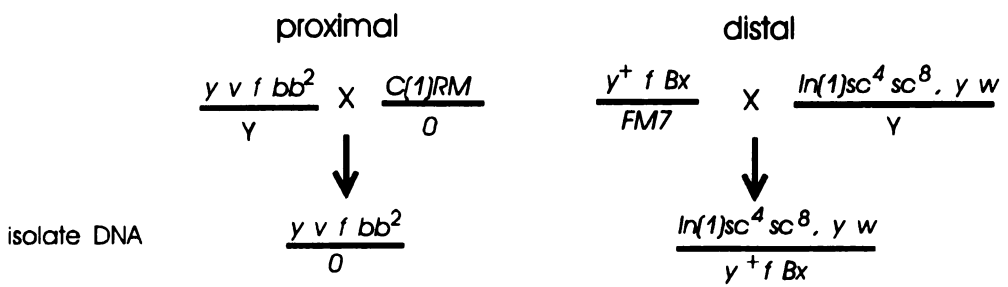

Figure 10 - Unique Bands in Proximal and Distal Arrays of *Dp(1:1)sc^{V2}, 3L bb^{2}R*

Southern blots of HaeIII digested genomic DNA from the flies bearing the proximal and distal arrays of *Dp(1:1)sc^{V2}, 3L bb^{2}R* were probed with ^{32}P-labeled IGS. Unique variants in the two ends are show as numbers (distal array) and letters (proximal array). Blots were scanned using a phosphorimager (see text for details) and bands were identified as peaks on an integration line graph.

Figure 10 - Unique Bands in Proximal and Distal Arrays of *Dp(1:1)sc*^{V2}

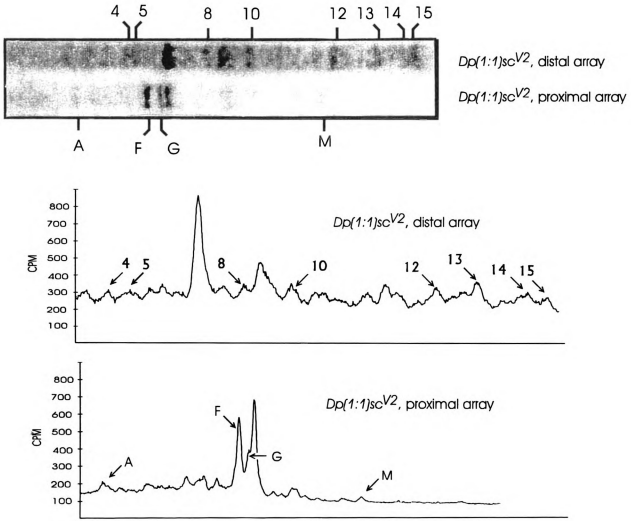

phosphorimager. Images were then analyzed with Imagequant software. Graphs in which each peak represents a particular band in a lane can be produced and these are shown in Figure 10.

In order to choose the most appropriate target, IGS variation from each of the four bobbed-viable left ends was compared to that of the proximal bb^2 NO. All four left ends had very similar IGS variants. There are multiple, clearly recognizable differences between the variants in the left end arrays and the bb^2 , right end variants.

In addition, bobbed penetrance of each of the four ends was measured (data not shown) under the assumption that the least bobbed left end would be least likely to produce bobbed spiral products that may themselves be difficult to isolate. Based on this criterion, *Dp(1:1)sc*^{V2}*bb*^{2}*, 3L* was chosen as the target for mapping bb^2.

Next, ten spiral exchange fragment chromosomes were generated and stocked from the *Dp(1:1)sc*^{V2}*bb*^{2}*, 3L* target . Genomic DNA was isolated from flies containing the spiral exchange fragment chromosomes/*C(1)DX* . *C(1)DX* is completely rDNA deficient, so that the only source of rDNA in these flies came from the recombinant fragment chromosome. Genomic DNA from each of these samples and the distal and proximal NO's of the parental *Dp(1:1)sc*^{V2}*bb*^{2}*, 3L* target were digested with *Hae*III. The cut DNA was then electrophoresed, blotted and probed with an IGS specific probe, DmHH102. Unique variants of the distal and proximal arrays of *Dp(1:1)sc*^{V2}*bb*^{2}*, 3L* in the ten spiral exchange chromosomes were first identified by inspection of autoradiograms or phosphor image figures of the blots. The unique bands were then matched with the equivalent bands on the computer image. The number of counts in each band is calculated using an integration technique that averages the counts/pixel across the length of the band for each ordinate pixel position. These values are then plotted against the ordinate values to generate a line graph of the counts along the length of an array, with peaks in the line graph representing bands in the autoradiogram (Fig. 10).

Once the unique bands are positionally defined for each of the two ends, the bands are scored as present or absent in each of the spiral exchange arrays. Figure 11 shows the bands from

Presence/Absence of Unique Variants Among Spiral Exchange Chromosomes

	Unique Variants											
Chromosome	**Distal Array**								**Proximal Array**			
	4	**5**	**8**	**10**	**12**	**13**	**14**	**15**	**A**	**F**	**G**	**M**
spiral 1	-	-	-	-	-	+	-	-	+	+	+	-
spiral 2	+	+	+	+	+	+	+	+	-	-	-	-
spiral 4	-	-	-	+	+	+	+	+	+	+	+	+
spiral 5	+	-	-	+	+	+	+	+	+	+	+	+
spiral 6	-	-	-	+	-	+	+	+	-	+	+	-
spiral 7	+	+	+	+	+	+	+	+	-	+	-	-
spiral 9	-	-	-	-	-	-	-	-	-	+	-	-
spiral 10	-	-	-	-	-	-	-	-	+	+	+	-
spiral 12	+	-	-	+	+	+	+	+	+	+	+	+
spiral 13	+	-	+	+	+	+	+	+	+	+	+	+

Figure 11 - The unique variants from the distal array are numbered and the unique variants from the proximal array are lettered. A (+) indicates the presence of the variant in the spiral exchange fragment chromosome. A (-) indicates that the variant is absent. Numbers are non-sequential because only unique bands are shown while all bands were scored. Similarly, lettered variants that are present in both arrays are not shown in the table.

each of the two ends of *Dp(1:1)sc*^{V2}*bb*^{2}, *3L* that are present or absent in each of the spiral exchange arrays.

As in spontaneous mapping, exchange positions in the two NO's are ordered on the basis of presence or absence of unique variants, and then the limit of each variant is defined in terms of the positions of these exchange points. Unlike either spontaneous exchanges, where we can recover both of recombinant arrays that bear one or the other parental centromere (designated as y^{+} or y in Fig. 3), or hairpin exchanges, where we can recover the reciprocal products of each exchange event, *Rex*-induced spiral exchanges only allow us to examine one of the reciprocal classes of recombinant arrays. The other recombinant array is lost because it is part of an acentric circular piece of DNA. Nevertheless, we can still map the proximal limits of the proximal array and the distal limits of the distal array with just presence/absence data. Moreover, using quantitative information, we can also locate the distal limit of the proximal array variants and the proximal limits of the distal array variants. These limits are found by determining the exchange points beyond which there is no increase in the number of copies of a particular variant. Again, the best way to explain the technique is with a simplified example, in this case, shown in Figure 12. A map of the variant limits is shown in Figure 13.

For simplicity, let us consider mapping the limits of just three unique variants in just one of the two arrays on our target chromosome, the proximal array. We will show how both presence and absence information in conjunction with quantitative data can be used to generate maps. The three variants are represented by squares, circles and triangles. In this example, we can order the exchange points unambiguously based on presence and absence data only. Exchange 1 contains only one variant and is therefore the most proximal exchange. Exchange 2 contains two variants and is therefore distal to exchange 1 and proximal to exchange 3 which contains all three types of variants.

By examination of quantitative data, we can determine distal limits. Although all three exchanges have the square variant, there is no measurable increase in copy number as we move distally from exchange 1 to exchange 3. This implies that all copies of the square variant are

Figure 12 - Spiral exchange mapping

The target chromosome has two rDNA arrays, shown as shaded boxes in the diagram. Euchromatin is shown as a curved line extending between the two arrays. The centromere is shown as a circle attached to the darker array. For the sake of simplicity, none of the heterochromatin that normally flanks the arrays is shown in the diagram. Three independent points of exchange and the fragment chromosomes that each exchange generates are shown. The unique variants in just one of the two arrays are shown as triangles, squares or circles. The presence of a particular variant in a recombinant array is indicated by a '+' in the presence/absence table. In addition, whether or not a recombinant chromosome contains all of the copies of a particular variant, as measured by quantitative southern blot analysis (see text), is indicated in the variant copy limit table. Here, a '+' indicates that there are the same number of copies of that particular variant in the recombinant array as there were present in the parental array, implying that we have reached the distal limit of that variant.

Figure 12- Spiral Exchange Mapping

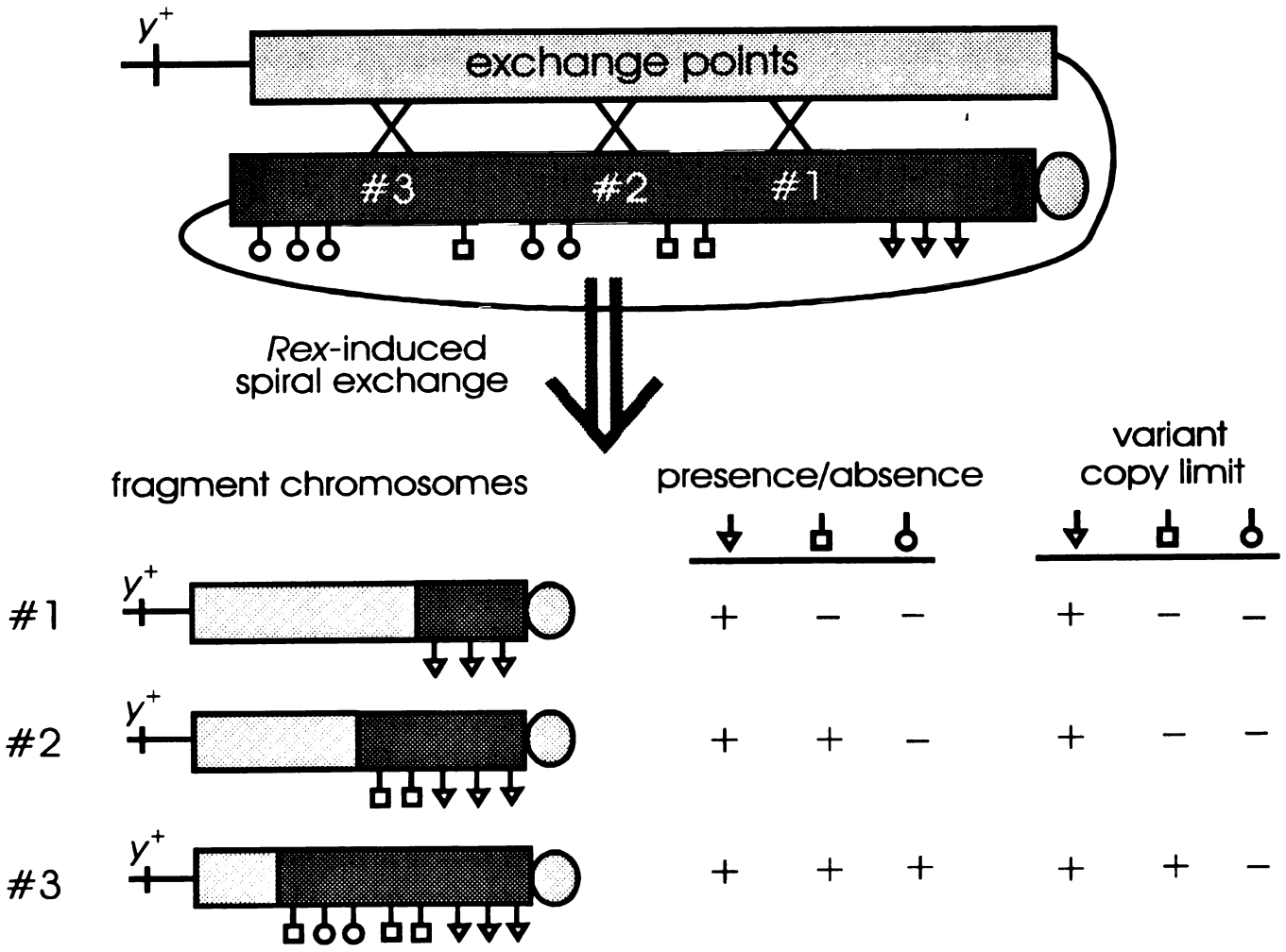

A Molecular Variant Map Generated From Spiral Exchanges

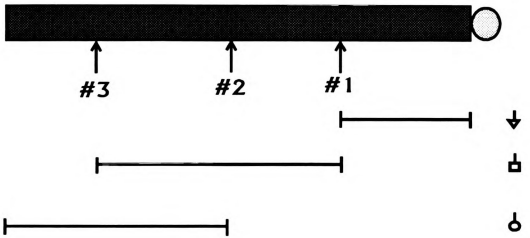

Figure 13- The relative positions of the unique variants in the proximal array of the target chromosomes are shown. The positions of three independent exchanges #1, #2 and #3 are indicated by arrows below the array. The positions of the three unique variants, shown as circles, squares and triangles, are defined with respect to the points of exchange (see text). The triangle variant does not extend beyond the first exchange point. Similarly, the square variant does not extend beyond the third exchange point. However, the square variant does not extend proximally (towards the centromere), beyond the first exchange point. Therefore, the position of the square variant is delimited by exchange point #1 and exchange point #2, as indicated by the line below the array.

proximal to exchange 1. Thus, exchange 1 defines the distal limit of the square type variant. Similarly, the triangular variant does not increase in copy number from exchange 2 to exchange 3, implying that there are no more copies of this variant distal to exchange 2. Finally, the copy number of the circle variant in the proximal array is the same as the number of the circle variant in the exchange 3 fragment chromosome. Thus, there are no copies of this particular variant distal to exchange 3. We now have all the information necessary to complete our map. The triangular variant extends from the centromere to exchange point #1. The square variant extends between exchange 2 and 3, and the circular variant runs from exchange point #2 to the distal end of the array.

The same procedure is followed for experimentally generated data. First, consider ordering the exchange points in the bb^2 end of the target chromosome based on the presence /absence data previously presented in Figure 11. There is one spiral exchange array, spiral 2, that does not contain any of the variants from the bb^2 array. Therefore, the exchange that generated this array must have been the most proximal of all the exchanges in the bb^2 NO. Next, we find that spiral exchange array 7 and spiral exchange 9 both have just one type of IGS variant from the bb^2 NO. The exchanges that generated these fragment chromosome must have occurred distal to the exchange that generated spiral 2, but proximal to all other exchanges. Continuing in a like manner for all the remaining spiral arrays we find that spiral 6 has two bb^2 variants and is therefore distal to spiral 2, spiral 7 and spiral 9. Spirals 1 and 10 each have three bb^2 variants and are inseparable based on presence/absence data alone, but both are distal to the three other exchanges. Finally, spirals 4, 5, 12, and 13 each contain at least one copy of each of the unique bb^2 variants and are therefore the most distal exchanges. We can now construct a partial genetic map based on presence/absence data alone. The exchange points are placed at arbitrarily equidistant positions along the length of an array. The proximal limit of a variant is then defined as the most proximal exchange point that does not carry that variant. For instance, spiral exchanges 7 and 9 do not contain variant type A. Furthermore, spiral exchanges 7 and 9 are the proximal most exchanges that do not contain this variant. Therefore, variant type A cannot extend

proximally beyond the spiral 7/spiral 9 exchange point. This defines the proximal limit of variant A. The map of the proximal limits of each unique variant is shown in Figure 14.

Defining the distal limit of unique variants in the bb^2 end of $Dp(1:1)sc^{V2}$, *3A* involves calculating the number of copies of each of the variants instead of just using presence/absence data. The distal limit of a variant type is defined as the exchange point after which there is no further increase in the number of copies of that variant. Provided that we have not reached the distal limit of a particular variant type, the number of copies of that variant should be greater in fragment chromosomes generated from more distal exchanges. How do we determine the copy number of a particular variant in a given array? First, we calculate the number of copies of each variant type in our right end, bb^2 array. If we assume the imager is able to detect single copy variants and that the lightest band in the bb^2 blot is a single copy variant, we can divide the number of counts in each peak in the integration curve by this single copy number value to arrive at an estimate of the total copy number of each variant in a particular array. Based on this procedure we should arrive at a value for the total number of repeats in an array. The bb^2 array contains approximately 120 copies (Lindsley and Zimm, 1987). By using the lightest band estimate as an estimate of a single copy variant, values for the total copy number of bb^2 of between 90-130 were found for several blots of bb^2 DNA.

Because the hybridization kinetics of membrane-bound sequences with homologous sequences in solution may not necessarily be first order, high copy number variants may be underestimated. Therefore, there is an adjustment factor that needs to be considered before a final determination of copy number can be made. The kinetic adjustment factor for a particular blot may be determined by finding an exponent such that when the calculated copy number of each variant in the bb^2 lane is raised to this value, the sum of all copies equals the total number of variants in bb^2, or 120.

Having calculated a kinetic factor for each blot based on the bb^2 adjustment, to find the copy number of the variants in a recombinant array, we first find the smallest peak in that lane. We define this peak as representing a single copy. We then divide all other peak values in the lane

Figure 14 - Proximal Limits of Unique Variants in bb^2

From the presence absence data collected from the *Rex*-induced spiral exchanges, we can determine the proximal limits of the unique variants in the bb^2 array. The different IGS variants are represented by letters. For instance, the 'F' variant does not extend proximally beyond the proximal-most exchange point, exchange #2. From the presence/absence data alone, we cannot determine how far the variants extend distally (see text). This uncertainty is represented by the dashed line next to the variant.

Figure 14 - Proximal Limits of Unique Variants in *bb*^{2}

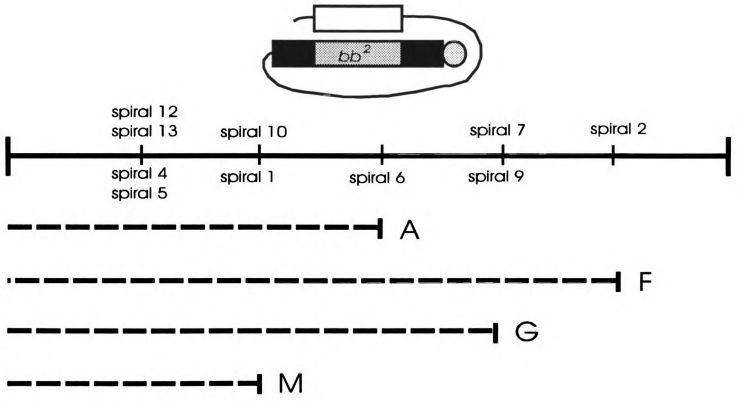

by the single copy peak value. Finally, we apply the same kinetic factors that give a value of 120 copies for the total copy number in the bb^2 lane to each of the bands in the recombinant lanes.

Because of the errors that are inherent in estimates of copy number, it is very difficult to detect changes from recombinant to recombinant of variants with a copy number of less than five. For this reason, we will only consider copy number data from unique variants that have more than five copies in the parental array. The copy numbers for those variants that have greater than five copies according to our estimates are shown in Table 4.

Once the copy number for each unique variant is determined in each of the recombinants, the distal limit of a variant is then defined as the exchange point after which there is no increase in that variant's copy number. For instance, consider the copies of variant F as we move distally along the array. The proximal most exchange, exchange 2, produces a spiral exchange fragment chromosome that has no copies of variant F. The next two exchange points, exchange 7 and 9 have 5.9-10.0 and 10.1-16.0 copies of variant F, respectively. The copy number in the right end parental array is 19.6-32.3. Therefore, we have not reached the distal limit of variant F at either of these exchange points. Moreover, this places exchange 9 distal to exchange 7. Looking at the next distal most exchange point, exchange point 6, we see that the copy number range of variant F in the recombinant generated from this exchange is 15.1-23.8. Here, the upper value of the range falls within the range of parental values and so it is possible that we have reached the limit of variant F at exchange point 6. Certainly by exchange points 1 and 10 we have reached the variant limit. This imprecision in finding distal limits is indicated by a dashed line on the variant map. We know that there are certainly copies of variant F between exchange points 7 and 9 and exchange point 6 as indicated by the solid line on our map. There may be additional copies between exchange point 6 and exchange points 1/10. consequently, the map shows a dashed line between these two exchange points. At exchange point 1/10 we have reached the distal limit of variant F since no further increases in copy number are found in the four remaining recombinant chromosomes. For low copy number variants, like variant M, we can define the proximal limit based on presence/absence data, but the distal limit remains undefined and is shown as a dashed line from

array	COPY NUMBER OF UNIQUE IGS VARIANTS						
	proximal array variants				distal array variants		
	4	5	12	13	A	F	G
proximal array					11.6 ± 3.0	25.9 ± 8.9	8.1 ± 1.8
distal array	9.2 ± 2.1	12.2 ± 3.3	6.3 ± 1.2	6.5 ± 1.3			
Spiral 1	absent	absent	absent	2.5 ± 0.3	6.6 ± 1.5	41.2 ± 8.5	17.2 ± 2.6
Spiral 2	10.1 ± 4.3	6.6 ± 2.2	4.7 ± 1.2	9.5 ± 3.8	absent	absent	absent
Spiral 4	absent	absent	4.0 ± 0.6	4.6 ± 0.7	2.4 ± 0.2	14.3 ± 4.0	3.8 ± 0.5
Spiral 5	4.1 ± 1.0	absent	3.3 ± 0.7	4.7 ± 1.2	4.6 ± 1.2	20.2 ± 10.4	7.5 ± 2.6
Spiral 6	absent	absent	absent	absent	absent	19.4 ± 6.1	5.9 ± 1.1
Spiral 7	6.9 ± 2.4	4.6 ± 1.6	5.8 ± 1.9	3.3 ± 0.7	absent	7.9 ± 2.8	absent
Spiral 9	absent	absent	absent	absent	absent	13.0 ± 4.1	absent
Spiral 10	absent	absent	absent	absent	5.1 ± 0.9	15.3 ± 4.4	7.8 ± 1.7
Spiral 12	4.3 ± 0.7	absent	3.6 ± 0.4	5.1 ± 0.9	3.3 ± 0.4	22.5 ± 7.2	6.7 ± 1.3
Spiral 13	12.0 ± 3.1	absent	4.9 ± 0.9	5.3 ± 1.2	7.4 ± 2.6	30.7 ± 17.8	3.9 ± 1.1

Table 4.
The estimated copy number of unique intergenic spacer length variants of parental and recombinant arrays *Dp(1:1)sc^{v2}*, 3aL *bb^{2}* R are shown. The recombinant arrays, labeled here as 'spirals', were generated from *Rex*-induced spiral exchange (see text). Originally, thirteen spiral exchange recombinant fragment chromosomes were recovered. Only the ten shown here survived and were not bobbed lethal in otherwise rDNA deficient backgrounds. Copy number estimation is described in the text.

the proximal limit to the end of the array. The complete spiral exchange variant maps for both the distal and proximal ends of *Dp(1:1)sc*^{V2}*,3A* are shown in Figures 15 and 16, respectively.

Figure 15 - Spiral Exchange Map of Distal NO of *Dp(1:1)sc^{V2}*

The limits of all unique variants identified in the distal NO of *Dp(1:1)sc^{V2}* are shown with respect to the positions of exchange points. Dashed lines indicate undefinable limits. In the distal NO, the proximal limit of low copy number variants is not defined (see text).

Figure 16 - Spiral Exchange Map of Proximal NO of *Dp(1:1)sc^{V2}*

The limits of all unique variants identified in the proximal NO of *Dp(1:1)sc^{V2}* are shown with respect to the positions of exchange points. Dashed lines indicate undefinable limits. In the proximal NO, the distal limit of low copy number variants is not defined (see text).

Figure 15 - Spiral Exchange Map of the Proximal NO of *Dp(1:1)sc*^{V2}, 3a*Lbb*^{2}R

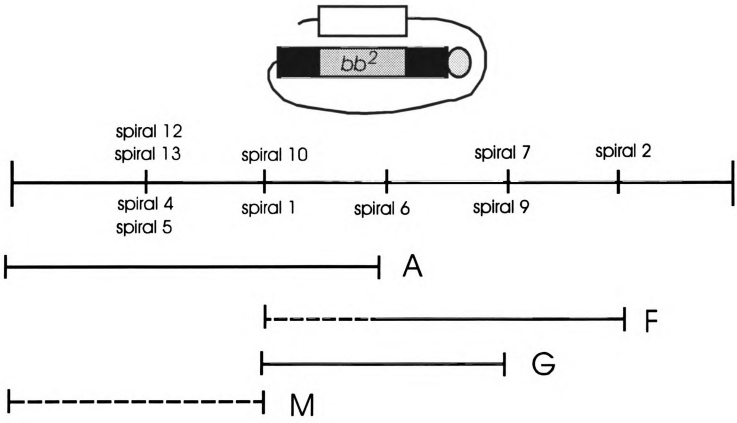

Figure 16 - Spiral Exchange Map of the Distal NO of *Dp(1:1)sc*^{V2}, 3a*Lbb*^{2}R

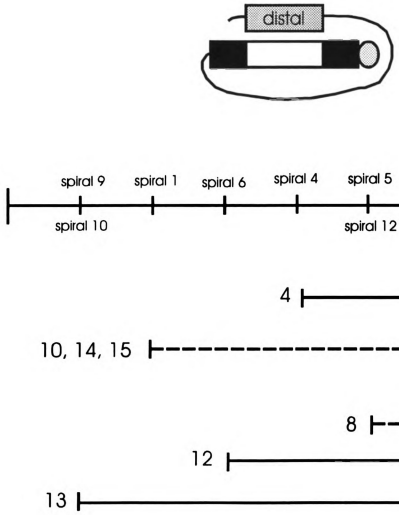

Discussion

Genetic maps of euchromatic regions have not only provided a basis for our current understanding of the structure of euchromatin, they have proven to be invaluable sources of information on tasks as mundane as stock keeping and processes as magical as cloning a gene. The power of high resolution genetic maps is illustrated over and over again by researchers working with organisms even distantly related to the fruit fly, such as a mosquito, for which there are only crude genetic maps or no maps at all. These researchers will often turn to the fly, a completely unfamiliar organism, clone the gene of interest from it, and then use the Drosophila gene as a heterologous probe to fish out the gene from their organism. They are able to do this, in large part, because of the existence of genetic maps.

There are two basic requirements for making a genetic map. First, there must be some detectable source of variation. This could either be a phenotype that one can see, like a difference in eye color or wing shape or a molecular difference like a RFLP. Second, mapping requires recombination. Mapping in the heterochromatin has been stymied both because of its repetitive nature, making the identification of variation difficult, and because there is very little recombination between heterochromatic regions. One of the main focuses of this thesis work was to develop a more efficient way of generating genetic maps of a particular heterochromatic region, the ribosomal DNA array. The mapping protocol that we have developed during the course of this study is, in terms of its requirements, no different from any other mapping technique. We use the highly polymorphic intergenic spacer region as a source of heterogeneity and we use *Rex* as a means of generating recombination.

The development of a mapping protocol based on spiral exchanges required a number of genetic components that were unique. First, a novel target chromosome had to be constructed. Previous mapping techniques relied either on spontaneous exchange or on *Rex*-induced hairpin exchanges in which there is no chromosomal loss. In order for spiral exchange mapping to be feasible, the new target had to be noninverted, in order to ensure that arrays of interest can be easily crossed onto the target, and it had to produce spiral exchange fragment chromosome that

could be stocked for further analysis. *Rex*-induced hairpin exchange of $In(1)sc^{V2}$ generated a series of five potential targets that met the two criteria. Second, because spiral exchange in the new target produces a fragment *X*-chromosome, *X*/fragment males resulting from a spiral event would not be fertile. Consequently, it was necessary to set up matings in which the female, *Rex*-bearing fly also carried an attached-*XY* chromosome. This ensures that half of the spiral exchange progeny will carry an attached-*XY* chromosome in addition to the fragment chromosome and therefore be recoverable as fertile males. Of course the use of the attached-*XY* in the female introduces one additional complication because many naturally occurring chromosomes carry suppressors of *Rex* (Boussaha, 1993). Thus, we had to find a suppressor-free attached-*XY*. Finally, a special chromosomes, an attached-*XY* with a deficiency and an attached-*X*, must be used in order to establish stocks that will stably maintain the fragment chromosomes.

In order to demonstrate the efficacy of the spiral mapping system, we have mapped two arrays, the bb^2 array, and the distal, sc^{V2} -derived, array of the target chromosome. The development of a spiral mapping technique is significant because it greatly enhances our ability to construct variant maps of rDNA arrays. Previous techniques relying either on spontaneous exchange or on *Rex*-induced hairpin exchange required intensive work to identify crossovers. *Rex*-induced spiral exchanges are easily identified. The labor demands for constructing a map are reduced from approximately two years of labor to two months for a single individual. Since the resolution of the map is dependent on the number of crossovers that are recovered, we are now in a position to map arrays to a high resolution or to map a larger sample of arrays than previously feasible.

There are still a number of technical difficulties in assessing the copy number of variants. However, even without this information, proximal limits of proximal variants and distal limits of distal variants can still be mapped. Even the high resolution single-ended maps generated from presence and absence data alone could potentially be used to address mechanistic questions. For example, we can now examine how changes in copy number of an array affect the positions of the variants relative to one another. Are particular regions amplified and then inserted somewhere in

an array or do the variants retain a constant relationship relative to one another as would be expected if copy number changes were the result of sister chromatid exchange.

Chapter 3

FURTHER EXAMINATION OF THE *Rex* TARGET SITE

Introduction

Prior to this study, the site of *Rex*-induced exchange had been mapped to the rDNA (Swanson, 1984). Those results did not tell us, however, if there are specific regions or sequences within the rDNA that *Rex* recognizes. We have taken a genetic approach in attempting to further define the target for *Rex*-induced exchange. We measured the *Rex* spiral exchange frequency, or *Rex* sensitivity, in twenty-one newly constructed target chromosomes that differ in both the amount and composition of rDNA repeat units that they contain. As detailed later, all of the twenty-one target chromosomes were constructed by combining distal and proximal recombinant arrays generated from *Rex*-induced hairpin exchange of the same parental $In(1)w^{m5}1bL_{w}m4R$ chromosome. The arrays prove to have significantly different sensitivities to *Rex*.

We also measured the total number of rDNA gene copies, the number of un-interrupted, presumably active copies, and phenotypically assessed the functional activity of each array. By un-interrupted, we mean repeating units that do not have retroviral-like elements inserted into the coding region of the 28S rRNA subunit. For reasons discussed later, the repeat units that do not contain insertion sequences are presumed to be transcriptionally active while those that do contain insertion sequences are thought to be transcriptionally silent. We compared the frequency of *Rex* sensitivity of the different arrays with our measures of absolute and active gene copy number, and with our phenotypic assessment of functional activity. We performed two different statistical analyses to look for correlations between *Rex*-induced spiral exchange frequencies and our various measurements. For the molecular measurements of total gene copy number and of active and inactive copy number, we used standard regression analyses. Because our phenotypic assessment

of functional activity was based on discrete data, we were able to do likelihood analyses and G-tests. Despite significant variation in Rex sensitivity, there is no correlation of sensitivity to any of these measures. Hence, sensitivity is not simply a quantitative property of the number of repeats or the number of active or inactive repeats.

Using a G-test, we have also shown that there are two distinct groups of arrays, high and low sensitivity groups, and used *Rex*-induced hairpin exchange mapping to construct an intergenic spacer (IGS) variant map of the two arrays in the parental $In(1)w^{m51Lb}{}_{w}{}^{m4}$ chromosome. The IGS map was used to attempt to localize a single region of high sensitivity. We have instead found that there is no single discrete highly-sensitive segment within the parental arrays.

Novel target chromosome construction

Two groups of novel target chromosomes were constructed for this study. Each group contains eleven chromosomes. Among the chromosomes of each group, only one of the two rDNA arrays differs . The members of one group have an identical proximal array but differ in the distal arrays, while the members of the other group have identical distal arrays but different proximal ones.

We had previously constructed eleven *Rex*-induced hairpin exchange chromosomes from $In(1)w^{m51bL}{}_{w}{}^{m4R}$ (Robbins and Swanson, 1982). Each of these eleven chromosomes contains recombinant proximal and distal arrays. Because the position of the exchange event within the two blocks of rDNA was different in each case, each of the eleven hairpin exchange chromosomes thus contains two different arrays, each with different segments of the two parental arrays. The mating scheme for generating the original hairpin exchange chromosomes is shown in Figure 17.

From these eleven original chromosomes we constructed twenty-one new combinations as diagrammed in Figure 18. Two arrays, the distal array from hairpin exchange #7 (7 left) and the

Figure 17 - *Rex*-induced Hairpin Exchanges of *In(1)w^{m51bL}w^{m4R}*

To illustrate the potential variability among *Rex*-induced recombinant arrays arising from *In(1)w^{m51bL}w^{m4R}* , two independent *Rex*-induced hairpin exchanges are shown. The proximal and distal arrays in *In(1)w^{m51bL}w^{m4R}* are shown as red and green blocks, respectively. The first exchange yields a product that carries only a small fraction of both parental arrays in the proximal recombinant NO and a large fraction of both parental arrays in the distal NO. The second exchange yields a large proximal and small distal array. As shown, *Rex*-induced hairpin exchange inverts all of the material between the exchange points. Because the original target chromosome is inverted, the products are normal.

Figure 17 - *Rex*-induced hairpin exchanges of $In(1)w^{m51Lb}{}_{w}{}^{m4R}$

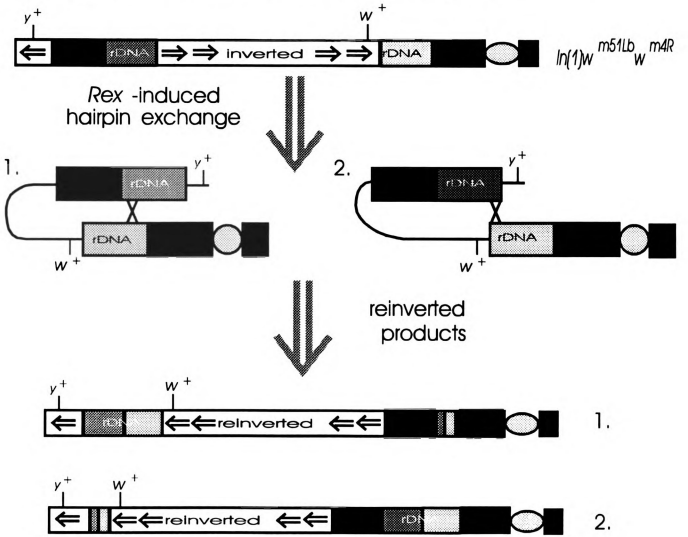

Figure 18 - Constructing Recombinant Chromosomes with 7 left and 5 right

A. Meiotic exchange between a chromosome bearing a left end recombinant array with one bearing a right end recombinant array gives rise to a new combination. Left end arrays were all combined with 5 right, while right end arrays were all combined with 7 left.

B. Mating scheme for generating new combinations. The left end arrays are stocked as females, because chromosomes bearing the left ends also carry the Df(1)X1 base. These females are mated to right end bearing males. Wild-type recombinants generated from meiotic exchange between the left and right end bearing chromosomes contain both left and right arrays.

Figure 18- Constructing Recombinant Chromosomes with 7 left and 5 right

A. chromosomes

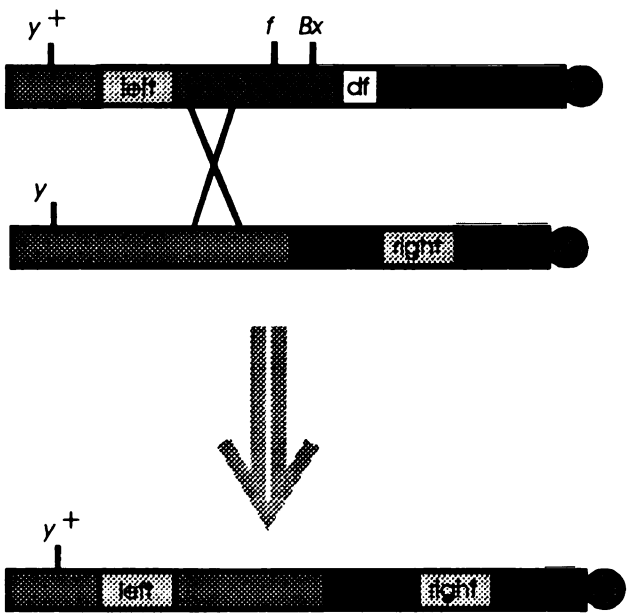

B. mating scheme

$$\frac{y \text{ left array, } f \text{ } Bx}{FM7} \times \frac{y, \text{ right array}}{Y}$$

$$\frac{y \text{ left array, } f \text{ } Bx}{y, \text{ right array}} \times \frac{FM7}{Y}$$

$$\frac{\text{left array + right array}}{Y} \quad \text{stock}$$

proximal array from hairpin exchange #5 (5 right) were chosen as the constant arrays for the two groups. All of the proximal arrays from the original eleven hairpins were recombined with a single distal array, 7 Left, and each of the distal arrays from the hairpins were recombined with a single proximal array, 5 Right. By constructing new targets that held either the proximal or distal array constant, we were able to assess differences in sensitivity to *Rex* in individual arrays.

Five right and 7 left are the two most bobbed arrays in the original set, (both by genetic and molecular measurements) and as such, presumably had the fewest active repeat units. By combining these two most-bobbed arrays with all the other arrays we had the greatest chance of uncovering differences in sensitivity. Whether all copies are sensitive, or only some regions contain *Rex*-sensitive copies, starting with a full-size array would be likely to hide the differences.

Materials and Methods

Hairpin exchange mapping

In an attempt to define *Rex*-sensitive regions of the two arrays of $In(1)w^{m51}bL_{w}^{m4}R$, we used *Rex*-induced hairpin exchanges to generate IGS variant maps. We then looked for cosegregation of regions of the map with high sensitivity to *Rex*.

Rex-induced hairpin exchanges have been used previously to map two functional elements within an array, *Rex* itself, and a dominant suppressor of *Rex*, *Su*(*Rex*), (Rasooly and Robbins, 1989). The strategy for constructing IGS variant maps using hairpin exchanges is very similar to that already discussed for mapping using spontaneous exchange (see Fig. 3). There are, however, several significant differences. Unlike spontaneous mapping, where the two arrays are on homologous chromosomes, hairpin exchanges are exchanges between two arrays on the same target chromosome. The entire chromosome, carrying both recombinant arrays is recovered. Because all products of the exchange are recovered, amounting to the equivalent of a complete tetrad, Rex-

induced hairpin exchanges have been instrumental in addressing questions about the mechanism of *Rex*-induced exchange (Rasooly and Robbins, 1989). For instance, hairpin exchange has been used to show that *Rex*-induced exchanges can be explained by simple single exchange events that are sometimes accompanied by deletions at the site of exchange (Rasooly and Robbins, 1989).

The major differences in methodology are pointed out in the following four-step hairpin mapping procedure;

1) **Identify unique IGS variants in the array(s) to be mapped.** In the spontaneous example, this is accomplished by separately placing the two arrays in rDNA$^-$ backgrounds. In order to identify unique variants in arrays on the same chromosome, however, the variants must first be meiotically separated from one another. Then the separated arrays can be placed in an rDNA$^-$ background and variants identified by Southern blotting.

2) **Recover recombinants.** Closely linked outside markers were used as a means of identifying spontaneous crossovers. There is no direct phenotypic assay for *Rex*-induced hairpin exchange. Hairpin exchange results in inversion of all of the material between the points of exchange. Therefore, if the original target chromosome were inverted, a *Rex*-induced hairpin would result in a normal sequence chromosome that can recombine freely with other normal sequence chromosomes. In order to recover recombinants, a second generation must be examined in order to determine whether or not the gene order has been reversed. Figure 19 illustrates the steps in identifying hairpin recombinants.

3) **Order the exchange points.** The procedure for ordering the exchange points is essentially identical to that discussed for spontaneous mapping. However, we have additional information

because we recover both reciprocal products of each exchange event. We can determine if, for instance, there has been a deletion at the site of exchange or if the exchange was unequal. A simplified example of the methodology used to generate an IGS map using *Rex*-induced hairpin exchanges is presented in Figures 20 and 21. In these figures, the two arrays are shown as shaded boxes. The darker array is referred to as the centromeric array and the lighter array is the telomeric array. Unique variants are shown as shaded circles (centromeric array) or shaded squares (telomeric array). For simplicity, we will map three variants, black, gray and white in the arrays.

Because we recover both products of the same exchange event, we are able to more clearly define the points of exchange than we are in the spontaneous case. For example, if two spontaneous recombinant centromeric arrays carried all the same unique centromeric variants, then the exchange points would be inseparable. In the case of hairpin mapping, however, we may be able to differentiate between two exchange points that carry the same centromeric variants. If, for example, the telomeric arrays produced from the exchanges mentioned above were different, the exchange that results in a recombinant telomeric array that carries more centromeric array variants occurred more proximally. In order to see this more clearly, refer to Figure 20. We recover two recombinant centromeric NO's from exchanges 2 and 3 that have the same centromeric variants. The position of the exchanges are indistinguishable based on these data alone. However, we see that the telomeric recombinant from exchange #2 has more centromeric variants compared to the telomeric recombinant array generated from exchange #3. Therefore, the order of the exchanges with the centromeric array was centromere - exchange #2 - exchange 3.

4) **Define the proximal and distal limits of each variant.** The procedure for defining variant limits in hairpin maps is exactly the same as that in spontaneous maps. Referring again to Figures 20 and 21, the proximal limit of a variant in the centromeric array is defined as the distal- most

Figure 19 - Identifying Hairpin Exchanges

Rex-induced hairpin exchange does not result in an immediately detectable phenotype. However, the target chromosome is inverted by the exchange. If the target chromosome is inverted to begin with, as is shown in this figure, then the hairpin exchange will reinvert the chromosome to its normal order. If the target chromosome had been normally ordered then a hairpin exchange would generate an inverted chromosome. By testing the frequency of recombination with a normal sequence chromosome, we can determine whether or not the target has undergone a *Rex*-induced hairpin. In this figure, because the target is inverted, those females in which a *Rex*-induced hairpin exchange occurred during the first mitotic division will not suppress recombination with a normal sequence chromosome.

Figure 19 - Identifying Hairpin Exchanges

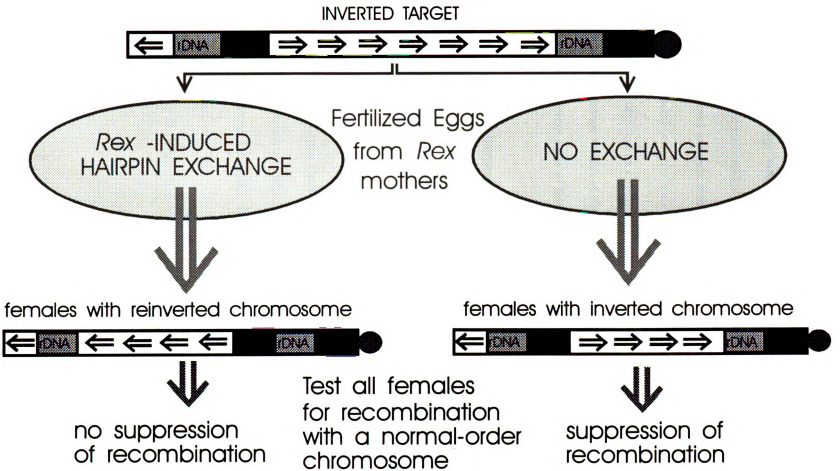

Figure 20 - Rex-induced Hairpin Exchange Mapping

Three chromosomes that result from *Rex*-induced hairpin exchange are shown. The positions of the exchange points in the parental arrays are indicated. The two parental arrays of the target chromosome are shown as lightly-shaded (centromeric) and darkly shaded (telomeric). Unique variants in the centromeric array are depicted as circles and those in the telomeric array are shown as squares. Rex-induced hairpin exchange results in chromosomes whose centromeric and telomeric arrays are comprised of different parts of the two parental arrays.

Figure 21 - Presence/Absence Data for Hairpin Exchange Mapping

After the two recombinant arrays are separated (see text) they are scored for the presence or absence of unique centromeric and telomeric IGS variants, a "+" indicates presence and a "-" indicates absence.

Figure 22 - IGS Variant Map From Hairpin Exchanges

The relative positions of the exchange points are determined using the presence/absence of unique parental variants in the recombinant arrays (see text). Once the relative exchange points are determined, the variants are placed relative to these exchange points. The map shows how far a variant extends proximally and distally in the parental array relative to the exchange points.

Figure 20 - *Rex*-Induced Hairpin Exchange Mapping

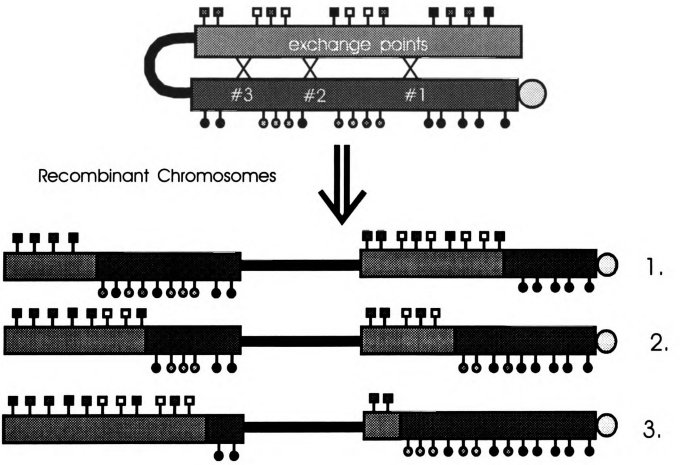

Figure 21 - Presence/Absence Data for Hairpin Exchange Mapping

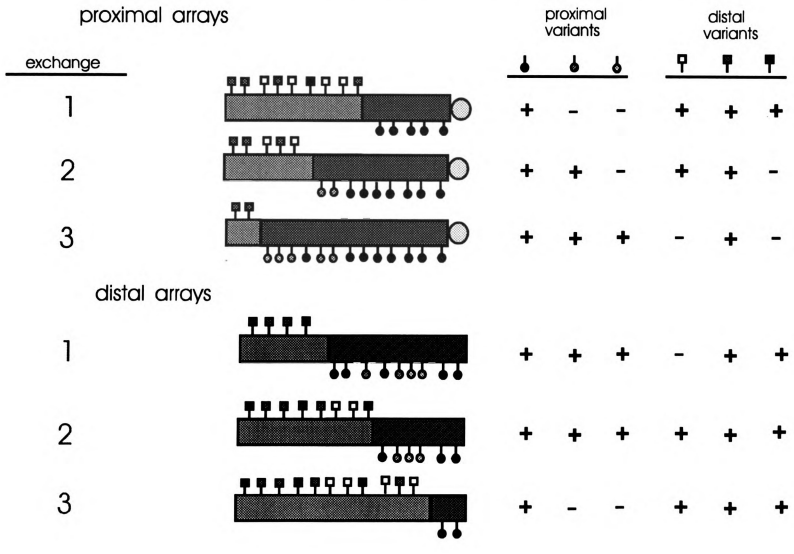

Figure 22 - IGS Variant Map From Hairpin Exchanges

A. Proximal Array

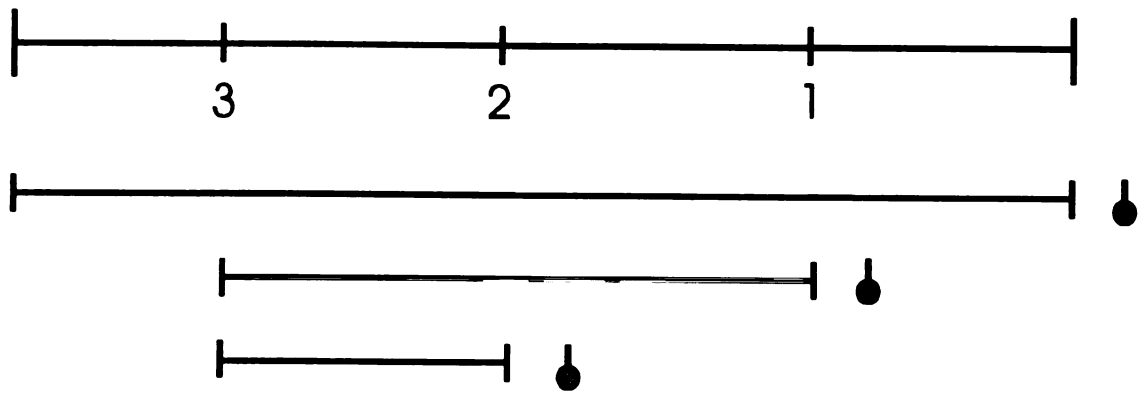

B. Distal Array

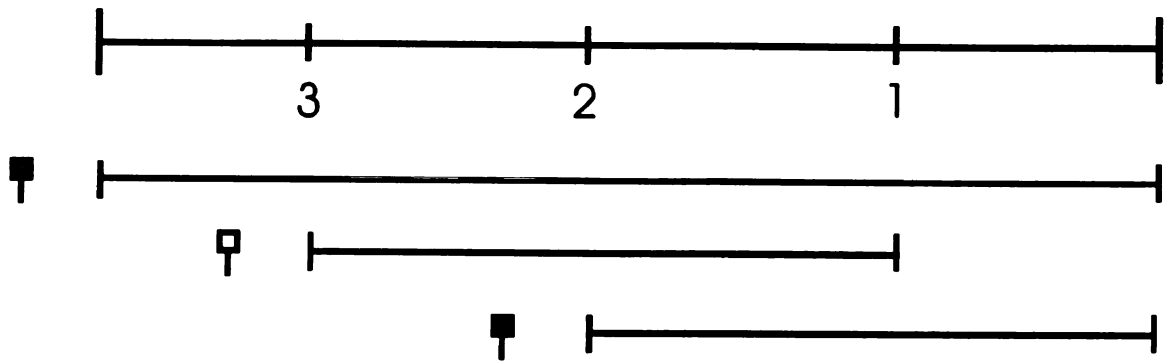

exchange that produces a recombinant centromeric array that does not carry that variant. Similarly, distal limits of a variant from the centromeric parental array are defined as the proximal most exchange that generates a recombinant telomeric array that does not carry that variant.

Dot blot analysis

The total copy number of rDNA repeat units in a given array was estimated by sequential hybridization of dot blots with pPA56, a probe that binds once to each rRNA gene copy, and with a probe for a single copy gene. The single copy probe served as an internal measure of the amount of DNA loaded on each dot. Dot blots were performed using modifications of conditions established by Boussaha (1992). Hybond-N (Amersham) nylon membranes and 4 sheets of Wattman's 3MM blotting paper were cut to blot size, presoaked in 20X SSC for 10 min. and loaded onto a Millipore dot blot apparatus. A brief vacuum (24"-30" Hg) was applied to remove excess liquid. Genomic DNA diluted to a concentration of 5μg/ml was boiled for 5' and then quenched for 10' on wet ice. 5M NaCl was added to a final concentration of 2.5M. DNA was added to wells under vacuum (24-30 Hg). Vacuum was turned off and 500μl of 1.5M NaCl, 0.5M NaOH was added to each sample to alkali denature. Vacuum was applied for 4' or until all liquid was drawn from every well. Samples were then neutralized by adding 500μl of 1.5M NaOH, 0.5M Tris, pH 7.2, 0.001M Na_2EDTA. Once again, vacuum was applied for 4' to remove liquid. The membrane was then removed from blotting apparatus, placed on a piece of blotting paper soaked in 10X SSC and UV fixed with 120 mJoules. Membranes were prehybridized in a Robbins hybridization incubator in 5 mls of 50% formamide, 0.5 mg/ml alkali-sheared salmon (or herring) sperm competitor DNA, 1X prehybridization mix (2.5X pre-hybridization stock = 250 mM Pipes, 2M NaCl, 0.5% sarkosyl, 0.25% Ficol, 0.25% PVP-40, 0.25% BSA, fraction V, pH 6.8). Prehybridization was carried out for 30' at 42°C. Blots were then hybridized with either a single

copy probe or the rDNA specific probe under conditions that allowed for pseudo-first-order kinetics (see below). Blots were washed 2X at 25°C for 10 min. in 2X SSC, 0.1%PPi, 0.1% Sarkosyl, 3X at 50°C for 15 min. in 0.1X SSC, 0.1%PPi, 0.1% Sarkosyl, and 1X at 60°C for 15 min. in 0.1X SSC, 0.1%PPi, 0.1% Sarkosyl.

Dot blot kinetics

For single copy probes, 50 ng of insert-containing plasmid was labeled and hybridizations were carried out at 42° overnight in hybridization solution (1X prehybridization mix; 40% formamide; 0.2% alkali-sheared salmon or herring sperm DNA; 10% dextran sulfate).

To ensure pseudo-first order kinetics for the pPA56 ribosomal probe, a combined 10X excess of radiolabeled fragment-purified insert DNA and non-labeled restriction enzyme cut plasmid was used in all multicopy hybridizations. In addition, the hybridization reaction was limited to one hour and no dextran sulfate was used. The amounts of labeled fragment-purified DNA and cut, cold carrier are calculated as follows;

1) the maximum amount of total DNA homologous to the multicopy probe on the membrane is:

(fraction of rDNA in wild-type genome)*(fraction of rDNA that is homologous to probe)*(total amount of DNA loaded on membrane)

2) the amount, in ng, of radiolabeled DNA is:

(1 X 10^6 CPM/ml hybridization soln.)* (total volume solution used)*(ng/ml probe)* (mls probe/total CPM)

3) the amount of homologous cold carrier probe sequence needed is:

(value calculated in step 2) - (10X the value calculated in step 1)

Since the probe is approximately 1/8 of the total (vector + insert) length, we multiply the difference by 8 to arrive at the total amount of cut (vector + insert) to be used as cold carrier. For example, a typical membrane will have 3.6μg genomic DNA. The fraction of sequence homologous to the probe is approximately 1/1500. This figure comes from an estimate that the rDNA occupies about

2% of the genome (3 X 10^6 rDNA/6 X 10^8 total haploid genome) and the probe sequence occupies about 1/30 of the rDNA. Therefore, the value from step 1 is equal to 2.7 ng. 100 ng of probe DNA was typically labeled to a specific activity of 5 X 10^8 CPM/μg DNA and collected in a volume of 200μl of 1X SET. For 5 mls of hybridization solution, 5 X 10^6 total CPM is required. Therefore, 20μl of labeled probe solution is required. This amounts to 10 ng of probe DNA in step 2. Consequently, 17 ng of homologous cold carrier sequence is required to ensure pseudo-first order kinetics, which is equivalent to 136 ng of cut (vector + insert).

Measurements of rDNA copy number for a given array requires that the array be placed in an otherwise rDNA$^-$ background. This was first accomplished by meiotically separating the two ends. Male flies bearing hairpin exchange chromosomes were crossed to females bearing a balancer *FM7* *X*-chromosome and a second *X*-chromosome, *Df(1)X1*, or simply *X1*, deficient for most of the basal heterochromatin including all of the rDNA. Female progeny were selected that carried both *X1* and the hairpin. Phenotypic markers were used to identify crossover progeny carrying either the distal or proximal arrays and these were stocked. Distal or left-end arrays carrying the *X1* base are stocked as females because the *X1* base is deleted for two euchromatic lethal loci. Proximal or right end arrays are stocked as males. For the left end stocks, DNA was extracted from females that carried the array over an rDNA$^-$ chromosome, $In(1)sc^{4L}sc^{8R}$. Right-end arrays were isolated either as *X/0* males or as $In(1)sc^{4L}sc^{8R}$ females. Eight wells were used for each genotype; four wells were loaded with 200 ng genomic DNA each and four wells were loaded with 400 ng. The Ore-R sample in each blot was loaded with half of this amount of DNA because it contains two NO's. The DNA was fixed on a nylon membrane and probed with a single copy gene; either the *D. melanaogaster* urate oxidase or ras genes. The blots were then stripped and reprobed with an rDNA specific probe, PA56, that hybridizes to a sequence in the 28S subunit

coding region (see description of probes). Blots were visualized and quantitated using a Molecular Dynamics Phosphor Imager. Any dots that had excessive background in either of the hybridizations were not used in the copy number calculations. For each usable dot we calculate the ratio of counts with PA56 to counts with a single copy probe. To account for blot to blot variation from, for instance, differences in specific activity of the probes, each blot contained a series of dots loaded with Oregon-R DNA. For each blot, a ratio of single copy counts to PA56 for each genotype was divided by the same ratio for Oregon-R to give the fraction of copies in a particular genotype relative to Oregon-R. We then multiply this fraction by 250, the total number of rRNA genes in an Oregon-R array, to arrive at the total number of copies in a particular genotype.

Molecular measurements of inserted and noninserted rRNA gene copy number

We used Southern blotting, combined with our measure of absolute copy number, to determine the number of inserted sequences in each array. Genomic DNA (400 ng), isolated from flies containing the array of interest in an otherwise rDNA$^-$ background, was cut simultaneously with *Hin*cII and *Hin*dIII (Boeringer Mannheim) following the recommended digestion protocols. These restriction enzymes cut a region of the 28S rDNA subunit that spans the R1 and R2 insertion sites (see Figure 1). Cut DNA was electrophoresed in 1% agarose gels. The DNA in the gels was alkali-denatured by soaking in 0.5M NaOH for 50 min. and then neutralized for 50 min. DNA was transferred to Hybond-N (Amersham) nylon membranes by capillary action or pressure blotting. Membranes were UV-fixed and prehybridized in a Robbins hybridization incubator in 7-10 mls of 50% formamide, 0.5 mg/ml alkali-sheared salmon (or herring) sperm competitor DNA, 1X prehybridization mix (2.5X pre-hybridization stock = 250 mM Pipes, 2M NaCl, 0.5% sarkosyl, 0.25% Ficol, 0.25% PVP-40, 0.25% BSA, fraction V, pH 6.8). Prehybridization was carried out overnight at 42°C. Membranes were then hybridized with 1-2 X 10^6 CPM of ^{32}P-

labeled PA56/ml of hybridization solution. Hybridizations were carried out at 42° for 8-12 hr. in 1X prehybridization mix; 40% formamide; 0.2% alkali-sheared salmon or herring sperm DNA; 10% dextran sulfate. After hybridization, membranes were washed twice at 25°C with mild scrubbing for 5-10 min. in 2X SSC, 0.1%SDS and 0.1% pyrophosphate. Membranes were then washed 3X for 15 min. at 50°C and 1X at 60°C in 0.1X SSC, 0.1% SDS, 0.1% pyrophosphate. After washing, membranes were immediately wrapped in saran wrap and placed in autoradiographic cassettes and later placed on storage-phosphor screens for quantification. PA56 hybridizes to the region of the 28S subunit that contains the insertion sites for both the Type 1 and the Type 2 insertion elements. Using this probe and the indicated enzymes, uninserted 28S subunits show up as 373bp bands. Each of the two types of insertion sequences have modal-length inserts; R1 shows a 5.5kb band while R2 shows a 3.0kb band (Jacubzak and Eickbush, 19..). Intermediate bands are presumably the result of an aborted reverse transcription of the RNA intermediate (Eickbush, 1994) whereby the 5' end of the element is deleted. There are also larger than modal- length bands that may be 28S coding subunits that have both elements inserted, or some combination of full length inserts and partial deletions. The vast majority of the counts (>90%) for any particular lane are found in the two modal length and the uninserted bands (data not shown).

To estimate the total number of inserted copies, we find the fraction of inserted repeat units within the array by summing the contributions from each of the two modal length insertion sequence bands and dividing this by the sum of inserted plus noninserted bands. we do not take into consideration the pseudo-first order kinetics of solution to membrane hybridization kinetics for two reasons. First, unlike the case for calculating IGS length variant copy numbers, where there are many bands with few copies and one or two with many copies, the modal length insertion sequences and the noninserted sequences are present in more equitable numbers. This means that

any deviations in copy number calculations would apply equally to all of the bands considered. Second, unlike the IGS case, where the probe contains repeated elements of the array, the probe used in the insertion sequence blots hybridizes to a unique sequence within the ribosomal array. This reduces the likelihood of underrepresentation of high copy number sequences because the ratio of the concentration of probe to homologous sequence bound to the membrane is much higher. The fraction of inserted copies for a given genotype multiplied by the total number of copies in that genotype calculated from the dot blot analysis is the number of inserted copies. A sample Southern blot of the insertion sequence variants is shown in Figure 23.

Phenotypic measurements of functional activity of arrays

Phenotypic assessments of the functional activity of each array were made using two different measures. First, as mentioned earlier, bobbed penetrance was scored as the frequency of phenotypically bobbed flies that contained the array of interest in an otherwise rDNA- background. Second, the scutellar bristle length of each genotype was measured. There are two pairs of bristles, a proximal pair and a distal pair, that are prominent on a triangular shaped region, called the scutellum, on the dorsal side of the fly. Using an optical micrometer, measurements of the lengths of each of the bristles were taken for all the genotypes. Only two of the arrays, 5 right and 7 left, show no overlap of standard errors with the other arrays. One interesting observation is that the molecular and phenotypic measurements are consistent. That is, 5 right and 7 left are phenotypically the most bobbed, showing significant bobbed penetrance and expressivity, while all other ends do not. The molecular data shows a much wider variation of noninserted copy numbers, but certainly 5 right and 7 left are grossly below the others.

Figure 23 - INSERTION SEQUENCE VARIANTS

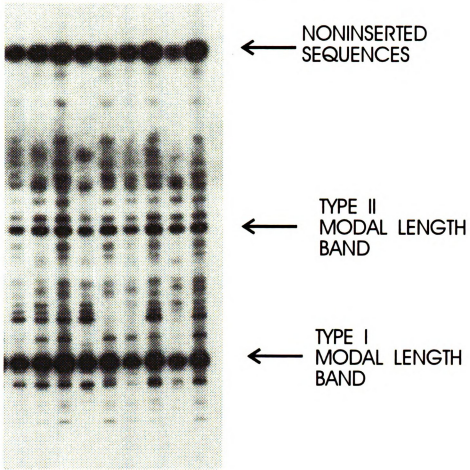

Southern blot showing modal length bands and length variants of insertion sequences in recombinant arrays. See text for details.

Testing for *Rex* response

In order to assess the sensitivity of novel target chromosomes to *Rex*, a standard cross is made. Individual males bearing the target chromosome to be tested are mated to female flies heterozygous for *Rex*. *Rex*-induced spiral exchanges produce phenotypically unique offspring (see Fig. 1) and the frequency of spiral events is calculated as:

spiral exchange progeny/(normal female progeny + spiral exchange progeny)

The G test

As mentioned in the introduction, we were interested in testing for a correlation between sensitivity of an array to *Rex* and: 1) the total number of rRNA genes in an array; 2) the number of non-interrupted, presumably active, rRNA gene copies; or 3) the functional activity of an array measured phenotypically. To determine whether or not our molecular measurements correlated with sensitivity we used standard regression analysis that will not be discussed. For comparisons of *bb* penetrance and *Rex* sensitivity, we used G tests. Because the G test is less frequently used, a brief explanation of the test is presented below. Precisely how it was used to address the questions of this study will be detailed in the Analysis section of this chapter.

Since much of what we do as fruit fly geneticists revolves around counting numbers of offspring, a statistic designed to deal with discrete data is a valuable tool. The G test is preferable to standard continuous-variable methods for examining correlations between discrete variables, like regression analysis, for two important reasons. First, because absolute numbers are used, the weight of each observation is taken into consideration, making the G-test a more powerful test. Second, unlike regression analysis, that only tells us whether two variables are significantly correlated, the G-test allows us to determine both significance and sufficiency. That is, we may find that two variables are correlated by means of a regression analysis, but we have no way of

knowing whether or not the correlation sufficiently explains all of the variation. The G test, on the other hand, allows us to determine whether or not there is a significant correlation between the chosen variables and whether the correlation is sufficient to explain most of the variation or if there is some source of extraneous variation that we have not considered.

Consider a simple example, like the one presented by the penetrance vs. sensitivity case. For each individual array we have the number of normal and spiral exchange progeny generated from crosses with *Rex*-bearing mothers to target-bearing males. We also have the number of bobbed and nonbobbed offspring among flies that carry the array of interest and no other rDNA. Therefore, we have four numbers associated with each array. Consider the following three hypotheses to describe what we see;

H_1: The sensitivity of each array is independent of bobbed penetrance for that array and differs for every array

H_2: The sensitivity is the same for every array

H_3 The sensitivity of an array is dependent on bobbed penetrance.

Each comparison, or the G value for each pair of hypotheses, will tell us something different about the data.. For instance, by comparing H_1 with H_2, we are asking whether the variation between the data points is significant (a contingency test based on maximum likelihood estimations). In other words, is the detachment frequency actually the same for each cross? By comparing H_2 with H_3, we can determine if the variation is explained by correlation. In other words, is the correlation significant, implying that the data points fall on the line that represents the best fit line as determined by the maximum likelihood solutions for slope and Y-intercept. Finally,

a comparison between H_1 with H_3, tells us if the correlation is sufficient to explain the variation. There may be instances where there exits a correlation among data points, yet the correlation explains little of the variation that we see. In these cases, we surmise that there is some additional source of variation that we have not considered in our model. Small G values in this final comparison represent models in which most of the variation can be explained by correlation. Large G values, on the other hand, imply that there are sources of variation other than the particular parameter examined. In other words, this final comparison gives a measure of how powerful the correlation is as an explanation of the data.

For each of these hypotheses, we can define a likelihood function, L, that describes the probability of observing the results. For instance, under the first hypothesis, we can define the probability of being a spiral exchange offspring from a target containing a particular array as D_{array}. Therefore, the probability of being a normal offspring is $1-D_{array}$. Similarly we can define the probability of being bobbed or not bobbed as P_{array} and $1-P_{array}$, respectively. The likelihood function is the product of each of these probabilities raised to the number of flies in that particular phenotypic group. For instance, let's assume we had data from only two arrays, array 1 and array 2, instead of twenty-two. If we observe M_1 spiral exchange offspring from array 1, M_2 spiral exchange offspring from array 2, N_1 normal offspring from array 1, N_2 normal offspring from array 2, R_1 bobbed offspring from array 1 and R_2 from array 2, and S_1 nonbobbed from array 1 and S_2 from array 2, then the likelihood function that describes these results is;

$$L = (D_{array1})^{M1} (1-D_{array1})^{N1} (P_{array1})^{R1} (1-P_{array1})^{S1} (D_{array2})^{M2} (1-D_{array2})^{N2} (P_{array2})^{R2} (1-P_{array2})^{S2}$$

Under the second hypothesis, the value of D remains constant for all of the arrays. The likelihood statement is simpler under this hypothesis since we can sum all the exponents of D and combine them into a single term;

$$L = (D)^{M1+M2}\,(1-D)^{N1+N2}\,(P_{array1})^{R1}\,(1-P_{array1})^{S1}\,(P_{array2})^{R2}\,(1-P_{array2})^{S2}$$

The third hypothesis assumes a correlation between sensitivity and penetrance. Expressed algebraically,

$$D_{array} = m\,(P_{array}) + b.$$

The likelihood statement under this third hypothesis is identical to the first hypothesis except that the right hand side of the linear equation above is substituted for each D_{array}.

Next, we find those values of our parameters that maximize the likelihood function. The maximum of the likelihood function is found at all values when the first derivative of the function is zero. In many instances, the likelihood equation is a function of more than a single parameter. In these cases, the system of equations that result from setting the partial derivatives equal to zero can sometimes be solved directly to obtain those values of the parameters that yield a maximum for the likelihood function. However, more often that not, a computer program designed to find maxima is used. One such program, MLIKELY (Robbins, personal communication) is an iterative program that accepts initial guesses for the values of the parameters and then searches for local maxima by incremental adjustments of the parameters that increase the value of the likelihood equation.

In this simple example, the parameter values that maximize the likelihood equations under the first two hypotheses are trivial. By first taking the natural log of both sides of the equation we can simplify the partial derivatives. The partial derivative of the likelihood equation for H_1 with respect to D_{array1}, only includes those terms that contain this parameter. All other terms are constants and drop out of the equation. Therefore, the derivative of the lnL under H_1 with respect to D_{array1} is:

$$M_1/(D_{array1}) - N_1/(1-D_{array1})$$

Setting the partial derivative equal to zero and solving for D_{array1}, we find that

$$D_{array1} = M_1/(M_1 + N_1),$$

which of course is the fraction of spiral exchange progeny that we observe. This tells us that under H_1, when our assumption is that the spiral exchange frequency is different for each array, the best estimate for the exchange frequency is that which we observe. Similarly, under H_2, the best estimate for the spiral exchange frequency is the weighted average of all of the individual frequencies.

The third hypothesis will give us the maximum algebraic likelihood estimates of the slope and Y-intercept of the 'best fit' line through our data points. Algebraically finding the maximum likelihood under H_3, however, is non-trivial, and we resort to computer-based numeric approximation. These values of D and P and m and b can then be substituted back into our original equations to give us values of the three different lnL's. G is then defined as twice the difference of the natural logs of the values of L under any two different hypotheses. G is distributed approximately as Chi-squared with degrees of freedom equal to the difference in the number of degrees of freedom used in each of the two hypotheses.

Results

Properties of arrays

Differences in *Rex* sensitivity among the recombinant arrays generated from *Rex*-induced hairpin exchanges in $In(1)w^{m51bL}\ w^{m4R}$ were detected by counting the number of *Rex*-induced spiral exchanges generated from a set of target chromosomes containing one common nucleolus organizer (see Materials and Methods). Proximal arrays were combined with 7 Left and distal arrays were combined with 5 Right. The percentage of spiral exchanges relative to a standard control cross for both proximal and distal arrays is defined as the sensitivity of an array.

Phenotypic measurements of bobbed penetrance and expressivity were performed to assess the functional activity of the arrays. Bobbed penetrance of arrays is defined as the percentage of flies showing any bobbed characteristics among a population that genotypically have the array and no other rDNA. Expressivity is calculated as the mean scuttellar bristle length of flies with a single array and no other ribosomal DNA. Figure 24 shows the experimentally determined values of penetrance, expressivity and sensitivity of the arrays.

The total number of repeat units, the number of repeat units containing insertion sequences and the number of uninterrupted repeat units have been measured molecularly. The molecular measurements of total copy number are calculated from sequentially probing of dot blots with a single copy and then a ribosomal DNA specific probe (see Materials and Methods). Samples of dot blots probed with single copy and rDNA probes are shown in Figures 25 and 26.

IGS Variant Map of *In(1)w^{m51bL}w^{m4R}*

Rex-induced hairpin exchange mapping was used to generate a map of the intergenic spacer variants in *In(1)w^{m51bL}w^{m4R}* . A sample Soutern blot showing IGS variants is shown in Figure 27. For mapping purposes, unique IGS variants originally in the proximal array of *In(1)w^{m51bL}w^{m4R}* are lettered while distal array variants are numbered. The presence/absence data for the *Rex*-induced hairpin recombinant arrays are shown in Figure 28. This figure also indicates those arrays that show a high sensitivity to *Rex*, the interpretation of which is discussed later in the text. The IGS map of *In(1)w^{m51bL}w^{m4R}* is shown in Figure 29. There are two components of the data that warrant mention. First, we have not positioned exchange 36 anywhere on the map. Both arrays of exchange 36 contain the full set of distal-array variants and none of the parental proximal array variants. Thus, our data suggest that this particular event resulted in a duplication of the entire distal array. It is difficult to imagine an event that would result in such a large duplication. One possibility is that there was a three strand double exchange occurring

outside the region of the arrays containing these unique variants. In any case, the event that produced the distal and proximal arrays in 36 was certainly not a simple single exchange. Second, exchange 40 is a large deletion; all of the parental distal bands are missing from both products of the exchange. Exchange 40 is clearly a recombinant, since variants were moved from the proximal to the distal array, but we cannot locate the point of exchange in the telomeric array and have arbitrarily placed 40 at the center of the telomeric array map, expressing the uncertainty of its position by showing that the exchange point may be at any position along the length of the map. The site of exchange 40 in the centromeric array is, however, well-defined.

Phenotypic Measurements of Functional Activity of Arrays

DISTAL NUCLEOLUS ORGANIZERS

LINE	EXPRESSIVITY	PENETRANCE	SENSITIVITY*
4	22.9 ± 2.00	0	49.28
5	22.1 ± 1.01	0.0017	37.16
6	23.4 ± 1.39	0	63.99
7	14.5 ± 1.69	1	29.67
18	22.6 ± 2.50	0.007	12.65
23	24.2 ± 1.26	0.0067	31.91
26	23.3 ± 0.92	0	30.13
36	21.9 ± 1.22	0.0016	8.96
40	21.3 ± 1.74	0.0037	14.23
44	22.4 ± 1.27	0.0059	40.01
60	21.7 ± 1.51	0.0034	18.96

PROXIMAL NUCLEOLUS ORGANIZERS

LINE	EXPRESSIVITY	PENETRANCE	SENSITIVITY*
4	23.5 ± 1.83	0.0017	97.66
5	17.8 ± 1.76	0.9	92.39
6	22.6 ± 2.03	0.0078	111.91
7	23.2 ± 2.03	0.0016	37.16
18	24.2 ± 1.00	0.21	0.00
23	24.6 ± 1.17	0.0014	16.43
26	25.1 ± 1.75	0.0016	39.00
36	22.8 ± 1.67	0.0094	33.36
40	21.7 ± 1.45	0.66	30.29
44	22.0 ± 2.12	0	33.74
60	21.8 ± 1.92	0.012	36.51

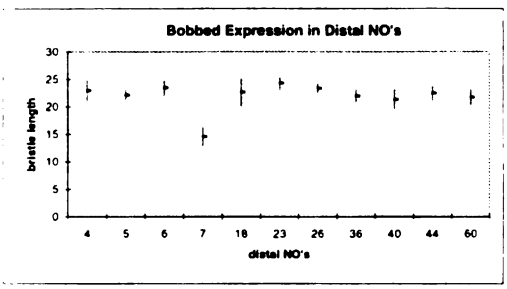

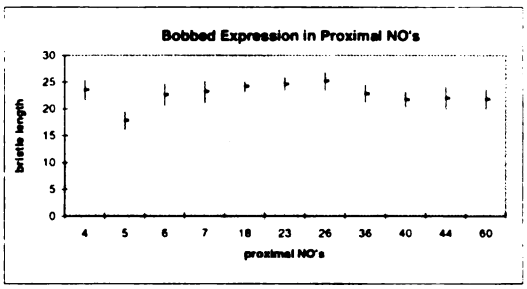

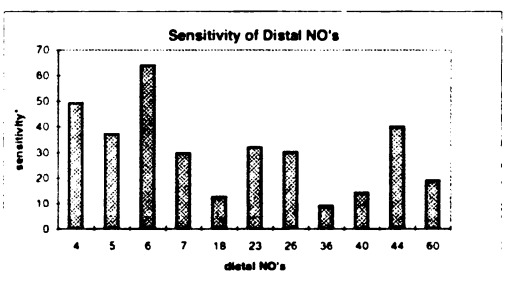

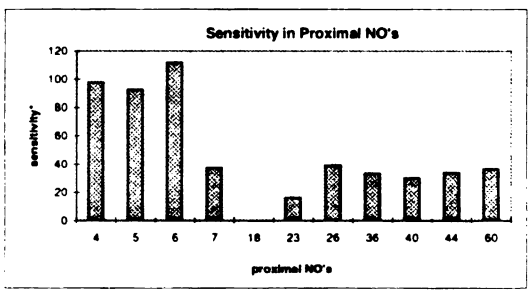

Figure 24
Three phenotypic measurements were made to assess the functional activity of the distal and proximal recombinant NO's derived from *Rex*-induced hairpin exchange of $In(1:1)w^{m51Lb}w^{m4R}$. All measurements were made in otherwise rDNA$^-$ backgrounds. Expressivity was measured as the average scutellar bristle length. Penetrance was measured as the percent of bobbed flies. Sensitivity was measured as the frequency of spiral exchange in target chromsomes containing either the distal or proximal array and a second constant array (see text for details). Sensitivities are expressed as a percent of spiral exchange frequency in the standard target chromsome. Graphs of sensitivity and expressivity are shwon for both proximal and distal arrays.

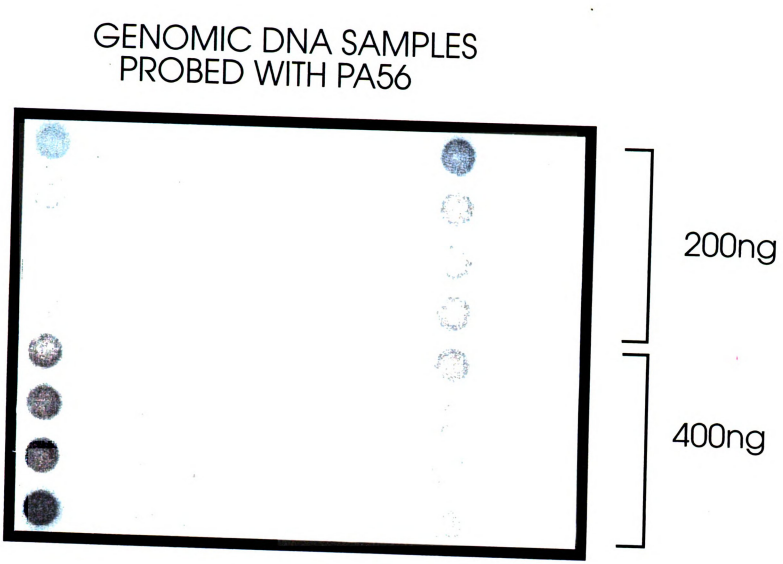

Figure 25 - Dot blot of recombinant arrays

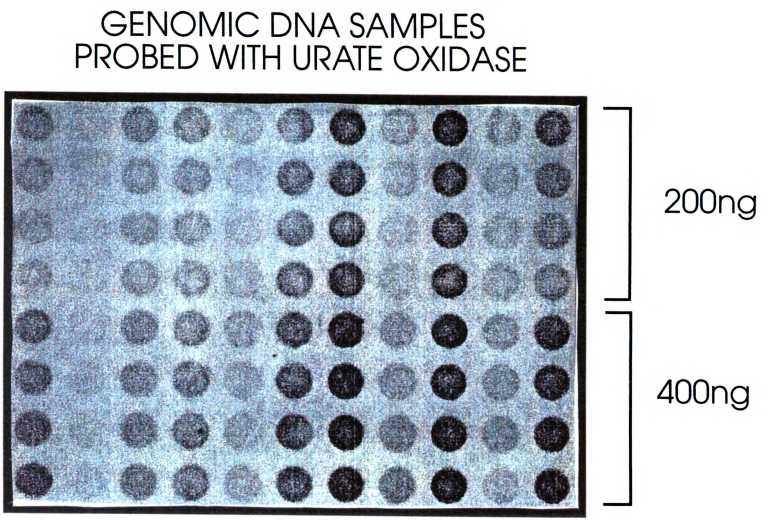

Figure 26

Intergenic Spacer Length Variants

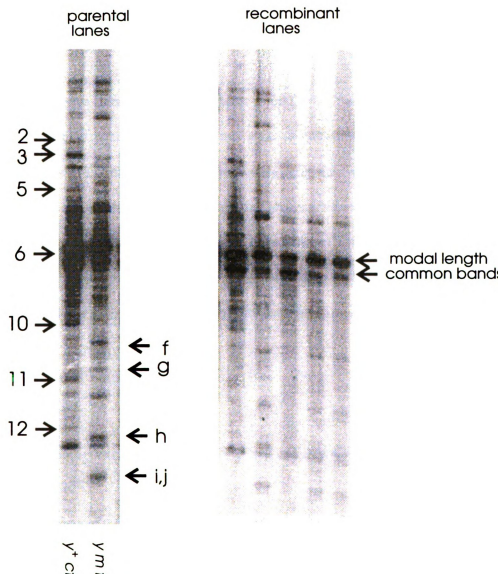

Figure 27

A Southern blot of the intergenic spacer length variants in both the distal and proximal arrays of *In(1:1)w^{m51Lb}w^{4R}*. Numbered bands represent variants that were mapped in the distal parental NO. Letters represent mapped variants in the proximal parental NO.

Figure 28 - Presence/Absence Data for Unique Variants in *In(1)w^{m51bL}w^{m4R}*

The presence or absence of the parental distal or proximal array unique variants among the recombinant arrays is shown. Proximal recombinant arrays are designated with an R (right) following the recombinant array number. Distal recombinant arrays are designated with an L (left) following the recombinant array number. A '+' indicates the presence of a particular variant. A minus sign indicates that the variant was absent in the recombinant array. The presence/absence of a putative element that induces exchange above the mean for each group of arrays is also indicated.

Figure 29 - Intergenic Spacer Variant Map of the Proximal and Distal NO's of *In(1)w^{m51bL}w^{m4R}*

Solid lines represent the limits of the indicated variant in the parental array. Numbers represent unique variants present in the parental distal array. Letters represent unique variants in the proximal array. The mapping methodology is detailed in the text.

Presence/Absence Data for Unique Variants in *In(1:1)w^{m51Lb} w^{m4R}*

distal variants in proximal array

	variants						
array	2	3	5	6	10	11	12
4R	+	+	+	-	+	-	+
5R	+	-	+	-	-	-	+
6R	+	+	+	-	+	+	+
7R	+	+	+	+	+	+	+
18R	+	+	+	-	-	-	+
23R	+	+	+	+	+	+	+
26R	+	+	+	+	+	+	+
36R	+	+	+	+	+	+	+
40R	-	-	-	-	-	-	-
44R	+	+	+	+	+	+	+
60R	+	+	+	-	+	+	+

proximal variants in proximal array

	variants					
array	f	g	h	i	j	high response element
4R	+	+	+	+	+	+
5R	+	+	+	+	+	+
6R	+	+	+	+	+	+
7R	+	+	+	+	+	-
18R	+	+	+	+	+	-
23R	+	-	-	+	+	-
26R	+	+	+	+	+	-
36R	-	-	-	-	-	-
40R	-	-	-	-	-	-
44R	+	-	-	+	+	-
60R	+	+	+	+	+	-

distal variants in distal array

	variants						
array	2	3	5	6	10	11	12
4L	+	+	+	+	+	+	+
5L	+	+	+	+	+	+	+
6L	+	+	+	+	+	+	+
7L	-	+	-	-	-	-	-
18L	+	+	+	+	+	+	+
23L	-	+	-	-	+	+	+
26L	+	+	+	+	+	+	+
36L	+	+	+	+	+	+	+
40L	-	-	-	-	-	-	-
44L	-	+	-	-	-	-	-
60L	-	+	+	+	+	+	+

proximal variants in distal array

	variants					
array	f	g	h	i	j	high response element
4L	-	-	-	-	-	+
5L	+	-	+	+	+	+
6L	-	-	-	-	-	+
7L	+	-	+	-	-	-
18L	+	+	+	+	+	-
23L	+	+	+	+	+	-
26L	+	-	-	-	-	-
36L	-	-	-	-	-	-
40L	+	+	+	+	+	-
44L	+	+	+	+	+	+
60L	+	-	-	-	-	-

Figure 28

Figure 29 - Intergenic Spacer Variant Map of Proximal and Distal NO's *In(1:1)w^{m51Lb}w^{4R}*

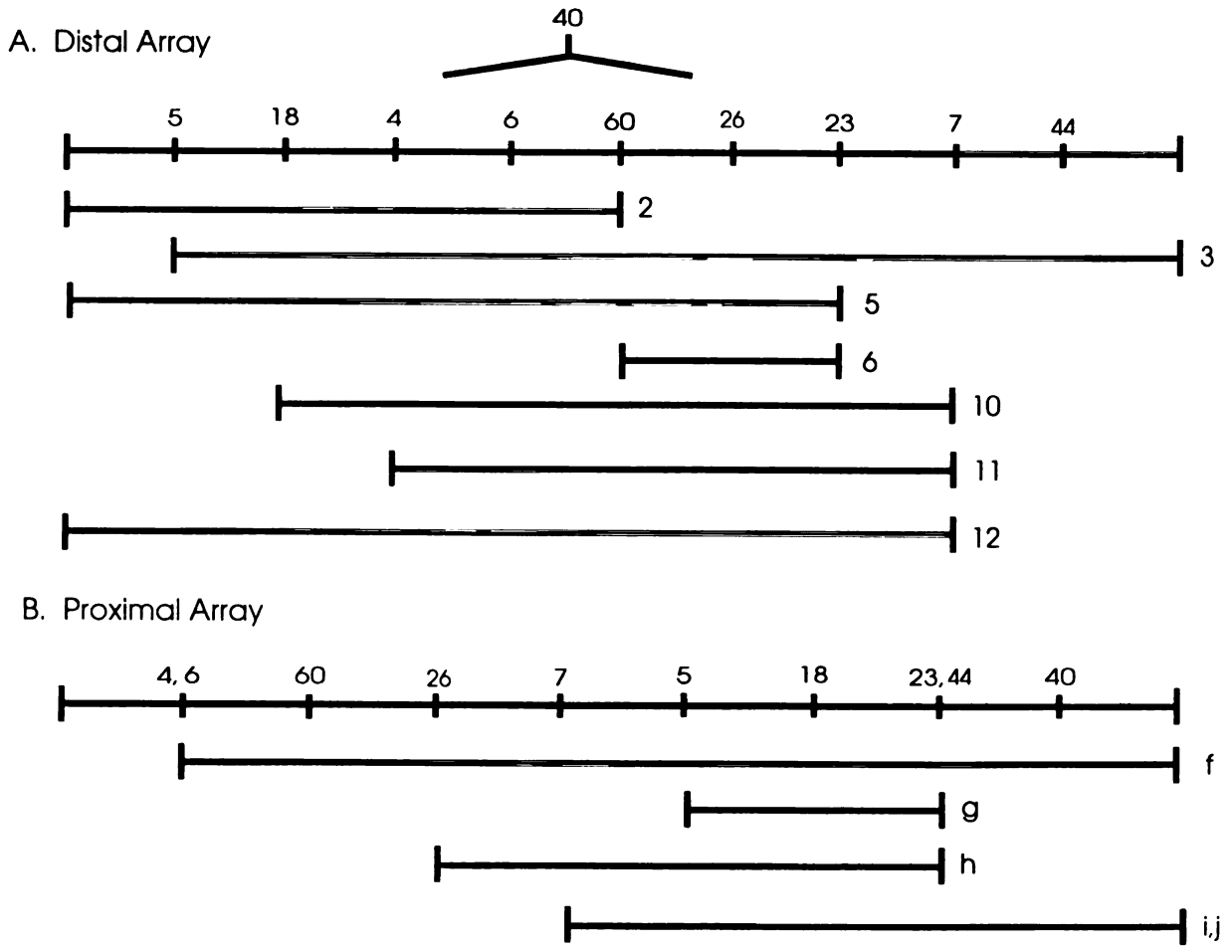

Analysis

Sensitivity

We analyzed the distal and proximal arrays separately to determine whether they differed significantly in sensitivity to *Rex*, . Contingency tests on both sets of data show that there is a significant difference in sensitivity among both proximal and distal arrays. (X^2 for proximal arrays = 36.5, 10 d.f.; X^2 for distal arrays = 61.4, 10 d.f.)

Correlations

We used two types of statistical analysis to determine whether any of the measured characteristics of the arrays were correlated with sensitivity. Standard regression analysis was used to determine whether any of the molecularly obtained measurements correlated with sensitivity. The results of these analyses are presented in Figure 30. There were three different molecular measurements that were compared with sensitivity; 1. the total number of repeat units, 2. the number of repeat units containing insertion sequences and 3. the number of repeat units that do not contain insert sequences. The data indicate that there is no significant correlation between any of the molecular measurements and sensitivity in either the distal or proximal arrays

We also measured bobbed expression and bobbed penetrance in all of the arrays. Bobbed expression was measured in terms of average bristle length expressed in optical micrometer units (see materials and methods). A regression analysis again showed no significant correlation between bobbed expression and sensitivity (see Fig. 30).

Because measurements of penetrance give discrete data, we used a G-test. As with the molecular data, we wanted to determine whether or not penetrance was correlated with sensitivity. Our three hypotheses to be compared using a G-test are:

H_1: the sensitivity of each array is different and is independent of bobbed penetrance

H_2: the sensitivity of each array is the same and is independent of bobbed penetrance

H_3: sensitivity is correlated with bobbed penetrance

Table 5 shows the G values for both the proximal and distal arrays, calculated as {2 *(lnL H_a-lnL H_b)}for each of the three comparisons.

Table 5 - G-TEST FOR SENSITIVITY VS.PENETRANCE

			DISTAL ARRAYS			PROXIMAL ARRAYS		
		G-tests	G	df	p	G	df	p
variation		H1 vs. H2	66.08	10	<<<.05	34.31	10	<<<.05
correlation	significance	H2 vs. H3	0.51	1	0.475	3.24	1	0.072
	sufficiency	H1 vs. H3	65.58	9	<<<.05	31.07	9	<<<.05

As with the molecular data, our phenotypic measurements show no significant correlation with *Rex* sensitivity.

The data do indicate, however, that there are two discrete groups of arrays, a high sensitivity and a low sensitivity group, among both the proximal and distal data sets. To show this, we again performed a G-test. Because we are only interested in sensitivity as a parameter, our three hypotheses do not include a parameter for penetrance. We are only interested in determining whether or not it is statistically sensible to define a high and a low sensitivity group within our sets of arrays. The high sensitivity group is defined as those arrays that have a sensitivity above the mean. The low group is defined as those that have a sensitivity below the mean. Our three hypotheses are:

Figure 30 - Regression Analysis

Different properties of arrays are compared to *Rex* sensitivity by regression analysis. The sensitivity values plotted on the Y-axis are % of sensitivity relative to a standard target chromosome. The total copy number, the number of insert-containing sequences and the number of noninterrupted repeat units for both proximal and distal recombinant arrays were compared. No significant correlation was found between sensitivity and any of the parameters examined. In addition, bobbed expression, as measured by the penetrance of the bobbed phenotype in individual arrays was compared to sensitivity values for the arrays. Again, no significant correlation was found (see text for discussion).

REGRESSION ANALYSIS

PROXIMAL NUCLEOLUS ORGANIZERS

LINE Right ends with 7 left	sensitivity (% control)	total copies	# of insertion containing sequences	# of noninterrupted sequences
4	49.28	270	140	130
5	37.16	98	78	20
6	63.99	260	174	86
7	29.67	465	282	183
18	12.65	140	92	48
23	31.91	222	180	42
26	30.13	303	205	98
36	8.96	213	167	46
40	14.23	140	105	35
44	40.01	585	409	176
60	18.96	465	342	123

DISTAL NUCLEOLUS ORGANIZERS

LINE Left ends with 5 right	sensitivity (% control)	total copies	# of insertion containing sequences	# of noninterupted sequences
4	97.66	294	166	128
5	92.39	314	134	180
6	111.91	187	114	74
7	37.16	121	103	19
18	0.00	402	279	123
23	16.43	388	303	85
26	39.00	274	227	48
36	33.36	202	132	70
40	30.29	402	316	86
44	33.74	388	287	102
60	36.51	274	168	106

Figure 30a

REGRESSION ANALYSIS

REGRESSION ANALYSIS OF PROXIMAL NO'S

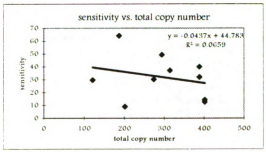

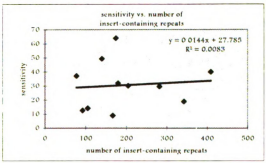

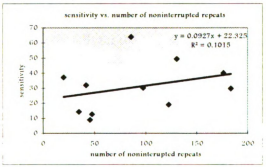

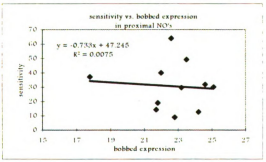

REGRESSION ANALYSIS OF DISTAL NO'S

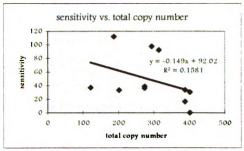

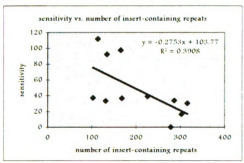

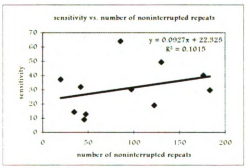

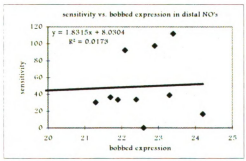

Figure 30b

H_1: the sensitivity of each array is different

H_2: the sensitivity of each array is the same

H_3: the sensitive of each array falls into one of two groups, a high or a low sensitivity group.

The likelihood expressions describing the first two of these hypotheses are similar to those already described in Materials and Methods. The only differences are that here, penetrance is not considered and we have only two observed classes. By not considering penetrance, we simplify the equations since all those factors that contained the penetrance parameter now disappear. The equation describing H_3 is a new equation, but is also simple. Under this hypothesis we consider two sensitivity values, S_1 and S_2, for high and low sensitivity respectively. Therefore, the probability of being a spiral exchange progeny is S_1 if the array is in the high sensitivity group and S_2 if the array is in the low sensitivity group. Similarly, the probability of being a regular offspring is $1-S_1$ for the high sensitivity group and $1-S_2$ for the low sensitivity group.

The ln of the overall likelihood equation for the proximal arrays becomes,

$$\ln L = \Sigma(\text{detachments in high sensitivity group}) * \ln(S_1) +$$
$$\Sigma(\text{regular offspring in high sensitivity group}) * \ln(1-S_1) +$$
$$\Sigma(\text{detachments in low sensitivity group}) * \ln(S_2) +$$
$$\Sigma(\text{regular offspring in low sensitivity group}) * \ln(1-S_2)$$

The maximum likelihood estimators for S_1 and S_2 are the weighted averages of the sensitivities of the arrays in each group. The G-values for each of the comparisons in both the proximal and distal data sets are shown in Table 6

Table 6 - G-TEST FOR HIGH/LOW SENSITIVITY GROUPS

		DISTAL ARRAYS				PROXIMAL ARRAYS		
		G-tests	G	df	p	G	df	p
variation		H1 vs. H2	66.08	10	<<<.05	34.31	10	<<<.05
correlation	significance	H2 vs. H3	47.14	1	<<<.05	23.81	1	<<<.05
	sufficiency	H1 vs. H3	18.94	9	0.026	10.49	9	0.312

For the H_2 vs. H_3 comparison, we must have use a much greater stringency than probability < 0.05 to determine whether or not there is a difference between our hypotheses. A critical value of .05 means that one out of twenty times we will observe that big of a difference between our hypotheses even though there is no biological basis for the difference. The two-group hypothesis creates an additional level of complexity by introducing an uncertainty about the choice of groupings. We have defined our groups based on values of sensitivity above and below the mean. This choice may or may not be correct. If we were to assign a critical value of .05 as the point at which we say there is a biological basis for the difference (generated using X^2 or the G-test), this would mean we would be giving the same chance of seeing a biological difference using a completely arbitrary grouping. That is, there are 11!/3!8! ways of grouping the distal arrays into groups of three and eight, any one of which has a one in twenty chance of producing a difference large enough for us to interpret as biologically significant. A conservative way of addressing this issue is to divide the standard critical value of .05 by the number of possible groupings. Even at this stringency, the difference between H_2, an hypothesis that assumes one average value for the sensitivity for any array and H_3, an hypothesis that considers two distinct sensitivities, high and low, is significant.

Each comparison tells us something different about the data. H_1 vs. H_2 is equivalent to a contingency test. We are comparing the weighted mean sensitivity against individual sensitivities and asking if there is a significant difference between them. Here we find that with 10 d.f., the G value is 66.08, indicating that there is a significant difference among arrays. The second comparison, H_2 vs. H_3 , tells us that we can reject the hypothesis that the high and low sensitivity groups are really the same. That is, there is a significant difference between H_3 , an hypothesis that breaks the arrays up into two groups, and H_2 , an hypothesis that suggests that there is a single sensitivity value. Finally, the third comparison, H_1 vs. H_3 tells us whether or not the two-group hypothesis is sufficient to explain the observed variation in sensitivity. For both distal and proximal arrays, the two-group, high/low sensitivity hypothesis sufficiently explains the variation that we observe among arrays. Although the G for this third comparison may be nearly significant at the .05 level, it is certainly not significant when the more stringent criteria is used. The G-test tells us that the two-group hypothesis fits the data, suggesting that there is a discrete region or element responsible for the either high or low *Rex* sensitivity. As with any phenotypically definable element within an array, it can potentially be mapped.

Mapping High Sensitivity

Using our IGS map (see Figure 29), we first attempted to define a single region that contains either a 'high sensitivity element' that, when present in either recombinant array, results in higher than average *Rex*-sensitivity or, a 'low sensitivity element' that when present results in a lower than average *Rex*-sensitivity. A diagram that helps to explain our logic is presented in Figure 31. In this figure, the centromeric parental array is lightly shaded while the distal array is darkened. The parts of each array present in the *Rex*-induced hairpin proximal recombinant arrays are shown. For instance, 44 right, contains a small part of the centromeric array and most of the

Figure 31- Mapping High/Low Sensitivity Elements

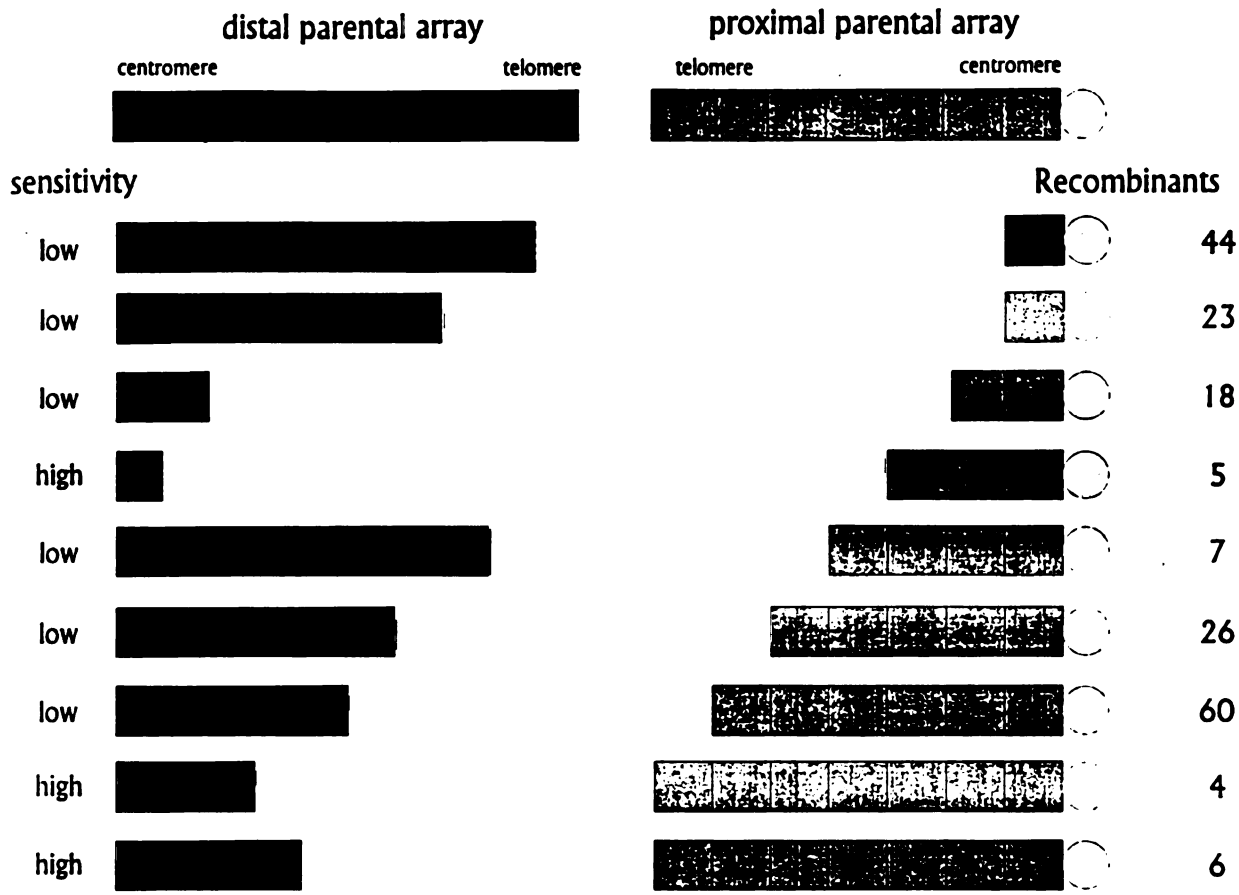

The parental variant composition of the proximal recombinant arrays is shown. Recombinant proximal arrays have variants from both the distal and proximal parental arrays. The amount of the distal or proximal parental array contained in the recombinantis determined by the point of the exchange. We can use this information to follow cosegregation of a high or low sensitivity element with particular regions of the parental arrays.

distal array. Do all of the highly sensitive arrays contain a region of either parental array that is not present in any of the low sensitivity arrays? The answer is, no. If there were in fact such a region, it would have to be contained within the parts of the parental arrays contained in 5 right since this is the smallest region contained in all three highly sensitive arrays. However, 7 left also contains all of the parts of the arrays contained in 5 right but is not itself a highly sensitive array. Following the same logic we can exclude the existence of a single 'low sensitive element and the existence of any combination of two elements, two highs, two lows, or a high and a low, as causing the high/low sensitivity divisions. There may, however, be multiple elements that create a complex interplay between promoting exchange and suppressing it to determine how a target will respond to *Rex*.

Discussion

We have further defined the properties of the target for *Rex*. First, we have shown that individual arrays show differences in sensitivity. We have also shown that there is no correlation between sensitivity and the total number of rRNA gene copies, the number of noninterrupted, presumably active, copies, or the number of insertion-sequence containing copies in an array.

We chose to look for correlations of sensitivity with these properties of the arrays for specific reasons. We have hypothesized that *Rex* can generate breaks in rDNA and that these breaks can be resolved via recombination to give rise to the types of exchanges we see. If this is in fact the case, *Rex* may be generating either random or site specific breaks in rDNA. A model that invokes random breaks predicts a correlation between the total number of repeat units in an array and the frequency of *Rex*-induced exchange. We have not found this to be the case. Thus, if *Rex* is in fact generating breaks in ribosomal arrays, the breakage is site specific. It has been proposed that *Rex* is an active version of a normally quiescent retrotransposable-like element residing in the

rDNA (Hawley and Marcus,1989; Rasooly and Robbins,1990). Two such elements are the Type 1 and Type 2 insertion sequences. *In vitro*, site specific endonucleolytic activity has already been demonstrated for an enzyme expressed from a Type 2 element (Jacubzac and Eickbush, 1990). If *Rex* were an active version of one of these elements, it could produce an endonuclease that would break DNA at the insertion sites. Repeat units that already contain inserts lack these sites and therefore would not act as targets for *Rex*. Thus, we would expect to see a correlation between *Rex* sensitivity and the number of noninterrupted sequences. Our data does not support this notion either.

We are currently pursuing a more direct means of addressing the possibility that *Rex* is an active Type 2 element. Germ line transformations with a P-element carrying a copy of a Type 2 insertion sequence under control of a Gal4 promotor have been constructed in the Eickbush lab and sent to us for testing.

We have also phenotypically measured functional activity of arrays in terms of bobbed expressivity and penetrance. We have attempted to correlate these observations with *Rex* sensitivity. Two observations, when taken together, support the notion that actively transcribed repeat units are non-interrupted repeat units. First, electron microscope studies of rDNA arrays in the process of transcription show that not all copies are transcribed. In any particular field of view, one typically sees Christmas tree shaped regions indicative of multiple rounds of transcription at a single promotor. Immediately adjacent these are regions of no transcriptional activity. Second, Northern analysis of rRNA transcript lengths does not show any transcripts large enough to contain inserts (Jamrich and Miller, 1984). Taken together, these observations suggest that it is insertion-containing sequences that are inactive and that it is the noninterrupted ones that are active. Nevertheless, analysis of our penetrance and expressivity data also showed that there is no significant correlation between rDNA function and *Rex* sensitivity.

We have also shown, using the G-test, that *Rex* sensitivity of recombinant arrays falls into two discrete groups, one with high sensitivity and one with low sensitivity. If the high response to *Rex* were due to a single region within the rDNA, then it could be mapped. We have attempted to place highly sensitive regions on an IGS variant map, but have found that the sensitivity cannot be localized to a particular region of the map. There are many hypotheses that could explain this inability to map sensitivity. One possibility, for example, is that there are interactions between multiple regions that promote exchange and regions that suppress it, and that the right combination of these elements must be present to see increased levels of exchange.

Chapter 4

REX-INDUCED rDNA MAGNIFICATION

Introduction

Ribosomal DNA magnification in *D. melanogaster* is an event that results in a heritable increase in the number of copies of rDNA genes (Ritossa, 1968 and Tartoff, 1974). Normally, the copy number is extraordinarily stable. However, in the presence of certain unusual *Y*-chromosomes, heritable increases in the number of genes on arrays carried on the *X*-chromosome can occur.

Magnification was first observed among the progeny of male flies that carried a *Y*-chromosome deficient for rDNA, Ybb^-. Males that are genotypically bb^2/Ybb^- are mated to females bearing one *bb*-deficient *X*-chromosome, $In(1)sc^4sc^8$, and one normal X-chromosome. The majority female offspring carrying the maternal deficiency, $In(1)sc^4sc^8$, and the paternal bb^2 *X*-chromosome are *bb*. However, depending on the particular Ybb^-, up to 18% of the bb^2/bb-deficiency F_1 females are phenotypically much less bobbed than expected (Tartoff, 1974). Furthermore, a significant fraction of the revertant alleles were shown to be stably inherited over subsequent generations. In controls, where the males do not carry the abnormal *Y*-chromosome, there are very few, if any, bb^2/bb-deficiency females that are phenotypically bb^+. These observations are summarized in Figure 32.

In crosses where a *Y*-chromosome that can induce magnification is used, most single pair matings do not result in any bb^+ progeny. There are however, some matings that give rise to a single bb^+ progeny among a population of *bb* siblings. Furthermore, in matings where there is one bb^+ among the progeny, there are often single flies that exhibit a much more severe bobbed phenotype, indicating a reduction in the number of functional rDNA genes. The reciprocal nature

Figure 32 -Detecting Magnification

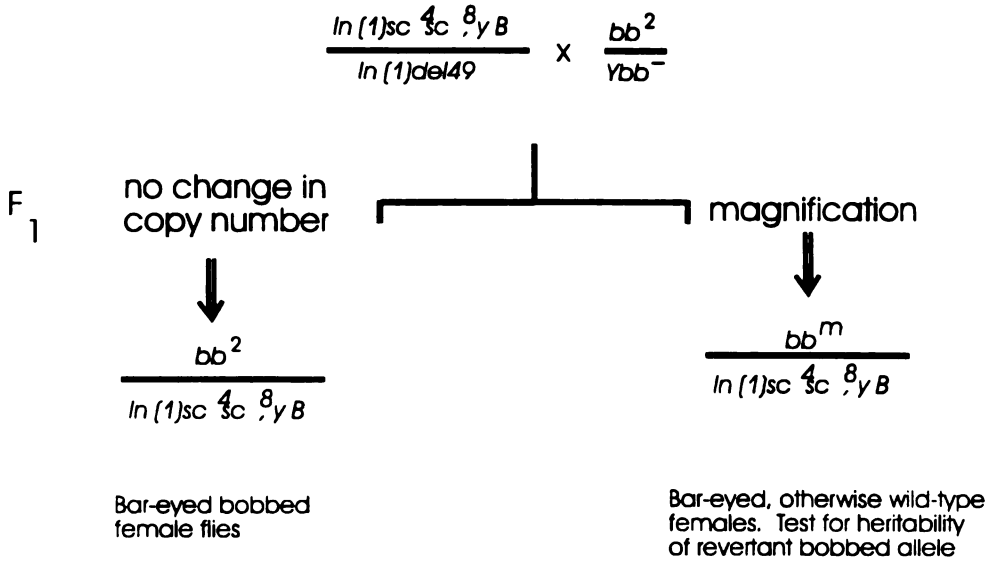

Sandard assay for magnification (see text for explanation).

of the single events supports the hypothesis that one meiotic mechanism for magnification is unequal sister chromosomal exchange (Tartoff, 1974).

There are also, however, single pair matings that give rise to many bb^+ progeny. Those matings that show clustering do not show equal numbers of reduced copy flies. The clustering is nonreciprocal. That is, among those matings that produce many bb^+ progeny, there are not equal numbers of flies that show a more severe bobbed phenotype. It has also been suggested that clustering could be the result of unequal sister chromatid exchange during a premeiotic stage of gametogenesis (Hawley and Marcus, 1989) . In this case, mitotically dividing germ-line cells that undergo magnification would be replicated during subsequent mitoses producing clusters, while the reciprocal reduced arrays would be selected against.

The unequal sister chromatid exchange hypothesis is supported by the observation that circular chromosomes do not magnify (Endow et al., 1984). Sister chromatid exchange within a circular chromosome would produce dicentric chromosomes. During meiosis II, when sister chromatids normally disjoin from one another, the centromeres of the dicentric circular chromosome become engaged in a tug of war leading either to breakage or loss. In either case, no functional gametes are produced. Therefore, the absence of magnification in circular chromosomes under conditions that would normally cause copy number changes is further evidence that unequal sister chromatid exchange is the mechanism for magnification.

The two types of magnification, meiotic and premeiotic, are genetically separable. That is, there are a number of mutations that effect one type of magnification but not the other. For instance, *mei-41* mutants suppress the frequency of meiotic magnification but have no effect on the frequency of premeiotic magnification (Hawley and Tartoff, 1983 and Marcus et al. 1986). In addition, premeiotic events are rDNA dosage dependent (Hawley and Marcus, 1989), while the meiotic events are apparently not the result of any type of compensatory mechanism. This has

been shown by testing the magnifying properties of a *Ybb*$^-$ chromosome with an appended *bb*$^+$ allele. This chromosome, designated *bb*$^+$*Ybb*$^-$, induces meiotic magnification in the male germ-line at frequencies comparable to the *Ybb*$^-$ chromosome (Hawley and Tartoff, 1983). In addition, other aberrant *Y*-chromosome that are not bobbed show some magnifying properties. Neither *bb*$^+$*Ybb*$^-$ nor the other *bb*$^+$ aberrant *Y*-chromosomes induce premeiotic magnification (Hawley and Tartoff, 1983). Both premeiotic and meiotic events, however, require the presence of an aberrant *Y*-chromosome. Hawley and Marcus have suggested that the presence of the aberrant *Y*-chromosome may disrupt sister chromatid alignment and that improper pairing between homologues may allow for sister chromatid exchange.

An alternative hypothesis for the nonreciprocal events has been proposed by Ritossa (Ritossa, 1968). He suggests that overreplication of a particular region of the array will produce the onion-skin structure seen in overreplication of the ribosomal array during oogenesis in Xenopus (Miller et al.,1969). In this hypothesis, magnification occurs when a fragment of the overreplicated region breaks off and reinserts into the array. This hypothesis is supported by electron microscopic studies that show small circular epichromosomal elements during gametogenesis under magnifying conditions (Graziani, et al., 1977). Epichromsosomal rDNA genes are found in a variety of other organisms, including amphibians, yeast, tetrahymena and other insects (Gall, 1974; Gall and Rochaix, 1974; Clark-Walker and Azad, 1980; Hourcade et al., 1973).

We present evidence that *Rex* , a heterochromatic element that causes gross chromosomal damage during the early stages of development and induces recombination between rDNA arrays, can also induce heritable increases in copy number in rDNA genes. *Rex* is a maternal effect locus. The recombination events that occur in crosses with *Rex*-bearing mothers occur in paternally-derived chromosomes present in the fertilized egg. *Rex*-induced magnification is also a maternal

effect. That is, *Rex* need be present only in the mother in order to induce magnification in paternally-derived chromosomes. The *Rex*-induced event therefore differs from the two other types of magnification - the *Rex*-induced event occurs in the zygote, while meiotic and premeiotic events occur during gametogenesis. Robbins has proposed that *Rex* generates breaks in rDNA arrays (Robbins and Pimpinelli, 1994 and Robbins, 1995 submitted). If the breakage is not repaired, the consequences are lethal. Occasionally, the breaks can be resolved via recombination with a second rDNA array. We propose that breaks in rDNA arrays may also be resolved through recombination between sister chromatids and that unequal sister chromatic exchange leads to heritable changes in rDNA copy number.

Initially, an observation made by Scott Hawley (personal communication), prompted us to examine whether *Rex* could induce changes in rDNA copy number. Hawley saw an unusually large number of unanticipated bb^+ offspring in crosses involving *Rex*. He suggested that the bb^+ offspring were the result of *Rex*-induced magnification. We have carried out experiments, detailed in the remainder of this chapter, that provide evidence that *Rex* can cause heritable changes in rDNA copy number.

Results

Evidence for *Rex*-induced magnification

Rex was originally identified because it induced intrachromosomal recombination between two separated blocks of rRNA genes. Depending on the alignment of the two arrays prior to the exchange, these events resulted in either a deletion or an inversion of the DNA between the exchange points. Detecting similar types of events within a single array is more difficult since deleting or inverting the repeat units within an array may have no phenotypic consequence. Currently, we have no way of detecting inversions of repeat units within a single array. Changes in

copy number of repeat units, on the other hand, can be detected. We addressed the question of whether *Rex* can induce copy number changes maternally by examining the frequency of reversion of a particular *bb* allele, bb^2, when exposed to *Rex*. We found that *Rex* maternally induces heritable changes in copy number of single arrays at frequencies comparable to the rates inter-array exchange.

The mating scheme for testing *Rex* for magnification is shown in Figure 33. Female flies that were genotypically *y cv v f Rex/In(1)*sc^4sc^8, *y sc B* were mated to bb^2/Y males. The *In(1)*sc^4sc^8, *y sc B*, chromosome or simply sc^4sc^8, is an inverted chromosome that is completely deficient for rDNA and carries a dominant *Bar* (*B*) marker that affects the shape of the fly's eye.

Because sc^4sc^8 carries a dominant marker, daughters bearing the bb^2 chromosome and the sc^4sc^8 homologue are phenotypically unique. They are y^+, since they carry y^+ from the bb^2 homologue and *B* because they also have sc^4sc^8, *y sc B*. Most bb^2/sc^4sc^8 daughters are bobbed. However, an occasional bb^2/sc^4sc^8 female that is phenotypically bb^+ is recovered. The bb^m homologue from each of the bb^m/sc^4sc^8 F_1 bb^+ females was then tested for the heritability of the bb^+ revertant allele. This was accomplished by mating the F_1 females to their brothers and examining the F_2. The bb^m alleles coming from F_1 females were scored as heritably revertant if the F_2 *Bar*-eyed females were all bb^+.

Double crossovers in the parental generation between the *Rex* and sc^4sc^8 chromosomes may occasionally result in bb^+ *Bar*-eyed females in the F_1. These F_1 females are genotypically *y B Rex/* y^+ bb^2. A *Rex* NO over bb^2 will sometimes appear bb^+ and therefore these females could be confused with y^+ bb^m / *y B* sc^4sc^8 . The double crossovers can be distinguished from themagnified chromosomes in the F_2. Double crossovers that bear the *Rex* base will be

Figure 33 - Mating scheme for detecting *Rex*-induced magnification events

Females heterozygous for *Rex* and bearing dominantly marked, $In(1)sc^{4R}sc^{8L}$ chromosomes, were mated to bb^2-bearing males. The F_1 were screened for females carrying $In(1)sc^{4R}sc^{8L}$ and the bb^2 paternal *X*-chromosome that nevertheless appeared bb^+. The revertants were further tested for heritability of the bb^+ phenotype. Only females that gave rise to progeny that were all bb^+ were scored as magnified (see text for details).

Figure 33 - Detecting *Rex*-induced Magnification

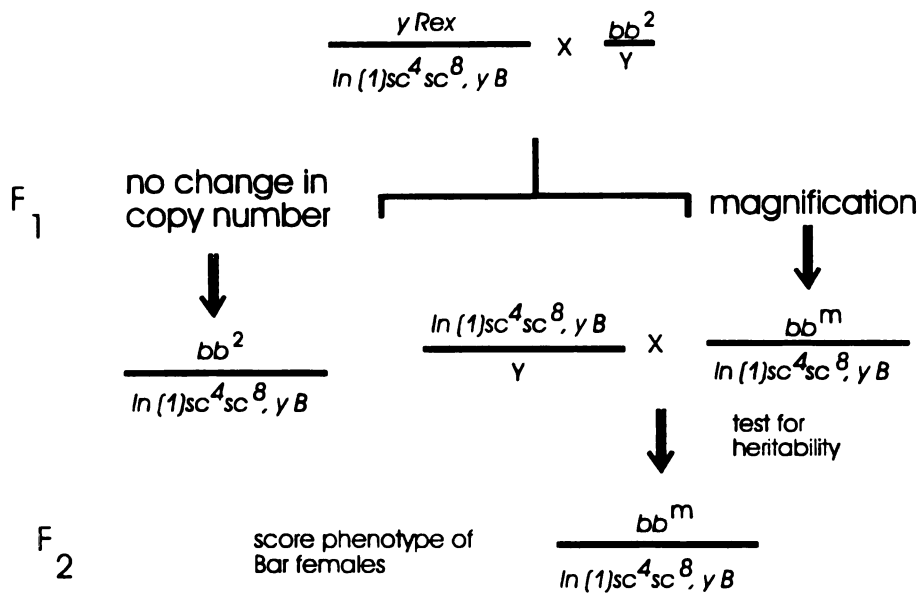

***Rex*-bearing female flies are mated to bb^2 males in the parental generation. Bar-eyed females that are not bobbed in the F_1 are further tested. They are mated to their Bar-eyed brothers and the F_2 Bar-eyed females are scored for the bobbed phenotype. F_1 females that do not bear any bobbed offspring are scored as magnified.**

noninverted, normal sequence chromosomes and will freely exchange with the bb^2 homologue in the F_1 females. Exchange will give rise to male flies that were phenotypically y^+ and *Bar*-eyed. The results of crosses using a number of different *Rex*-bearing chromosomes are presented in Table 7.

Mapping the magnifying element in *Rex*-bearing chromosomes

Although a number of different *Rex*-bearing chromosomes induced heritable copy number changes, the cause could be something other than *Rex* itself. Thus, we decided to map the region of the chromosome that induced magnification. We reasoned that if the element responsible for magnification could be mapped to the base of the *Rex*-bearing chromosome, we would be much more confident that *Rex* itself is the magnification inducing element. We mapped the magnifying element proximal to forked, a marker ten map units from the basal heterochromatin.

Comparing frequencies of *Rex*-induced events with *Ybb*$^-$-induced events.

As a means of comparing the frequency of *Rex*-induced magnification to the meiotic and premeiotic magnification induced by *Ybb*$^-$, we also performed parallel experiments with a *Ybb*$^-$ derivative, B^SYbb^-. In these experiments, male flies bearing a bb^2 allele and an aberrant Y-chromosome, B^SYbb^-, were mated to females carrying a dominantly marked sc^4sc^8 chromosome. Again, bb^+ F_1 female flies bearing sc^4sc^8, and a potentially magnified bb^2 allele were further tested. In these experiments F_1 females were crossed not to their *Ybb*$^-$ brothers but to sc^4sc^8, *y B/Y* males. The mating scheme is presented is Figure 34. Only those F_1 females that produce bb^+ *Bar*-eyed female offspring were scored as magnified. The results are presented together with the *Rex* results in Table 6.

Testing for the ability of *Ybb*$^-$ to induce *Rex*-like recombination events

Because both *Ybb*$^-$ and *Rex*-bearing chromosomes were capable of inducing magnification, we wondered if the *Ybb*$^-$ chromosome might induce *Rex*-like exchanges maternally. Christin Glogowski, a rotation student in our lab, carried out the matings designed to determine whether *Ybb*$^-$ could produce *Rex*-like events. The mating scheme for this experiment shown in Figure 36. The results are straight forward; out of a total of 2606 females scored there were no spiral exchanges. The maternal presence of *Ybb*$^-$ does not cause Rex-like inter-array exchange events.

Figure 34 - Detecting *Ybb*$^{-}$-induced Magnification

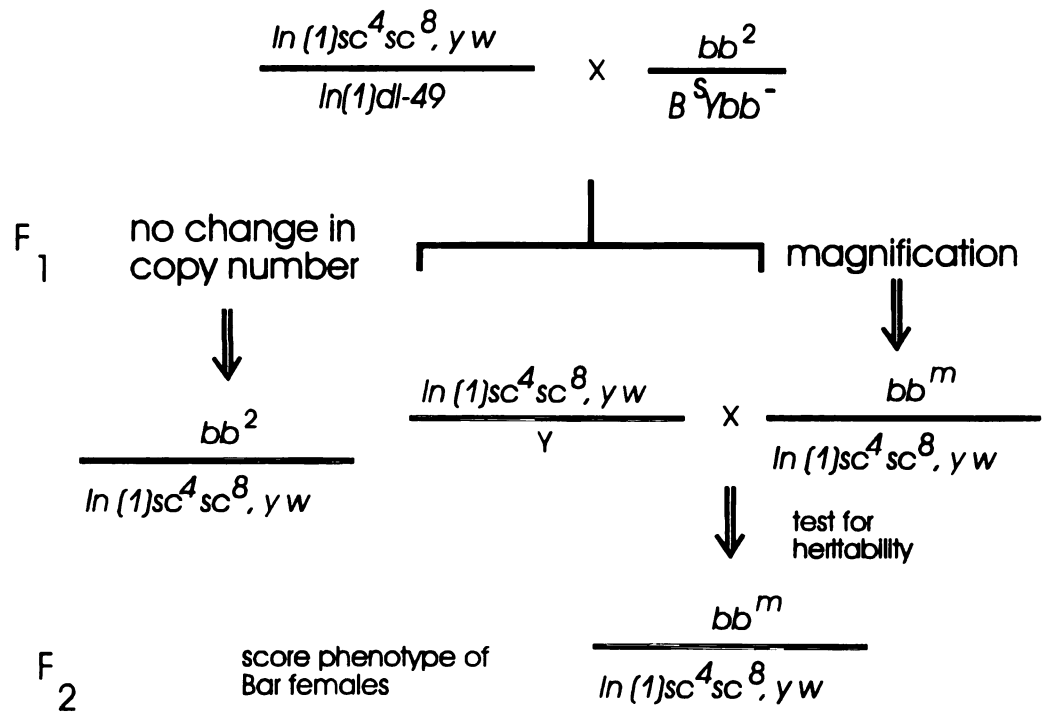

Figure 34 - Females carrying marked In(1)sc^{4}sc^{8} chromosomes are mated to Ybb^{-}- bearing males. Potentially magnified bb^{2} alleles are recovered in the F_1 generation as bb^{+} female flies carrying In(1)sc^{4}sc^{8}. These females are further tested for the heritability of the revertant allele

Table 7 - *Rex* and *Ybb*$^-$ magnification data

The results of magnification tests from both *Rex*-bearing females and Ybb$^-$-bearing males. Using the criteria explained in the text, approximately equal frequencies of magnified chromosomes were recovered from both types of experiments. The figure shows the maternal and paternal genotypes of the parental mating. Final frequencies represent those events that led to heritable changes in rDNA expression (see text for details).

Table 7 - *Rex* and *Ybb*$^-$-induced rDNA magnification

mother	father	*In(1)sc* $^{4L}_{sc}$ ^{8R} daughters	*bb*$^+$	fertile and fully penetrant
$\frac{y\ Rex}{In(1)sc\ ^{4L}_{sc}\ ^{8R}}$	$\frac{bb^2}{Y}$	2658	3.8%	0.8%
$\frac{y}{In(1)sc\ ^{4L}_{sc}\ ^{8R}}$		4741	1.6%	0.08%
$\frac{y}{In(1)sc\ ^{4L}_{sc}\ ^{8R}}$		1382	1.2%	0.3%
$\frac{In(1)dl\text{-}49}{In(1)sc\ ^{4L}_{sc}\ ^{8R}}$	$\frac{bb^2}{Ybb^-}$	2352	3.4%	1.1%
$\frac{FM7}{In(1)sc\ ^{4L}_{sc}\ ^{8R}}$		1732	1.4%	0.6%

Figure 35 - Mating scheme to test for the ability of *Ybb*$^-$ to induce *Rex*-like events

Ybb$^-$-bearing females were mated to target-bearing males. The cross is designed such that spiral exchange progeny can be detected. Spiral exchange in the target will generate y^+-bearing *Y*-chromosomes, giving rise to a unique male phenotype (see text for explanation). Controls are designed to test for the ability of either of the two maternal *X*-chromosomes to produce *Rex* events.

Figure 35 - Testing the ability of *Ybb*$^{-}$ to induce *Rex*-like exchange

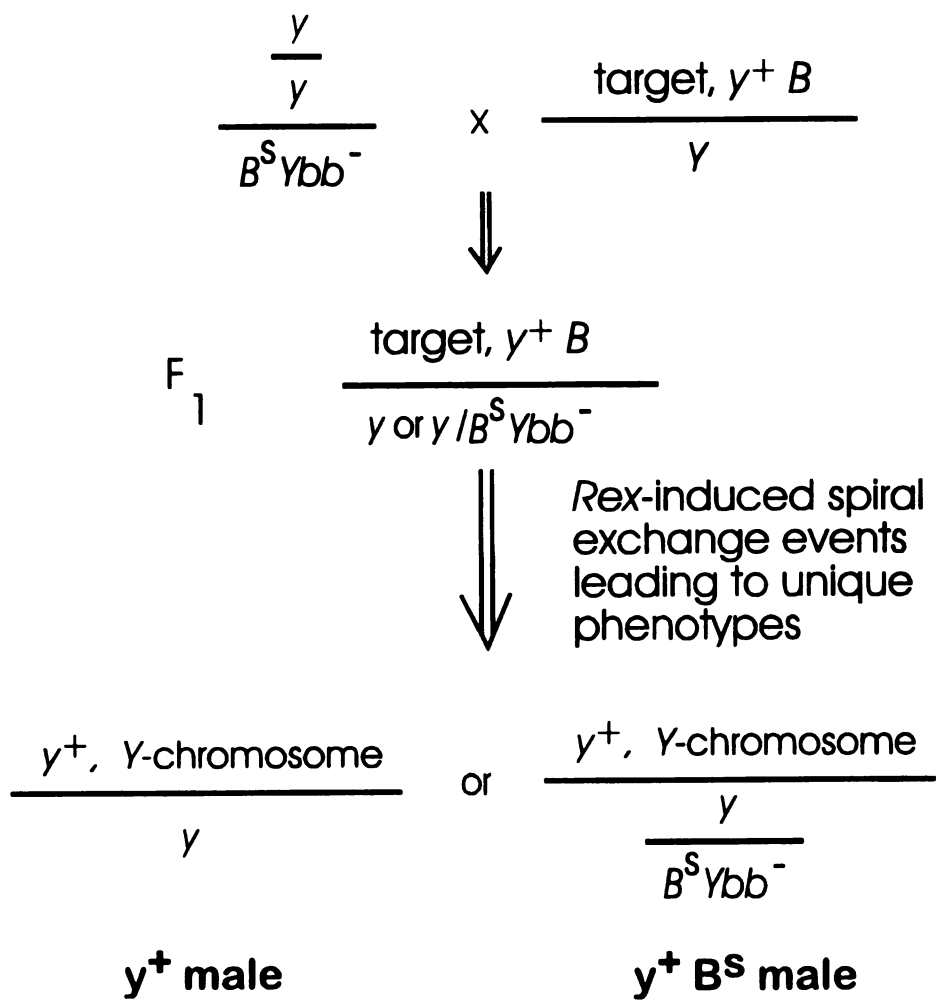

Discussion

Like other *Rex* phenotypes, *Rex*-induced magnification is caused by maternal action. This means that the event must be mitotic. The results can be explained in terms of our current model of how *Rex* works. There are several lines of evidence that suggest that *Rex* activity generates breaks in rDNA arrays. *Rex* may be an activated version of a normally quiescent retrotranspon-like element that inserts into rDNA. Activation of this element could cause expression of a site-specific endonuclease that generates breaks within the rDNA. Depending on how or if these breaks are resolved accounts for the number of different events that we associate with *Rex*. If the breaks go unresolved, the developing embryo arrests very early. Evidence for this comes from cytological examination of early embryos produced from *Rex*-bearing mothers. Upwards of 60% of the embryos fail to reach gastrulation and show gross chromosomal damage (Robbins, 1995). On the other hand, if the breaks are resolved through recombination between two separated arrays on the same chromosome, the classical *Rex* exchange phenotype is exhibited. Molecular analysis of arrays derived from *Rex*-induced hairpin exchanges indicates that, at least for some of the exchange events, there are deletions at the site of exchange, consistent with loss of a piece from rDNA arrays broken in two places.

The magnifying phenotype now associated with *Rex* can also be explained in terms of *Rex*-generated breaks in rDNA. *Rex*-generated breaks within a single array could be resolved by exchange, just as they are in *Rex*-induced spiral and hairpin events. Resolution of such breaks via recombination would involve unequal sister exchange occurring after the first round of DNA synthesis in the zygote. Mitotic unequal sister exchange would produce one array with more copies and one array with fewer copies. It may be that the flies that appear wild-type are actually mosaics with a subset of cells containing fewer than wild type array copy numbers and the remainder containing the reciprocal product of the unequal exchange product, an array with wild-type or close

to wild-type copy number. Phenotypically this fly would appear normal. The other possible fate for the reduced arrays is one that has been suggested for reduced arrays in pre-meiotic events (Tartoff, 1974). They are selected against during the developmental process. In the case of pre-meiotic magnification those germ line cells that have too few copies are outcompeted by cells that contain arrays that have expanded because of unequal exchange. Only expanded arrays proliferate successfully. Cells with reduced arrays may be slower to divide and never make it into mature sperm. A similar type of selection could occur during *Rex*-induced magnification. After the exchange, two homologues with different numbers of rDNA repeat units are generated. One homologue will have an expanded array and the other a reduced array. Cells that derive from the homologue with a reduced number of repeat units may die during fly development.

One of the ultimate aims of this line of research was to determine the mechanism for *Rex*-induced mitotic magnification. We now have a 'quick' mapping approach using *Rex*-induced spiral exchanges that would allow us to address mechanistic questions. We have collected ten *Rex*-induced and ten Ybb^- induced arrays that are all derived from a single bb^2 allele. These could be crossed immediately onto the $Tp(1:1)sc^{V2}$, *3a* target and *Rex*-induced spirals could be generated and stocked in a manner identical to that already described for bb^2 itself (see Chapter 2). If unequal exchange is the mechanism responsible for changes in copy number, then we would predict that maps generated from the magnified arrays would be identical to the parental map. This is because unequal exchange does not change the position of one variant relative to another variant. Therefore the limits of these variants as determined by the exchange points would remain the same and the map as a whole, because it is defined by the variant limits, will also remain unchanged. If, on the other hand, a replicative mode is occurring where one section of the array is replicated and then inserted at a distant site, the relative positions of the variants will change.

Taken together, these experiments indicate that *Rex* can in fact act on a single isolated rDNA array to induce copy number changes. In addition, the frequency of intra-array events, as measured by the frequency of magnification, is comparable to the frequency of inter-array events as measured by the frequency of spiral exchange.

BIBLIOGRAPHY

Aimi, T., Yamada, T. and Murooka, Y. (1994). A group-I self-splicing intron in the nuclear small subunit rRNA-encoding gene of the green alga, *Chloralla ellipsoidea* C-87. Gene 139(1):65-71.

Bonaccorsi, S., Gatti, M., Pisano, C., and Lohe, A. (1990). Transcription of a satellite DNA on two *Y* chromosome loops of *Drosophila melanogaster*. Chromosoma 99: 260-66.

Boussaha, M. (1993). *Rex* and suppressors of *Rex* in natural populations. Masters thesis. Michigan State University.

Brittnacher, J.G. and B. Ganetzky (1983). On the component of segregation distortion in *Drosophila melanogaster*. Deletion maping and dosage analysis of the Sd locus. Genetics 103:659-73.

Brown, S.W. (1966). Heterochromatin. Science 151, 418-425.

Brutlag, D., Appels, R., Dennis, E. S. and Peacock, W. J. (1977). Highly repeated DNA in *Drosophila melanogaster*. J. Mol. Biol. 135, 565-582.

Carbone, I., Anderson, J.B. and Kohn, L.M. (1995). A group-I intron in the mitochondrial small subunit ribosomal RNA gene of *Sclerotiorum sclerotiorum*. Current Genetics 27(2):166-76.

Christman, M. F., Dietrich, F.S., and Fink, G.R. (1988). Mitotic Recombination in the rDNA of *S. Cerevisiae* is suppressed by the combined action of DNA topoisomerases I and II. Cell 55, 413-425.

Christman, M.F., Dietrich, F.S., Levin, N.A., Sadoff, B.U. and Fink, G.R. (1993). The rRNA-encoding DNA array has an altered structure in topoisomerase I mutants of *Saccharomyces cerevisiae*. Proceedings of the National Academy of Science of the U.S.A. 90(16):7637-41.

Clark-Walker, G.D., and A.A. Azad (1980). Hybridizable sequences between cytoplasmic ribosomal RNAs and 3 micron circular DNAs of *Sacchromyces cerevisiea* and *Torulopsis glabrata*. Nucleic Acid Res. 8, 1009-1022.

Condon, C., Liveris, D., Squires, C., Schwartz I. and Squires, C.L. (1995). rRNA operon multiplicity in Escherichia coli and the physiological implications of rrn inactivation. Journal of Bacteriology 177(14):4152-6.

Delany, M.E., Muscarella, D.E. and Bloom, S.E. (1994). Effects of rRNA gene copy number and nucleolar variation on early development: inhibition of gastrulation in rDNA-deficient chick embryos. Journal of Heredity 85(3):211-7.

DePriest, P.T. and M.D. Been (1992). Numerous group I interons with variable distributions in the ribosomal DNA of a lichen fungus. Journal of Molecular Biology 228(2):315-21.

Du, C., Sanzgiri, R.P., Shaiu, W.L., Choi, J.K., Hou, Z., Benbow, R.M. and Dobbs, D.L. (1995). Modular structural elements in the replication origin region of Tetrahymena rDNA. Nucleic acids research 23(10):1766-74.

Endow, S.A. (1980). On ribosomal gene compensation in Drosophila. Cell 22:145-155.

Endow, S.A., and K. C. Atwood (1988). Magnification: gene amplification by an inducible system of sister chromatid exchange. Genetics 100:375-85.

Eissenberg, J.C., Morris, G.D., Reuter, G., and Harnett, T. (1992). The heterochromatin-associated HP-1 Is an essential protein in Drosophila with dosage-dependent effects on position-effect variegation. Genetics 131, 345-352

Ellison, E.L. and V.M. Vogt (1993). Interaction of the intron-encoded mobility endonuclease I-PpoI with its target site. Molecular & Cellular Biology 13(12):7531-9.

Feinberg, A.P. and B. Vogelstein (1983). Addendum to: "A technique for radiolabeling DNA restriction endonuclease fragments to high specific activity." Anal. Biochem. 137:266-267.

Franz, G. and W. Kunz. (1981). Intervening sequences in ribosomal RNA genes and bobbed phenotype in *Drosophila hydei*. Nature 292:638-640.

Fukui, K., Kamisugi, Y. and Sakai, F. (1994). Physical mapping of 5S rDNA loci by direct-cloned biotinylated probes in barley chromosomes. Genome 37(1):105-11.

Gall, J. G. (1974). Free ribosomal RNA genes in the macronucleus of Tetrahymena. Proc. Natl. Acad. Sci. USA 71, 3078-3081.

Gall, J.G., and Rochaix, J.D. (1974). The amlified ribosomal DNA of Dytisid beetles. Proc. Natl. Acad. Sci. USA 71, 1819-1823.

Ganetzky, B. (1977). On the component of segregation distortion in *Drosophila melanogaster*. Genetics 86: 325-55.

Giuntoli, D., Stringer, S.L. and Stringer, J.R. (1994) Extraordinaryily low number of ribosomal RNA genes in P. carinii. Journal of Eukaryotic Microbiology 41(5):88S.

Glatzer, K. H. (1979). Lengths of transcribed rDNA repeating units in spermatocytes of *Drosophila hydei*: only genes without an intervening sequence are expressed. Chromosoma 75:161-175

Glover, D.M. (1981). The rDNA of *Drosophila melanogaster*. Cell 26:297-298.

Goggin, C.L. (1994). Variation in the two internal transcribed spacers and 5.8S ribosomal RNA from five isolates of the marine parasite Perkinsus (Protista, Apicomlexa). Molecular and Biochemical Parasitology 65 (1):179-82.

Graziani, F., Caizzi, R., and Gargano, S. (1977). Circular ribosomal DNA during ribosomal magnification in *Drosophila melanogaster*. J. Mol. Biol. 112, 49-63.

Graziani, F., and S. Gargano (1976). Ribosomal DNA transcription products during the first stages of magnification in *Drosophila melanogaster*. J. Mol. Biol. 100, 59-71.

Hartl, D. L., Hiraizumi, Y. and Crow, J.F. (1967). Evidence for sperm dysfunction as the mechanism of segregation distortion in *Drosophila melanogaster*. Proc. Natl. Acad Sci. USA 58:2240-45.

Hawley, R.S. and K. D. Tartoff (1983). The ribosomal DNA of *Drosophila melanogaster* is organized differently from that of *Drosophila hydei*. J. Mol. Biol. 163:499-503.

Hawley, R.S. and K.D. Tartoff (1983). The effect of *mei-41* on rDNA redundancy in *Drosophila melanogaster*. Genetics 104: 63-80.

Heitz, E. (1928). Das Heterochromatin der Moose. I. Jb. wiss Bot. 69, 762-818

Henikoff, S. (1990). Trends in Genetics vol. 6, no. 12, 422-426.

Higuchi R., Stang, H.D., Browne, J.K., Martin, M.O., Hout, M., Lipeles, J. and Salser, W. (1981). Human ribosomal RNA gene spacer sequences are found interspersed elsewhere in the genome. Gene 15(2):177-86.

Hilliker, A.J. and R. Appels (1982). Pleiotropic Effects Associated with the Deletion of Heterochromatin Surrounding the rDNA of the *X* chromosome of Drosophila. Chromosoma 86, 469-490.

Holmdahl, O.J., Mattsson, J.G., Uggla, A. and Johansson, K.E. (1993). Oligonucleotide probes complimentary to variable regions of 18S rRNA from Sarcocystis species. Mollecular and Cellular Probes 7(6):481-6.

Hourcade, D., Dressler, D., and Wolfson, J. (1973). The amplification of ribosomal RNA genes involves a rolling circle intermediate. Proc. Natl. Acad Sci. USA 70, 2926-2930.

Jacob, S.T. (1995). Regulation of ribosomal gene transcription. (Review) Biomedical Journal 306(Pt3):617-26.

Jakubczak, J.L., Burke, W.D. and Eickbush, T.H. (1991). Retrotransposable elements R1 and R2 interrupt the rRNA genes of most insects. Proceedings of the National Academy of Science of the U.S.A. 88(8):3295-9.

Jakubzak, J.L., Xiong, Y. and Eickbush, T.H. (1990). type I (R1) and type 2 (R2) ribosomal DNA insertions of *Drosophila melanogaster* are retrotransposable elements closely related to those of Bombyx mori.

Jakubczak, J.L., Zenni, M.K., Woodruff, R.C. and Eickbush, T.H. (1992). Turnover of R1 (type I) and R2 (type II) retrotransposable elements in the ribosomal DNA of *Drosophila melanogaster*. Genetics 131(1):129-42.

Jamrich, M. and O.L. Miller, Jr. (1984). The rare transcripts of interupted rRNA genes in *Drosophila melonogaster* are processes or degraded during synthesis. EMBO J. 3:1541-1545.

John, B. and G. Milos. The Eukaryotic Genome in Development and Evolution. (Allen and Unwin, London, 1989).

Kaback, D.B., and H. O. Halvorson (1977). Magnification of genes coding for ribosomal RNA in *Sacchromyces cerevisea*. Proc. Natl. Acad. Sci. USA 74, 1177-1180.

Kamisugi, Y., Nakayama, S., Nakajima, R., Ohtsubo, E. and Fukui, K.(1994). Physical mapping of the ribosomal RNA genes on rice chromosome 11. Molecular & General Genetics, 245(2):133-8.

Kapier, G.M. and E. H. Blackburn (1994). A weak germ-line excision mutation blocks developmentally controlled amplification of the rDNA minichromosome of *Tetrahymena thermophila*. Genes & Development 8(1):84-95.

Karpen H.G., and A. Spradling (1992). Analysis of subtelomeric heterochromatin in the Drosophila minichromosome Dp1187 by single P element insertional mutagenesis. Genetics 132, 737-745.

Kapier, G.M., Orias, E. and Blackburn, E.H. (1994). *Tetrahymena thermophilia* mutants defective in the developmantally programmed matuation and maintenance of the rDNA minichromosome. Genetics 137(2):455-66.

Kaufmann, B. P. (1934). Somatic mitoses of *Drosophila melanogaster*. J. Morphol. 56:125-55.

Keil, R.L., and G.S. Roeder (1984). Cis-acting, recombination-stimulating activity in a fragment of the ribosomal DNA of *S. cerevisiae*. Cell 39, 377-386.

Kidd, S.J. and D.M. Glover (1981). *Drosophila melanogaster* ribosomal DNA containing type II insertions is variably transcribed in different strains and tissues. J. Mol. Biol. 151:645-622.

Komma, D.J. and K.C. Atwood (1994). Magnification in Drosophila: evidence for an inducible rDNA-specific recombination system. Molecular & General Genetics 242(3):321-6.

Leffers, H. and A.H. Anderson (1993). The sequence of 28S ribosomal RNA varies within and between human cell lines. Nucleic Acids Research 21(6):1449-55.

Linares, A.R., Bowen, T. and Dover, G.A. (1994). Aspects of nonrandom turnover involved in the concerted evolution of intergenic spacers within the ribosomal DNA of *Drosophila melangaster*. Journal of Molecular Evolution 39(2):151-9.

Long, E.O. and I. B. Dawid. (1979). Expression of ribosomal DNA insertions in *Drosophila melanogaster*. Cell 18:1185-1196.

Luan, D.D., Korman, M.H., Jakubczak, J.L. and Eickbush, T.H. (1993). Reverse transcriptoin of R28m RNA is primed by a nick at the chromosomal target site: a mechanism for non-LTR retrptransposition. Cell 72(4):595-605.

Luccini, R. (1995). Replication of transcriptionally active chromatin. Nature, 374(6519):276-80.

Maleska, R. and G. D. Clark-Walker (1990). Magnification of the rDNA cluster in *Kluyvermyces lactis*. Mol. Gen. Genet. 223:342-344.

Marrow, Bernice E., Qida Ju, and Warner Jonathan (1990). Purification and characterizaion of the yeast rDNA binding protein REB1. Journal of Biological Chemistry, vol. 34, 20778-20783.

McKee, B.D., Habera, L., Vrana, J.A. (1992). Evidence that intergenic spacer repeats of *Drosophila melanogaster* rRNA genes function as *X-Y* pairing sites in male meiosis, and a general model for achiasmatic pairing. Genetics 132(2):529-44.

Meng-Chao Yao, Ching-Ho Yao, and Bob Monks (1990). The controlling sequence for site-specific chromosome breakage in tetrahymena. Cell, vol. 63, 763-772.

Miklos, G.L.G. in Molecular Evolutionary Genetics (ed. McIntyre, R.J.) 241-322 (Plenum, New York, 1985).

Miller, O.L. and B. Beatty (1969). Extrachromosomal nucleolar genes in amphibian oocytes. Genetics 61, 133-143.

Morgan, G.T. and K.M. Middleton (1992). Conservation of intergenic spacer length in ribosomal DNA of the tailed frog, *Ascaphus truei*. Gene 110(2):219-23.

Muller, H. J. (1930). J. Genet. 22, 299-334.

Muscarella, D.E. and V.M. Vogt (1993). A mobile group-I intron from Physarum polycephalum can insert itself and induce point mutation in the nuclear ribosomal DNA of *Saccharomyces cerevisiae*. Molecular & Cellular Biology 13(2):1023-33.

Neuveglise, C. and Y. Brygoo (1994). Identification of group-I introns in the 28s rDNA of the entomopathogenic fungus *Beauveria brongniartii*. Current Genetics 27(1):38-45.

Oberbaumer, I. (1992). Retroposons do jump: a B2 element recently integrated in an 18S rDNA gene. Nucleic Acids Research 20(4):671-7.

Ohno, S. in Evolution of Genetic Systems (ed. H. H. Smith) 366-370. (Gordon and Breach, New York, 1970).

Paalman, M.H., Henderson, S.L., Sollner-Web, B. (1995). Stimulation of the mouse rRNA gene promoter by a distal spacer promoter. Molecular & Cellular Biology 15(8):4648-56.

Paule, M.R. (1993). Polymerase I transcription, termination, and processing. Gene Expression 3(1):1-9.

Peacock, W.J., Lohe, A.R., Gerlach, W. L., Dunsmuir, P., Dennis, E.S. and Appels, R. (1977). Fine structure and evolution of DNA in heterochromatin. Cold Spring Harbor Symp. Quant. Biol. 42, 1121-1135.

Pikaard, C.S. (1994). Ribosomal gene promoter domains can funtion as artificial enhancers of RNA polymerase I transcription, supporting a promoter origin for natual enhancers in Xenopus. Proceedings of the National Academy of Sciences of the U.S.A. 91(2):464-8.

Raymond A. Kim and James C. Wang (1989). A subthreshold level of DNA topoisomerases leads to the excision of yeast rDNA as extrachromosomal rings. Cell, vol. 57, 975-985.

Reeder R.H. (1990). rRNA synthesis in the nucleolus. Trends in Genetics. 6(12): 390-5.

Ritossa, F.M., Atwood, K.C., Spiegelman, S. 1966. A molecular explanation of *bobbed* mutants in Drosophila as partial deficiencies of ribosomal DNA. Genetics 54: 819-34.

Robbins, L.G. (1981). Genetically induced mitotic exchange in the heterochromatin of *Drosophila melanogaster*. Genetics 99:443-45.

Robbins, L.G.' and S. Pimpinelli (1994). Chromosome damage and early developmental arrest by the *Rex* element of *Drosophila melanogaster*. Genetics 138(2):401-11.

Robbins, L.G. and E.E. Swanson (1988). *Rex*-induced recombination implies bipolar organization of the ribosomal RNA genes of *Drosophila melanogaster*. Genetics 120:1053-1059.

Rochaix, J.D., Bird, A., and Bakken, A. (1974). Ribosomal RNA gene amplification by rolling circles. J.Mol.Biol. 87, 473-487.

Sandler, L. (1977). Evidence for a set of closely linked auosomal genes that interact with sex-chromosome heterochromatin in *Drosohila melanogaster*. Genetics 86, 567-582.

Schwarzacher, H.G. and F. Wachtler (1993). The nucleolus. (Review) Anatomy & Embryology 188(6):515-36.-36.

Smith, G.P. Science 191, 528-535 (1976).

Southern, E. (1975). Detection of specific sequences among DNA fragments sparated by gel electrophoresis. J.MOl. Biol. 98,503-517.

Spofford, J.B. (1976) in Genetics and Biology of Drosophila (Ashburner, M. and Novitski, E., eds), pp. 955-1019, Academic Press

Srivastava, A.K. and D. Schlessinger (1991). Structure and organisation of ribosomal DNA. (review) Biochimie 73(6):631-8.

Stewart, A. (1990). The functional organization of chromosomes and the nucleus. Trends in Genetics vol. 6, no.12, 377-379.

Sullivan, W., Minden, J.S., and Alberts, B.M. (1990). daughterless-abo-like, a Drosophila maternal-effect mutation that exhibits abnormal centrosome separation during the late blastoderm divisions. Development 110, 311-323.

Swanson, E.E. (1984). Parameters of the *Rex* phenotype in *Drosophila melanogaster*. PhD. thesis. Michigan State University.

Swanson, E.E. (1987). The responding site of the *Rex* locus of *Drosophila melanogaster*. Genetics 115: 271-276.

Tartoff, K.D. (1973). Regulation of ribosomal RNA gene multiplicity in *Drosophila melanogaster*. Genetics 73:57-71.

Terracol, R. (1987). Differential magnification of rDNA gene types in *bobbed* mutants of *Drosophila melanogaster*. Mol. Gen. Genet. 208:168-176.

Tomkiel, J.E., Pimpinelli, S. and Sandler, L. (1992). Rescue from the abnormal oocyte maternal effect lethality by ABO heterochromatin in *Drosophila melanogaster*. Genetics 128:583-94.

Trendelenburg, M.F., Scheer, U., Zentgraf, H., and Franke, W.W. (1976). Recombination-stimulating sequences in yeast ribosomal DNA correspond to sequences regulating transcription by RNA polymerase I. Cell 48,1071-1079.

Wakamoto, B.T. and Mark Hearn (1990). The Effects of chromosome rearrangements on the Expression of Heterochromatin genes in chromosome 2L of *Drosophila melanogaster*. Genetics 125, 141-54.

Wallrath, L., and Thomas Friedman (1991). Species differences in the temporal pattern of Drosophila *urate oxidase* gene expression are attributed to trans-acting regulatory changes. Proc. Natl. Acad. Sci. USA Vol.88, 5489-93.

Wiesendanger, B., Lucchini, R., Koller, T. and Sogo, JM. (1994). Replication fork barriers in the xenopus rDNA. Nucleic Acids Research 22(23):5038-46.

Williams, S. M., Kennison, J. A., Robbins, L. G. and Strobeck, C. Recipricol recombination and the evolution of the ribosomal gene family of Drosophila melanogaster. Genetics.

Williams, S. M. and L. G. Robbins (1992). Molecular genetic analysis of Drosophila rDNA arrays. Trends in Genetics. Vol. 8, No. 10 335-340.

Wilson, G.N., Szura, L.L., Rushford, C., Jackson, D. and Erickson, J. (1982). Structure and variation of human ribosomal DNA: the external transcribed spacer and adjacent regions. American Journal of Human Genetics. 349(1):32-49.

Wolffe, A.P. (1994). The role of transcription factors, chromatin structure and DNA replication in 5 S RNA gene regulation. (review) Journal of Cell Science 107(Pt 8):2055-63.

Xiong,Y. and T. H. Eickbush (1988). Functional expression of a sequence-specific encoded by the retrotransposon R2Bm. Cell 55:235-46.

Zhang, H., Wang, J.C., and Liu, L.F. (1988). Involvement of DNA topoisomerase I in transcription of human ribosomal RNA genes. Proc. Natl. Acad. Sci. USA 85, 1060-1064.